Atmosphere and Climate (NS-154B)

2012-2013

C. H. Tijm-Reijmer

Institute for Marine and Atmospheric Research,
Utrecht University, the Netherlands

Contents

1 Introductie **3**

2 The static atmosphere **4**

2.1 Radiation balance of the Sun-Earth system 4

2.1.1 Laws for black body radiation 4

2.1.2 Incoming solar radiation at the top of the atmosphere 7

2.1.3 Solar radiation on geological time scales: Milankovich cycles 9

2.1.4 The planetary and surface albedo 11

2.1.5 The radiation balance 12

2.1.6 Climate sensitivity 13

2.2 Physical properties of the dry atmosphere 15

2.2.1 Composition of the atmosphere 15

2.2.2 Atmospheric density and temperature 16

2.2.3 The hydrostatic balance 18

2.2.4 The dry adiabatic lapse rate 19

2.2.5 Potential temperature 22

2.3 Atmospheric moisture 23

2.3.1 Measures of humidity 23

2.3.2 Global distribution of moisture 26

2.3.3 Stability of the moist atmosphere 27

2.4 Aerosols and clouds 30

2.4.1 Characteristics 31

2.4.2 Cloud formation 34

2.4.3 Cloud classification 36

2.4.4 Precipitation 37

2.4.5 Brunt Väisälä frequency 37

2.4.6 Clouds and radiation 39

2.5 Temperature and radiation in the clear atmosphere 40

2.5.1 The vertical structure of the atmosphere 40

2.5.2 Transport of radiation in the atmosphere 43

2.5.3 Short and longwave radiation in the atmosphere: clear sky 45

2.5.4 Vertical distribution of atmospheric oxygen 47

2.5.5 Radiation transport and the atmospheric temperature profile 48

3 The dynamic atmosphere **50**

3.1 Introduction 50

3.2 Motion in the atmosphere 50

3.2.1 Coordinate systems . . . 51
3.2.2 Apparent forces . . . 52
3.2.3 The pressure gradient force . . . 57
3.2.4 The momentum equations . . . 58
3.2.5 Total and local derivatives . . . 58
3.3 Applications of the equations of motion . . . 61
3.3.1 The Rossby number . . . 61
3.3.2 Geostrophic flow . . . 61
3.3.3 Cyclostrophic flow . . . 62
3.3.4 Gradient flow . . . 62
3.3.5 Geostrophic wind in cartesian coordinates . . . 64
3.3.6 Thermal wind . . . 66
3.4 Synoptic scale motions in mid-latitudes . . . 69
3.4.1 The polar front . . . 70
3.4.2 Mass conservation . . . 72
3.4.3 Vorticity . . . 73
3.5 The atmospheric boundary layer . . . 82
3.5.1 The clear weather ABL over land . . . 83
3.5.2 Exchange of heat and moisture: the surface energy balance . . . 83
3.5.3 Growth of the mixed layer . . . 85
3.5.4 The neutral ABL over land (Ekman or friction layer) . . . 87

4 List of constants **93**

5 Course information **94**
5.1 Course programme . . . 94
5.2 Contact information . . . 94
5.3 Examination . . . 95
5.4 Project information . . . 95
5.4.1 Topic examples . . . 95
5.4.2 Workplan example . . . 96
5.4.3 Presentation information . . . 96
5.5 Hints for the written exam . . . 97
5.5.1 Formulas to know by heart . . . 97
5.5.2 Formulas to recognise / able to work with / able to apply . . . 98

6 Exercises **99**
6.1 Radiation balance of the Sun-Earth system . . . 99
6.2 Physical properties of the dry atmosphere . . . 100
6.3 Atmospheric moisture . . . 101
6.4 Aerosols and clouds . . . 102
6.5 Temperature and radiation in the clear atmosphere . . . 103
6.6 Motion in the atmosphere . . . 104

Bibliography **108**

Chapter 1

Introductie

Het college Atmosfeer en Klimaat beschrijft met behulp van fysische basisprincipes de processen in the atmosfeer.

We beginnen met de stralingsbalans van het zon/aarde/atmosfeer systeem en het natuurlijke broeikaseffect. Vervolgens wordt voor de statische atmosfeer de vertikale verdeling van druk en temperatuur behandeld, de vertikale stabiliteit van deze verdeling en de invloed die vocht hierop heeft.

In het tweede deel van dit college stappen we over naar de dynamica. Hierin worden de basisprincipes van een stroming op een roterende bol behandeld. De krachten die hierbij een rol spelen zijn Coriolis, gravitatie, drukgradiënt en wrijving. Hiermee beschrijven we de geostrofische wind en enkele cirkelsymmetrische systemen zoals tropische cyclonen en tornado's. Verder wordt ook de variatie van de geostrofische wind met de hoogte behandeld en zullen begrippen als straalstroom en polair front de revue passeren.

Vervolgens dalen we af naar de planetaire grenslaag, waar we het grootste deel van ons leven doorbrengen. Hierin leiden we de wrijvingstermen af en wordt de energie uitwisseling met het oppervlak behandeld.

Het statische en dynamische deel komen samen in het derde deel van dit college waarin we zullen stilstaan bij de invloed van natuurlijke klimatologische variaties zoals ijstijden en de invloed die de mens op het klimaat uitoefent (versterkt broeikaseffect).

Dit dictaat ondersteunt het college dat bestaat uit hoorcolleges en werkcolleges. Verder zullen er drie gastcolleges worden verzorgd die ingaan op het meteorologische onderzoek dat plaatsvindt op het Instituut voor Marien en Atmosferisch onderzoek utrecht, IMAU: prof. Hans Oerlemans over IJs en Klimaat, dr. Geert Jan Roelofs over aerosolen in de atmosfeer, dr. Aarnout van Delden over mesoschaal meteorologie. Andere verplichte onderdelen van de cursus zijn studentpresentaties over een zelf gekozen onderwerp uit de meteorologie en/of klimatologie en een excursie naar het KNMI.

Gedurende het college zal op blackboard de college ppts gepubliceerd worden, informatie over de excursie, antwoorden op de oefeningen van het werkcollege etc.

Veel plezier, Carleen Tijm-Reijmer

Chapter 2

The static atmosphere

2.1 Radiation balance of the Sun-Earth system

Among the billion stars in the universe the Sun is the closest to Earth. As a result, virtually all of the energy received by the Earth and that drives the Earth's atmospheric motions, comes from the Sun. Therefore, to understand the Earth's atmosphere the first step is to understand the radiative properties of the Sun-atmosphere system. The basics of the radiative balance of the Sun-Earth system are described here. More information on atmospheric radiation can be found in e.g. Liou (1980); Wallace and Hobbs (2006).

2.1.1 Laws for black body radiation

Each body with a temperature above absolute zero (-273.16 °C), including the Sun and the Earth, emits and absorbs radiation. How effective a body emits and absorbs radiation is expressed by the emissivity (ε_λ) and absorptivity (α_λ) of the body. ε_λ and α_λ vary between 0 and 1. An emissivity of 1 means that all radiation absorbed by the body is also emitted, while an emissivity of 0 means that nothing is emitted. Similar, an absorptivity of 1 means that all radiation that falls on a body is absorbed while 0 means that nothing is absorbed.

The amount of radiation a body emits or absorbs, the way it depends on temperature and wavelength is described by the laws for black body radiation, which are the basis for describing thermal emission of a body. For a black body $\varepsilon_\lambda = 1$ (and $\alpha_\lambda = 1$). Other characteristics are that the radiation emitted is uniquely determined by the temperature of the emitter, for a given temperature the radiant energy emitted is the maximum possible at all wavelengths and the radiation is isotropic, equally strong in all directions. The distribution of black body radiation over the spectrum is given by Planck's law for black body radiation:

$$B_\lambda(T) = \frac{2hc^2}{\lambda^5\left(e^{hc/k\lambda T}-1\right)} = \frac{c_1}{\lambda^5\left(e^{c_2/\lambda T}-1\right)} \tag{2.1}$$

Here, $B_\lambda(T)$ is the monochromatic flux intensity or monochromatic radiance (flux intensity for a single wavelength) in $\mathrm{W\,m^{-3}}$, T is temperature in K and λ is wavelength in m. Furthermore:

$h =$	$6.63\times10^{-34}\ \mathrm{J\,s}$	Planck constant
$k =$	$1.38\times10^{-23}\ \mathrm{J\,K^{-1}}$	Boltzmann constant
$c =$	$2.9973\times10^{8}\ \mathrm{m\,s^{-1}}$	Speed of light.

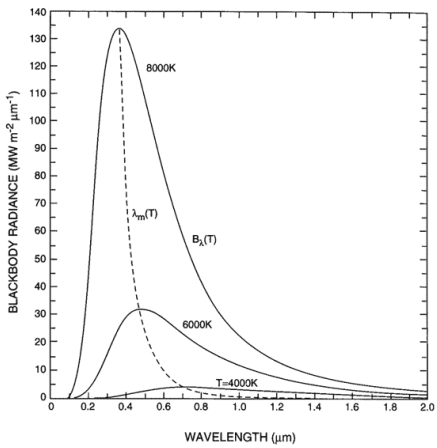

Figure 2.1: Black body intensity per wavelength for a number of emitting temperatures.

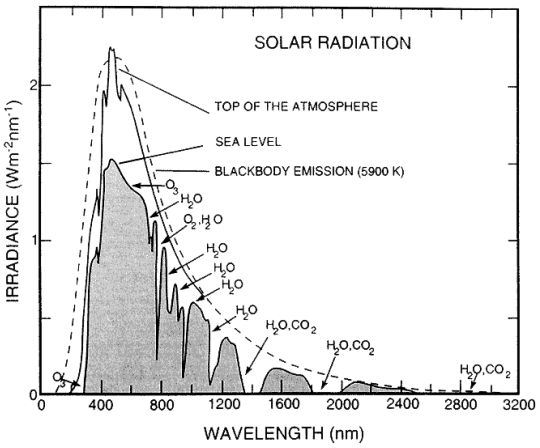

Figure 2.2: Solar spectrum at the top of the atmosphere as observed with satellites, and at sea level for clear sky conditions. Note that the irradiance (F_λ) is plotted, which is the radiance (B_λ) integrated over half a sphere ($F_\lambda = \pi B_\lambda$).

Eq. 2.1 shows that for a given emitting temperature of a black body the energy emitted at each wave length is fixed and can be calculated. Curves of the monochromatic radiance ($B_\lambda(T)$) as function of wave length are called Planck curves and a few examples for several values of emitting temperature are plotted in Figure 2.1. The Figure shows that at a certain wavelength a maximum in radiative intensity occurs. The wavelength at which this maximum occurs (λ_{max}) is given by Wien's displacement law:

$$\frac{\delta B_\lambda(T)}{\delta \lambda} = 0 \qquad \Rightarrow \qquad \lambda_{max} = \frac{2897}{T}\,,$$

where λ_{max} is in μm. Some examples:

$T =$	255 K	$\Rightarrow$	$\lambda_{max} =$	11.4 μm	Earth
$T =$	288 K	$\Rightarrow$	$\lambda_{max} =$	10.1 μm	Earth
$T =$	5780 K	$\Rightarrow$	$\lambda_{max} =$	0.50 μm	Sun

If we now look at the Sun, we know from observations that the main part of the energy emitted by the Sun is in the visible range of the spectrum, between 0.4 and 0.7 μm. The largest intensity is at $\sim$0.5 μm. Figure 2.2 shows the solar spectrum as received at the top of the atmosphere (ToA). The dashed line represents a black body emission curve at 5900 K. It is clear that the spectrum at ToA does not equal a Planck curve. The reason for this is that the temperature of the Sun's photosphere, where the radiation originates, fluctuates. Additionally, the Sun also contains an atmosphere in which radiation is absorbed. The best fit with a Planck curve is obtained for an effective solar radiation temperature between 5800 - 6000 K. The Figure also shows that the Earth's atmosphere is reasonable transparent to solar radiation.

We will take an emission temperature of 5780 K to be representative for the Sun and an emission temperature of 255 K to be representative for the Earth. The corresponding Planck curves are plotted in Figure 2.3. The spectra barely show any overlap, the overlap is only about 5 μm or $\sim$0.4%. Because of this distinction and the fact that solar radiation has the shortest observed wavelengths in the Earth-atmosphere system, solar radiation is often referred to as shortwave radiation (Shw) while terrestrial radiation is often referred to as longwave radiation (Lw). They can also be integrated separately to yield the radiation fluxes for both intervals. Because scientist are often interested in the radiation

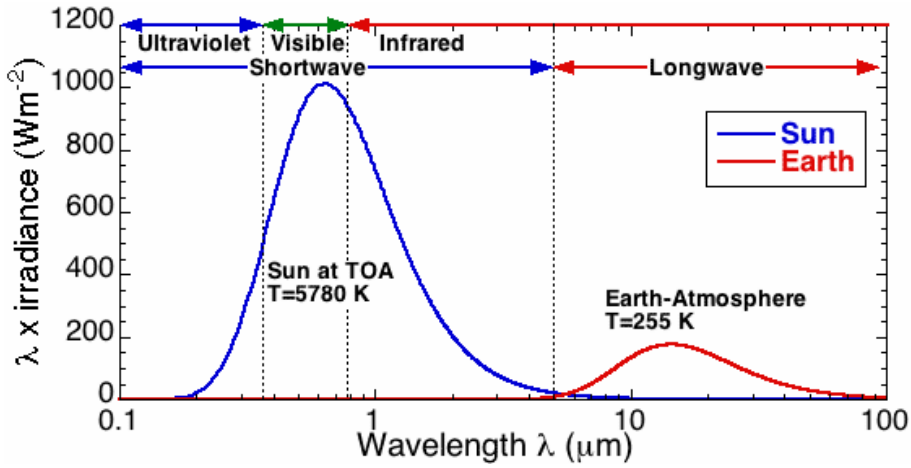

Figure 2.3: Planck's black body curves representative for the Sun at ToA (5780 K) and the Earth (255 K). The irradiance is multiplied by wavelength, which is plotted on a logarithmic scale. The surface below the curves is proportional to the wavelength integrated irradiance ($F(T)$).

balance of a horizontal surface in the atmosphere or at the surface (to calculate e.g. how its temperature will change), it is useful to integrate the radiative fluxes over the upward and downward facing hemispheres and only distinguish between downward (incoming) and upward (outgoing) radiative fluxes: $Shw\uparrow$, $Shw\downarrow$, $Lw\uparrow$, $Lw\downarrow$.

To obtain the total radiation flux ($F(T)$) emitted by a unit surface we integrate $B_\lambda(T)$ (Eq. 2.1) over half a sphere and over the wavelength domain. Integration of the vertical component of $B_\lambda(T)$ over half a sphere results in a factor π:

$$\int_0^{2\pi}\int_0^{\pi/2} \cos\theta \sin\theta \, d\theta d\phi = \int_0^{2\pi} -\frac{\cos^2\theta}{2}\Big|_0^{\pi/2} d\phi \;=\; \pi$$

Thus:

$$F(T) = \int_0^\infty \pi B_\lambda(T) d\lambda = \int_0^\infty \left[\frac{\pi c_1}{\lambda^5\left(e^{c_2/\lambda T}-1\right)}\right] d\lambda = \sigma T^4 \;,$$

in which $F(T)$ is the total radiation flux or irradiance in $\mathrm{W\,m^{-2}}$, equal to $\pi B(T)$, and σ is the Stefan Boltzmann constant ($5.67\times10^{-8}\,\mathrm{W\,m^{-2}\,K^{-4}}$). This equation is often refered to as the Stefan Boltzmann law for black body radiation. Based on $F(T)$ the best fit with total solar radiation outside the Earth's atmosphere is obtained for effective solar radiation temperature of 5780 K.

The last law concerning radiation emission and absorption is Kirchhoff's law. Kirchhoff's law states that for a body in thermodynamic equilibrium, characterized by a uniform temperature and isotropic radiation, absorptivity at a given wavelength equals emissivity at a certain wavelength: $\alpha_\lambda = \varepsilon_\lambda$. In other words, because there is an equilibrium, the same amount of radiation absorbed is also emitted. In case of a black body, the maximum amount of radiation is absorbed and therefore also the maximum amount of radiation is emitted, and $\alpha_\lambda = \varepsilon_\lambda = 1$. A gray body is then characterized by incomplete absorption and emission, and described as $\alpha_\lambda = \varepsilon_\lambda < 1$. All natural surfaces are gray bodies. The Stefan Boltzmann law for natural surfaces is:

$$F(T) = \pi B(T) = \varepsilon\sigma T^4 \;.$$

ε is the wavelength integrated emissivity with values between 0 and 1.

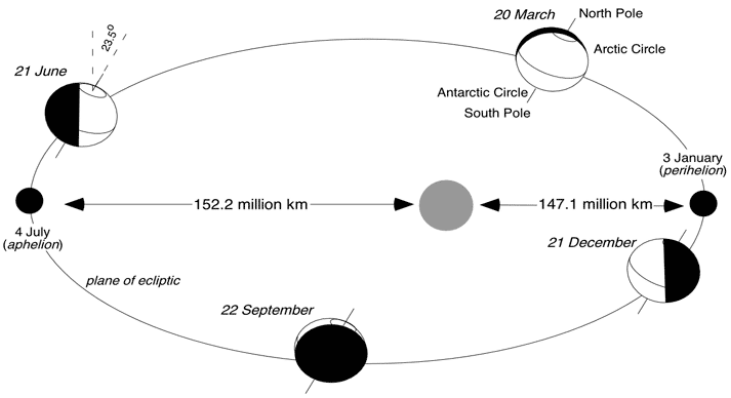

Figure 2.4: Present-day orbit of the Earth around the Sun.

2.1.2 Incoming solar radiation at the top of the atmosphere

From the previous section we know how much energy the Sun is emitting. Based on the energy conservation principle, the total energy emitted by the surface of the Sun must remain the same at any distance of the Sun, and also at the distance of the Earth. This defines the solar constant S_0, which is the instantaneous flux of solar radiation through a surface of 1 m^2 perpendicular to the beam, at average Sun-Earth distance (d_{s-e}).

$$F_s 4\pi r_s^2 = S_0 4\pi d_{s-e}^2 \ ,$$

where F_s is the solar irradiance ($= \sigma T_{Sun}^4$). For a radiant black body temperature of 5780 K, F_s is 63.3×10^6 W m^{-2}. Furthermore, r_s is the radius of the visible disk of the Sun (~700,000 km) and d_{s-e} is the average Sun-Earth distance (~150×10^6 km). This results in a value for S_0 of 1372 W m^{-2}, which corresponds to the surface under the blue curve in Figure 2.3. Variations in S_0 due to variations in solar temperature (e.g. sunspots) are small, ~0.1%. So, the total energy intercepted by the Earth (mean radius r_e = 6371 km) is $S_0\pi r_e^2$. If this energy is spread uniformly over the surface of the globe, we find the insolation at ToA, averaged over a year:

$$Shw{\downarrow}_{ToA}(ann) = \frac{S_0\pi r_e^2}{4\pi r_e^2} = \frac{S_0}{4} \cong 343 \text{ W m}^{-2} \ . \tag{2.2}$$

This means that the average rate at which the Earth and its atmosphere are absorbing solar radiation, and emitting radiation back to space, assuming the Earth-atmosphere system to be in radiative equilibrium with the Sun, is $S = S_0/4 = 343$ W m^{-2}.

The solar constant S_0 represents an (approximate) maximum to be received at the surface of the Earth, if solar incidence is normal and no atmosphere would be present. However, in the present day Sun-Earth configuration, instantaneous ToA incoming solar radiation is a function of several parameters. (1) Latitude, which determines the angle of incidence, (2) time of day or longitude, and (3) time of year, due to the tilted rotation angle of the Earth with respect to the plane in which the Earth rotates around the Sun, and the elliptical form of the Earth's orbit around the Sun. Figure 2.4 illustrates the orbit of the Earth around the Sun.

If the Earth's rotation angle would be perpendicular to the plane in which the Earth revolves about the Sun (the plane of the ecliptic, Figure 2.4) and the orbit of the Earth would be circular, there would be no seasonal variations, the rays of the Sun would hit the top of the atmosphere above the equator at right angles, and the poles would receive no solar radiation at all (Figure 2.5a). However, the rotation axis of the Earth is inclined

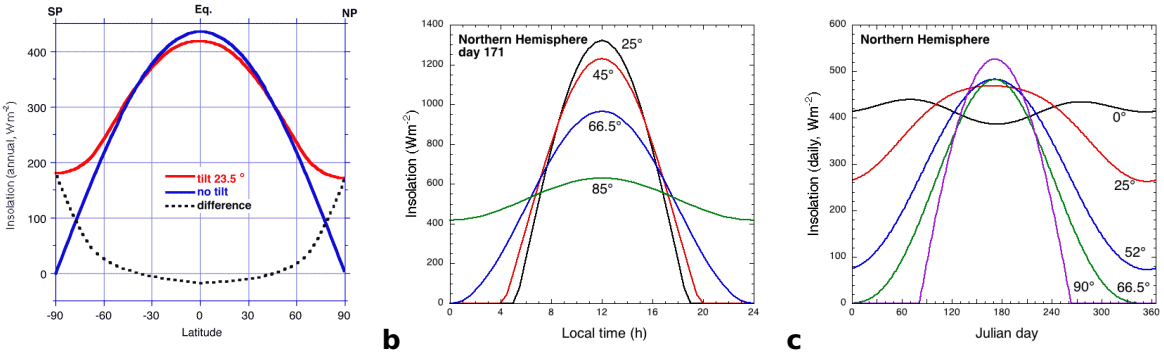

Figure 2.5: a) Latitudinal variation of annual mean insolation as a function of tilt of the rotational axis of the Earth. b) Daily variation of insolation for four latitudes on the Northern Hemisphere on 21 June. c) Seasonal variation of daily mean insolation for five latitudes on the Northern Hemisphere.

by a substantial angle of tilt, measuring ~23.5° from the perpendicular, and its northern extremity pointing to the North Star (Polaris). This means that the latitude where the Sun is directly overhead at solar noon migrates from 23.5°N (Tropic of Cancer) on June 21 (summer solstice) to 23.5°S (Tropic of Capricorn) on December 21 (winter solstice). The regions north of 66.5°N (the Arctic circle) and south of 66.5°S (the Antarctic circle) have one or more days in the winter/summer season during which the Sun is continuously below/above the horizon. On March 20 (the vernal or spring equinox) and September 22 (the autumnal equinox) the Sun is at solar noon directly overhead on the equator and on these days the length of day and night is equal at all latitudes except the poles. The effect of a change in tilt on solar insolation is small between 60°N and 60°S. In the present day configuration the insolation at the poles is about 40% of that at the equator, when integrated over the year.

Figure 2.5b presents the theoretical amount of insolation, i.e. the amount of solar radiation, at ToA for June 21 for several latitudes in the Northern Hemisphere. It illustrates that north of 66.5°N the Sun does not set and that in the tropics the noon insolation is maximum. Figure 2.5c illustrates the seasonal variation of daily mean solar insolation at some selected latitudes. Obviously, the annual cycle of insolation in the polar regions is much greater than at lower latitudes. The daily mean insolation in summer at the pole is larger than at the equator. This is due to the 24 hours sun light at the pole in summer that offsets the effect of the low incidence angle. Note also the higher insolation values in the equinoxes at the equator when the Sun is exactly over the equator.

On a sub-annual time-scale, the rotation of the Earth about its axis and the shape of the orbit of the Earth around the Sun are the most important factors determining the local insolation. The local insolation depends strongly on the solar zenith angle θ_0, which is the angle between the Sun and the normal of the surface and is defined zero when the Sun is right overhead. θ_0 depends on latitude (λ), solar inclination or time of year (δ), and hour angle or time of day (h). The insolation received per one day (or daily insolation) is obtained by integrating the time dependent insolation, which results in:

$$Shw{\downarrow}_{ToA}(daily) = \frac{S_0}{\pi}\left(\frac{d_{s-e}}{d}\right)^2 (\sin\lambda \sin\delta H + \cos\lambda \cos\delta \sin H) \tag{2.3}$$

in which H is the half-day, the time between sunrise or sunset to solar noon. Frame 2.1 derives and illustrates this equation.

The Earth's orbit around the Sun is an ellipse rather than a circle, so $d_{s-e}\, d^{-1}$ does not equal unity: d is ~152.5 million km when the Earth is in aphelion on July 4 and 147.1 million

The solar zenith angle θ_0 is given by (Liou, 1980; Wallace and Hobbs, 2006):

$$\cos\theta_0 = \sin\lambda\sin\delta + \cos\lambda\cos\delta\cos h$$

where λ is latitude, δ solar inclination or time of year, which is the angle between rotation axis and the plane normal to Sun rays, varying between -23.5° and +23.5°, and h is the hour angle or time of day (= ωt, ω is the angular velocity of the Earth). The daily insolation is obtained by integrating the time dependent insolation:

$$Shw{\downarrow}_{ToA}(t) = S_0\left(\frac{d_{s-e}}{d}\right)^2\cos\theta_0(t)$$

over the daylight hours of one day and dividing it by the period (P, 24 hours):

$$Shw{\downarrow}_{ToA}(daily) = \frac{1}{P}S_0\left(\frac{d_{s-e}}{d}\right)^2\int_{t_{sunrise}}^{t_{sunset}}\cos\theta_0(t)dt\ .$$

d is the actual distance between Earth and Sun and d_{s-e} de average distance. t is time with respect to solar noon, with t at solar noon is 0, $t_{sunrise}$ is negative and t_{sunset} is positive defined. Substitute $\cos\theta_0$ and write out results in Eq. 2.3. The term π results from expressing P in an angle ($P = 2\pi$).

Example Calculate $Shw{\downarrow}_{ToA}(daily)$ at equinox (spring or autumn) at the equator. Then λ = 0, δ = 0 thus $\cos\theta_0 = \cos\omega t = \cos 2\pi t/P$. Assume $d_{s-e}\,d^{-1}$ = 1 and use that P = 24 h, $t_{sunrise}$ = -6 h and t_{sunset} = 6 h. Expres time t in hours and solve Eq. 2.3:

$$Shw{\downarrow}_{ToA}(daily) = \frac{S_0}{P}\left(\frac{d_{s-e}}{d}\right)^2\int_{t_{sunrise}}^{t_{sunset}}\cos\left(\frac{2\pi}{P}t\right)dt = \frac{S_0}{P}\frac{P}{2\pi}\left[\sin\left(\frac{2\pi}{P}t\right)\right]_{t_{sunrise}}^{t_{sunset}} = \frac{S_0}{\pi} \qquad \approx 437\,\mathrm{W\,m^{-2}}$$

This value corresponds to the daily insolation on the equator at equinox in Figure 2.5c.

Frame 2.1: Daily mean incoming solar radiation.

km when the Earth is in perihelion on January 3. Note that these dates do not coincide with the summer and winter solstice. Taking the ellipse form into account, the actual seasonal variation of daily insolation at ToA can be calculated (Figure 2.6).

As a result of the eccentricity of the Earth's orbit about the Sun, global insolation at ToA falls from 354 $\mathrm{W\,m^{-2}}$ to 331 $\mathrm{W\,m^{-2}}$, or nearly 7% between early January to early July, so that summertime radiation intensity at ToA is significantly higher in the Southern Hemisphere (SH) than in the Northern hemisphere (NH). In fact, the top of the atmosphere over South Pole at winter solstice (December 21) has the highest daily insolation on Earth at any day of the year. Given the high altitude of South Pole (2900 m), the low cloud amount and the dry atmosphere, this also holds for insolation at the surface. The high summer values of daily mean insolation at high latitudes are due solely to the fact that the Sun is above the horizon for such a large part of the day. Note that the instantaneous highest insolation at ToA (over 1400 $\mathrm{W\,m^{-2}}$) is observed at noon on a day close to the winter solstice at the latitude of the tropic of Capricorn (23.5°S). At this time, the Earth is in perihelion and the incidence angle of the radiation is nearly perpendicular to the surface.

2.1.3 Solar radiation on geological time scales: Milankovich cycles

Interestingly enough, on long time scales variations in the amount of incoming solar radiation and its spatial and temporal variations can explain the occurence of large climate variations such as glacial-interglacial cycles. These variations are brought about by variations in the orbit of the Earth around the Sun.

Figure 2.4 presents the present day orbit of the Earth around the Sun. This orbit has not been constant through time but changes on time scales of thousands of years. As a result the amount of radiation at ToA changes on these time scales as well. The incoming solar

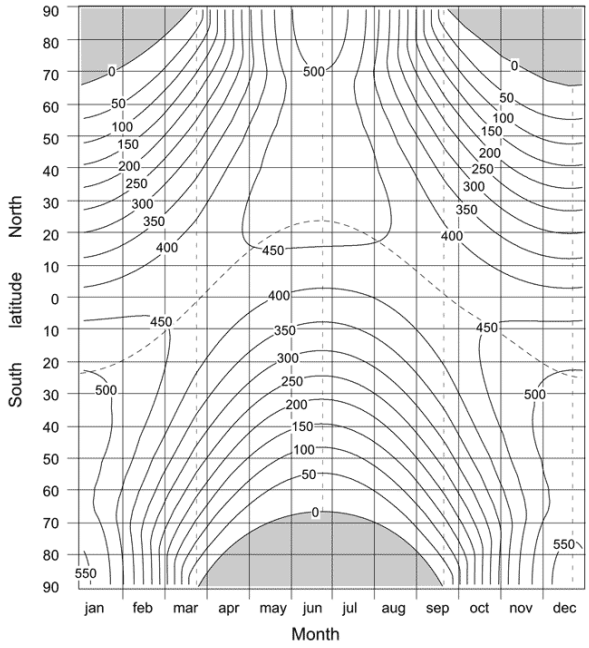

Figure 2.6: Seasonal variation of daily mean TOA insolation as a function of latitude. The curved dotted line indicates the inclination, the angle between the Earth's rotation axis and the plane normal to Sun rays.

radiation at ToA is, on geological time scales, a function of three parameters: 1) Eccentricity of Earth's orbit about the Sun, 2) Obliquity of Earth's rotation axis and 3) Longitude of the perihelion. The variations in these parameters are often called the Milankovitch variations.

The eccentricity of Earth's orbit about the Sun is a measure for the ellipse shape of the Earth's orbit. An eccentricity of 0 represents a circle, an eccentricity between 0 and 1 is an ellipse. The eccentricity of the Earth's orbit varies between 0.005 and 0.060 over a period of 100 kyr. The present day value is ∼0.017. This present day value produces a difference of 10% in radiation incident on Earth between perihelion and aphelion. Annually averaged the difference in incident radiation between maximum and minimum eccentricity is small, ∼0.18%.

The obliquity of Earth's rotation axis is the tilt of the axis with respect to the perpendicular to the plane of ecliptic (Figure 2.7). It varies between ∼22° and ∼24.5° over a period of 41 kyr. The present day value is ∼23.5°. The obliquity changes the amplitude of the seasonal cycle. Obliquity variations within the observed range can produce ∼10% variations in summer insolation in high latitudes.

The precession is the third parameter and describes the longitude of the perihelion. The longitude of the perihelion is the angle between the vernal equinox and the perihelion (Figure 2.7) and describes the location of the seasons on the Earth's orbit about the Sun. It precesses by 360° with a period of 21 kyr. The precession controls the modulation in

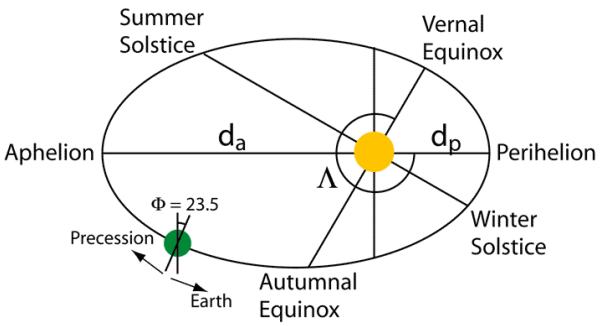

Figure 2.7: Orbit of the Earth around the Sun. Λ is the longitude of the Perihelion, Φ is the obliquity, and d_a and d_p are the distances from the Sun to the Aphelion and Perihelion, respectively, determining the eccentricity (e) of the orbit. $e = (d_a - d_p) / (d_a + d_p)$.

seasonal insolation due to eccentricity. The combined effects of precession and eccentricity can result in ∼15% changes in high latitude summer insolation.

Together these parameters determine the incoming solar radiation at ToA for a given location on Earth and variations in them cause variations in incoming solar radiation and with that influence climate. In high latitudes the combined effect of the three orbital parameters can cause variations in seasonal insolation as large as 30%. These variations are also thought to be responsible for the occurrence of ice ages. The optimum conditions for ice ages to occur are the conditions which result in the survival of winter snow through the summer. Additionally, ice caps need large landmasses to build up. These conditions require the Earth to be in aphelion in the Northern Hemisphere summer, the eccentricity must be large to maximize the Sun-Earth distance in the Northern Hemispheric summer and the obliquity must be small to minimize the seasonal amplitude.

2.1.4 The planetary and surface albedo

In the previous sections solar radiation at the top of the atmosphere, annual and globally averaged as well as as a function of location and time is derived. However, when looking at the Earth-atmosphere system, not all solar radiation reaching the Earth is absorbed by the system, part of it is reflected or scattered back to space. The fraction of solar radiation that is reflected/scattered back to space is determined by the planetary albedo α_p defined as the ratio of incoming and reflected shortwave radiation at ToA:

$$\alpha_p = \frac{Shw\uparrow_{ToA}}{Shw\downarrow_{ToA}} .$$

Similar to α_p, the surface albedo α, is defined as the ratio of incoming and reflected shortwave radiation at the Earth surface:

$$\alpha = \frac{Shw\uparrow_{surface}}{Shw\downarrow_{surface}} .$$

The largest contribution to α_p is from reflection at clouds and absorption by atmospheric constituents, while smaller contributions derive from surface reflection and reflection at aerosols in the troposphere (the lowest 8-10 km of the atmosphere). Figures 2.8a and b present the annual mean cloud cover and surface albedo. Cloud cover is high at mid latitudes over the ocean, and is relatively low over dessert areas. The surface albedo is high over snow and ice surfaces; Antarctica and Greenland. In areas with perennial snow cover the average surface albedo is also relatively high, as for the ocean areas with sea ice cover in winter. Note also the relatively high surface albedo of the Saharan dessert. Combining cloud cover and surface albedo results approximately in the planetary albedo (Figure 2.8c). The annual and global averaged planetary albedo determined from satellites is 0.3±0.02.

The net radiation at the top of the atmosphere ($Shw_{ToA,net}$) can now be defined as:

$$Shw_{ToA,net} = Shw\downarrow_{ToA} - Shw\uparrow_{ToA} = Shw\downarrow_{ToA}(1 - \alpha_p)$$

Figure 2.8d shows that $Shw_{ToA,net}$ is zonally rather evenly distribution, and ranges from 50 W m^{-2} on Antarctica to 250 W m^{-2} at the equator. This decrease in $Shw_{ToA,net}$ is stronger than expected when only looking at the $Shw\downarrow_{ToA}$. This is due to the high surface albedo at the poles.

The longwave radiation balance at the surface is much more heterogeneous: it is strongly negative in areas where cloudiness is low (limited incoming longwave radiation) and the surface is relatively warm (much outgoing longwave radiation). These conditions are met in

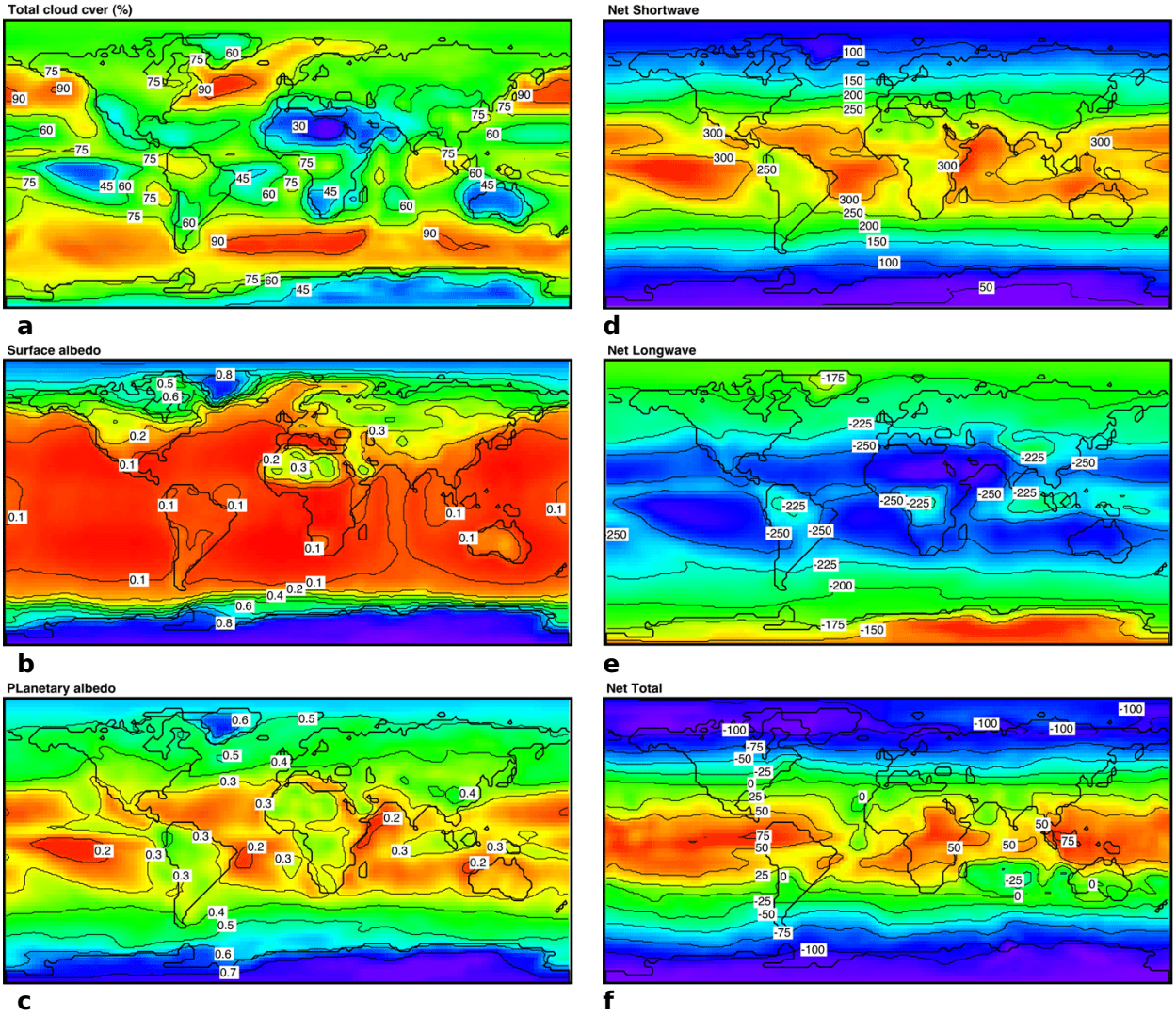

Figure 2.8: a) Annual mean cloud cover in %. b) Annual mean surface albedo. c) Annual mean planetary albedo. d) Annual mean shortwave radiation at TOA. e) Annual mean longwave radiation at TOA. f) Net annual mean radiation at TOA.

desert regions, which are easily discernible, e.g. the Saharan desert. In the tropics the loss of longwave radiation is limited because of the high moisture content and temperature of the atmosphere. The poles are interesting because due to the high surface albedo most of the solar radiation is reflected and cannot be used to warm the surface. As a result the longwave radiation loss is large enough to create a negative net radiation flux over large parts of the surface of the Greenland and Antarctic ice sheets in spite of the low temperatures and low cloud amounts.

2.1.5 The radiation balance

Based solely on radiation we can already study the sensitivity of our climate to changes in incoming solar radiation. For a climate system in balance, at the top of the atmosphere the following balance holds:

$$Shw\downarrow_{ToA}(1-\alpha_p) = \sigma T^4_{e-a} \, . \tag{2.4}$$

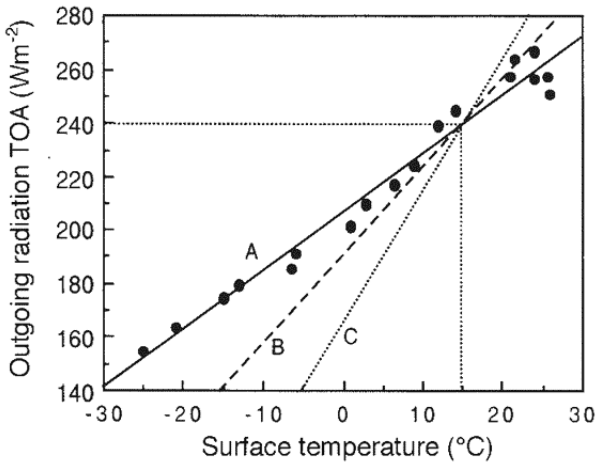

Figure 2.9: Outgoing radiation at ToA as a function of surface temperature, based on satellite measurements. Values are zonally averaged and representative for latitude bands of 10° width. Line A represents measurements, line B present conditions, and line C the black body value. Slope of the line is $\delta L/\delta T = b$.

Which states that the gain of energy by the climate system through shortwave radiation is balanced by a loss of longwave radiation, assuming the Earth-atmosphere system to act as a black body. From this you can calculate the radiation temperature of the climate system T_{e-a} (temperature of the earth-atmosphere system). When we now substitute the result of Eq. 2.2, $Shw{\downarrow}_{ToA} = S = S_0/4 = 343\,\mathrm{W\,m^{-2}}$, $\alpha_p = 0.3$ and the Stefan-Boltzman constant in Eq. 2.4 a radiation temperature of the Earth-atmosphere system of ∼255 K = -18°C results. This is much lower than the actual average surface temperature of the Earth, which is ∼15°C! In fact, a temperature of -18°C is in the atmosphere found at an altitude of about 5 km. It appears that the largest part of the longwave radiation emitted to space is not emitted by the surface but by the atmosphere. Or, most of the longwave radiation emitted by the Earth surface is absorbed by the atmosphere, which in turn, emits longwave radiation upward as well as downward. This effect is called the greenhouse effect of the atmosphere.

To include the effect of the greenhouse effect and to obtain the emitted longwave radiation at ToA in terms of the surface temperature (T) we write:

$$S(1-\alpha_p) = \sigma T_{e-a}^4 = \tau\sigma T^4 \ . \tag{2.5}$$

Here, τ is the effective transmissivity of the atmosphere to longwave radiation emitted by the surface. τ is per definition a value between 0 and 1 and the smaller τ the larger the greenhouse effect of the atmosphere. For the present conditions ($\alpha_p = 0.3$, $T = 288\,\mathrm{K}$) a value of 0.61 is found for τ. Since τ depends on atmospheric conditions, as we will show below, we cannot assume τ to remain constant when climate changes.

2.1.6 Climate sensitivity

To investigate the sensitivity of T for changes in S we perform a perturbation analyses (see Frame 2.2). The result of the analyses is:

$$\delta T = \frac{(1-\alpha_p)\delta S}{b} \ , \tag{2.6}$$

expressing the sensitivity of T to changes in S.

In the present condition $b = \delta L/\delta T = 4\tau\sigma T_c^3$ is $\sim 3.3\,\mathrm{W\,m^{-2}\,K^{-1}}$ and for a change in S of 1% ($\delta S = 3.43\,\mathrm{W\,m^{-2}}$) a temperature change for the present conditions, of 0.72 K is found. For a pure black body ($\tau = 1$, $T = 288\,\mathrm{K}$), $b = 5.42\,\mathrm{W\,m^{-2}\,K^{-1}}$ resulting in $\delta T = 0.44\,\mathrm{K}$. This

To derive Eq. 2.6 first assume: $T = T_c + \delta T$, $S = S_c + \delta S$, $L = L_c + \delta L$ and α is constant. Linearize the balance equation (Eq. 2.5):

$$\begin{aligned} \tau\sigma(T_c+\delta T)^4 &= L_c + \delta L \\ &= L_c + (\delta L/\delta T)\delta T \\ &= \tau\sigma T_c^4 + 4\tau\sigma T_c^3 \delta T \\ &= a + b\delta T \ , \end{aligned}$$

with $a = \tau\sigma T_c^4$ and $b = \delta L/\delta T = 4\tau\sigma T_c^3$. Substitute the result in Eq. 2.5:

$$(S_c + \delta S)(1-\alpha_p) = a + b\delta T$$

Using the fact that $S_c(1-\alpha_p) = a$ reduces the equation to:

$$\delta S(1-\alpha_p) = b\delta T \ .$$

Rearranging the terms results in Eq. 2.6.

Now assume also a perturbation in α_p: $\alpha_p = \alpha_c + \delta\alpha$
Include the above and substitute all in Eq. 2.5:

$$(S_c + \delta S)(1-\alpha_c-\delta\alpha) = a + b\delta T$$

We assume $\delta\alpha$ to be a function of δT by writing:

$$\delta\alpha = -\beta\delta T \qquad \beta \geq 0 \ ,$$

in which β is the strength of the albedo feedback. Substituted in the equation, and using $S_c(1-\alpha_c) = a$, and neglecting higher order perturbation terms ($\delta\alpha\delta S$), the temperature sensitivity including albedo feedback is given with Eq. 2.7.

Frame 2.2: Perturbation analysis.

shows that the greenhouse effect of our atmosphere enhances the climate sensitivity of the atmosphere.

A value for b can also be derived from observations. Figure 2.9 presents zonal averaged measurements of T and L for 18 latitude bands. Each point represents a 10° latitude band. The slope of the lines in the figure represent b. Compared to the above, b derived from the figure is exceptionally low. The reason is feedback mechanisms in the atmosphere, mainly the water vapor feedback. The water vapor feedback mechanism results from the fact that when temperature increases air can contain more moisture and will absorb more longwave radiation. A linear regression from this Figure gives a value of $2.2\,\mathrm{W\,m^{-2}\,K^{-1}}$ for b, and therefore $\delta T = 1.09\,\mathrm{K}$ for a change in S_0 of 1%. Thus, the water vapor feedback mechanism enhances the sensitivity of the climate system.

In the above we assumed the surface albedo remained constant, which is not a realistic assumption since the extent of area covered with snow and ice is directly related to temperature. To investigate the sensitivity of the surface temperature to S changes including the albedo feedback effect we include the albedo variations in the perturbation analyses (Frame 2.2). The result is:

$$\delta T = \frac{(1-\alpha_c)\delta S}{b - \beta S_c} \ . \tag{2.7}$$

β is the strength of the albedo feedback with an estimated value of $\sim 0.003\,\mathrm{K^{-1}}$, $\beta S_c \approx 1\,\mathrm{W\,m^{-2}\,K^{-1}}$. For a value of b of $2.2\,\mathrm{W\,m^{-2}\,K^{-1}}$ this means that the albedo feedback doubles climate sensitivity for a change in solar insolation. For δS is 1% of S and $\alpha_p = 0.3$, δT becomes 2.0 K.

To summarize:

Table 2.1: Composition of the atmosphere (lowest 100 km)(* Stratospheric value).

Gas	Molar mass (M_i)	Molar (volume) fraction	Molar mass fraction (M_i/M_{tot})	Vertical distribution	Controlling process
H_2O	18	<0.030		Decreases sharply in troposphere; highly variable	Evaporation, condensation transport
N_2	28	0.7808	0.7552	Homogeneous	Vertical mixing
O_2	32	0.2095	0.2315	Homogeneous	Vertical mixing
Ar	40	0.0093	0.0128	Homogeneous	Vertical mixing
CO_2	44	0.0003	0.0005	Homogeneous	Vertical mixing; production by surface and anthropogenic processes
O_3	48	10 ppmv*		Increases sharply in stratosphere; highly variable	Photochemical production in stratosphere
CH_4	16	1.6 ppmv		Homogeneous in troposphere	Production by surface processes
N_2O	44	350 ppbv		Homogeneous in troposphere	Production by surface and anthropogenic processes
CO	28	70 ppbv		Decreases in troposphere	Production by anthropogenic processes
NO	30	0.1 ppbv*		Increases vertically	Dissociation of N_2O
CFC-11		0.2 ppbv		Homogeneous in troposphere	Industrial production, mixing
CFC-12		0.3 ppbv		Homogeneous in troposphere	Industrial production, mixing

no greenhouse effect (black body):
$\delta T =$ 0.44 K $b =$ 5.42 $\mathrm{W\,m^{-2}\,K^{-1}}$
constant greenhouse effect:
$\delta T =$ 0.72 K $b =$ 3.3 $\mathrm{W\,m^{-2}\,K^{-1}}$
plus water vapor feedback:
$\delta T =$ 1.09 K $b =$ 2.2 $\mathrm{W\,m^{-2}\,K^{-1}}$
plus albedo feedback:
$\delta T =$ 2.00 K $b =$ 2.2 $\mathrm{W\,m^{-2}\,K^{-1}}$

The vertical temperature profile will be discussed later. Note however, that temperature at certain altitude is not only determined by radiation balance. Heat exchange also occurs at the Earth surface and in the atmosphere by turbulence (heat exchange through temperature differences and moisture differences). The vertical profiles of longwave radiation are therefore not monotonous.

2.2 Physical properties of the dry atmosphere

The second step in understanding the Earth's atmosphere is to understand the physical properties of the atmosphere, i.e. its composition and structure. We will first discuss the dry atmosphere and then extend the description to include moisture.

2.2.1 Composition of the atmosphere

The atmosphere is a mixture of gasses. Some of these gasses occur only incidentally or/and in very small amounts. These are mainly the industrial produced gasses. Table 2.1 presents the most important permanent gasses present in the atmosphere, among which oxygen (O_2), carbon dioxide (CO_2) and water vapor (H_2O). The table also presents other characteristics such as the vertical distribution and the processes controlling the gas in the at-

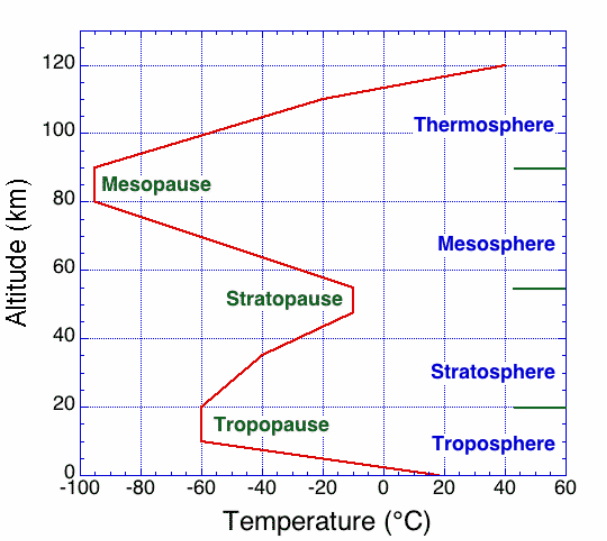

Figure 2.10: Schematic view of the atmospheric temperature structure.

mosphere. Note that the total amount is not a measure for the importance of a gas. The residence time of the gas is important too. It appears that when the residence time of a gas becomes larger, the temporal and spatial variability becomes smaller. This is an important feature in the climate system. Besides the gasses, the atmosphere also contains hydrometeors (e.g. water droplets and ice crystals) and aerosols, which are small solid particles in the air.

The lowest 150 km of the atmosphere is divided in the thermosphere (>90 km), the mesosphere (50 to 90 km), the stratosphere (15 to 50 km), and the troposphere (to 15 km) (Figure 2.10). The daily variations in weather mainly occur in the troposphere. The different layers are separated by the mesopause, the stratopause and the tropopause, respectively. These are the regions where the sign of the temperature gradient changes.

In the troposphere the temperature generally decreases with altitude. Solar radiation is absorbed at the surface and heats the atmosphere from below. In the stratosphere the temperature increases again, which is due to the absorption of solar radiation, mainly in the ozone layer at about 20 km altitude. This ozone layer is also very important for life on Earth because the layer strongly reduces the amount of ultraviolet radiation that reaches the Earth surface. Above the stratosphere the air becomes extremely thin and in the thermosphere the air temperature may vary between 200 and 2000 K, depending on the solar activity. Above the stratopause the vertical exchange is suppressed. A more extensive description of the vertical structure of the atmosphere is given in section 2.5.

2.2.2 Atmospheric density and temperature

To describe the state of the atmosphere in terms of pressure and temperature we make use of equations of state. In general, for a given substance or mixture of substances, equations of state attempt to describe the relationship between temperature, pressure, and volume of that substance. One of the most simple equations of state is the ideal gas law. The ideal gas law is reasonably accurate for gasses at low pressures and high temperatures, but it becomes increasingly inaccurate at higher pressures and lower temperatures. Gasses that behave according to the ideal gas law are called ideal gasses. The atmosphere is a mixture of gasses and behaves to a good approximation as an ideal gas. For a single component

Avogadro's number The mass of a gas is often expressed in terms of the molar (or molecular) mass, which is the number of grams in one mole of gas. One mole is defined by Avogadro's number: $N_A \approx 6.02\,10^{23}$ molecules per mole gas. This number of molecules in one mole of gas is defined such that one mole of gas is the amount of molecules needed to obtain a mass in grams equal to the molecular mass of a certain gas. For example, the molecular mass of Carbon (C) is 12, and therefore, 1 mole = $6.02\,10^{23}$ molecules of ^{12}C contains 12 g of mass.

Avogadro's law states that at given pressure and temperature, the same number of molecules of different gases occupy the same volume, independent of their mass. Under standard atmospheric conditions:
Pressure p_0 = 101300 Pa = 1013 hPa = 1 atm
Temperature T_0 = 0°C = 273.16 K
this volume (V_0) is found to be 22.4 m^3 for 1 kmole of molecules.

Newton's first law of motion pertains to the behavior of objects for which the forces acting on it are balanced. It states that an object at rest tends to stay at rest and an object in motion tends to stay in motion with the same speed and in the same direction unless acted upon by an unbalanced force.

The first law of thermodynamics is the application of the conservation of energy principle to heat and thermodynamic processes. The change in internal energy of a system (dIE) is equal to the heat added to the system (dQ) minus the work done by the system (dW).

$$dIE = dQ - dW \tag{2.8}$$

Dalton's law states that the total pressure exerted by a mixture of gasses is equal to the sum of the pressures that would be exerted by the gasses if they alone were present and occupied the total volume: $p = \sum p_i$.

Frame 2.3: Fundamentals.

gas the ideal gas law is given by:

$$p = \rho R T \ ,$$

where p is pressure in Pa, ρ density in kg m^{-3}, R is the specific gas constant for the single component gas (in J kg^{-1} K^{-1}) and T is temperature in K.

However, the atmosphere is a mixture of gasses. Table 2.1 presents the most important permanent gasses present in the atmosphere with some of their properties, such as the molar mass M, molar (volume) fraction and molar mass fraction. Each gas in the atmosphere behaves to a good approximation as an ideal gas. Using the Law of Dalton ($p = \sum p_i$), the ideal gas law for a single gas can be rewritten for a mixture of gasses. The equation of state then becomes:

$$p = \rho R_d T \ , \tag{2.9}$$

where R_d is the gas constant of dry air, which is the universal gas constant (R^*) divided by the molecular weight of dry air (see Frame 2.4). This end result shows that the ideal gas law for the dry atmosphere is similar to that for a single gas if R is replaced by R_d as defined in Frame 2.4.

The weighted average molecular mass of dry air (M_d) based on the four major constituents of the dry atmosphere can be calculated using the numbers for the molecular mass and mass fraction given in Table 2.1, and is 28.9. Given this value the gas constant of dry air ($R_d = R^*/M_d$) is 287.05 J kg^{-1} K^{-1}. Furthermore, we can also calculate the density of dry air (ρ) if we know the air pressure and air temperature. The next step is to look at the vertical distribution of temperature and pressure.

A single component gas: The ideal gas law describes p of a single component gas in terms of T and ρ:

$$p = \frac{nR^*}{V}T = \frac{mR^*}{MV}T = \rho R T \ .$$

p	pressure	Pa
$n = \frac{m}{M}$	number of moles	kmol
m	mass	kg
M	molecular weight	$\mathrm{kg\,kmol^{-1}}$
R^*	universal gas constant	$\mathrm{J\,K^{-1}\,kmol^{-1}}$
V	volume	$\mathrm{m^3}$
T	temperature	K
$\rho = m/V$	density	$\mathrm{kg\,m^{-3}}$
$R = R^*/M$	specific gas constant	$\mathrm{J\,kg^{-1}\,K^{-1}}$

R^* follows from the standard conditions (see Avogadro's law in Frame 2.3): $p_0 = 101300\,\mathrm{Pa}$, $T_0 = 273.16\,\mathrm{K}$, $V_0 = 22.4\,\mathrm{m^3}$, $n = 1\,\mathrm{kmol}$, substituted in a rearanged ideal gas law:

$$R^* = \frac{p_0 V_0}{n T_0} = 8.314 \times 10^3\,\mathrm{J\,K^{-1}kmol^{-1}}.$$

A mixture of gasses: Dalton's law ($p = \sum p_i$) is used to derive the equation of state. Assume that each gas (i) is characterized by mass m_i ($\rho_i = m_i/V$), pressure p_i and gas constant R_i, then the ideal gas law for a mixture of gasses (excluding water vapor) becomes:

$$\begin{aligned} p &= \sum p_i \\ &= \frac{\sum m_i R_i}{V} T \\ &= \rho T \sum \frac{m_i}{m_{tot}} R_i \\ &= \rho R_d T \ , \end{aligned}$$

where $m_{tot} \equiv \sum m_i$, $\rho = \frac{m_{tot}}{V}$, and R_d is the gas constant of dry air, which can be written as:

$$R_d \equiv \sum \frac{m_i}{m_{tot}} R_i = R^* \sum \frac{\frac{m_i}{M_i}}{m_{tot}} = \frac{R^*}{M_d} \ .$$

with M_d the weighted average molecular mass of dry air.

Frame 2.4: The ideal gas law.

2.2.3 The hydrostatic balance

The air is not evenly distributed over the vertical (and horizontal) extent of the atmosphere, but the amount of air decreases with increasing altitude. Air pressure is defined as the force acted on a unit surface by the air and it decreases upwards in the atmosphere. If we assume a homogenic isothermal atmosphere without motion, the upward pressure gradient force is balanced by gravity. The resulting balance is known as the hydrostatic balance and basically states that air pressure is the weight of the column of air above you. Hydrostatic balance requires an isothermal (constant temperature) motionless fluid. This means that the atmosphere never quite satisfies hydrostatic equilibrium. But for most atmospheric motions it is a very good approximation. It only gives problems in areas where there are strong vertical accelerations, like in thunderstorms.

The hydrostatic balance is derived from Newton's first law (Frame 2.3) with pressure and gravity acting as the balancing forces (Frame 2.5). The hydrostatic balance is given by:

$$\frac{dp}{dz} = -\rho g \ . \tag{2.10}$$

According to the equation of state, pressure depends on the density and temperature of

Consider a column of air between two vertical levels with pressures p at z, and $p+dp$ at $z+dz$ (note $dp < 0$) (see Figure). In absence of a vertical acceleration Newton's first law requires that the forces acting on the column balance, i.e. the total vertical pressure force balances the downward gravitational force (downward force is defined negative, and note that pressure is force per unit surface, Pa = Nm^{-2}):

$$\begin{aligned} pdA - (p+dp)dA - mg &= 0 \\ (p - p - dp)dA &= mg \\ -dpdA &= \rho dVg \\ -dpdA &= \rho dzdAg \\ -dp &= \rho dzg \\ \frac{dp}{dz} &= -\rho g \end{aligned}$$

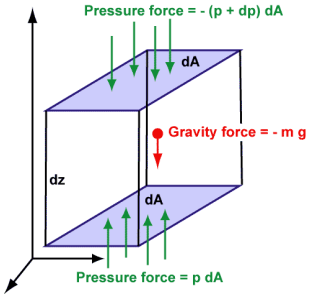

pdA is the pressure force acting on the column from the air below, dA is the surface area of the column, $(p+dp)dA$ is the pressure force acting on the column from above, mg is the gravitational force, g is the gravitational acceleration, m is mass, ρ is the air density, dV the volume of the column, dz de height of the column defined positive in the upward direction.
The result is the hydrostatic balance, Eq. 2.10.

Frame 2.5: The hydrostatic balance.

the gas. Therefore, the combination of the equation of state for a dry atmosphere (Eq. 2.9) and the hydrostatic balance (Eq. 2.10) provides an expression which can be used to derive the vertical variation in pressure (Frame 2.6):

$$p(z) = p_0 \exp\left[\frac{-g}{R_d}\int_{z=0}^{z}\frac{dz}{T(z)}\right]$$

This relation shows that pressure decreases exponentially with height. Assuming an isothermal atmosphere (constant T) this equation can be solved:

$$p(z) = p_0 \exp\left(\frac{-zg}{R_d T}\right) ,$$

which is called the barometric equation. An example of the barometric relation is given in Figure 2.11 for an isothermal atmosphere of -18°C. The relation can also be solved for a linear decreasing temperature (see exercises). Furthermore, the term $R_d T/g$ in the barometric equation provides a scaling height for pressure. A scaling height is the height at which a parameter has decreased by factor $1/e$. For an atmosphere with an average temperature of 15°C, the scaling height for pressure is about 8.4 km.

2.2.4 The dry adiabatic lapse rate

In the previous section the assumption is made that the atmosphere is isothermal. This is in reality not the case, temperature varies with elevation. For a dry atmosphere, the dry-adiabatic lapse rate describes the rate of temperature change with elevation. Using the first law of thermodynamics and the assumption that there is no heat exchange between parcel and surroundings results in the dry-adiabatic lapse rate γ_d (Frame 2.7):

$$\gamma_d = -\frac{g}{c_p} = -9.8\ \mathrm{K\,km^{-1}} ,$$

with g the gravity acceleration and c_p the heat capacity of air at constant pressure ($1004\,\mathrm{J\,kg^{-1}K^{-1}}$).

Combine the equation of state : $p = \rho R_d T \rightarrow \rho = \frac{p}{R_d T}$

and the hydrostatic balance : $\frac{dp}{dz} = -\rho g \rightarrow dp = -\rho g dz$.

to obtain : $\frac{dp}{p} = \frac{-g dz}{R_d T}$

Integrate this expression between the surface z=0 ($p = p_0$ at $z = 0$) and a given level z ($p = p(z)$ at z) to obtain an expression for the vertical variations in pressure as a function of the vertical variations in temperature:

$$\begin{aligned}
\int_{p_0}^{p(z)} \frac{dp}{p} &= \int_{z=0}^{z} \frac{-g}{R_d} \frac{dz}{T(z)} \\
\ln(p(z)) - \ln(p_0) &= \frac{-g}{R_d} \int_{z=0}^{z} \frac{dz}{T(z)} \\
\ln\left(\frac{p(z)}{p_0}\right) &= \frac{-g}{R_d} \int_{z=0}^{z} \frac{dz}{T(z)} \\
p(z) &= p_0 \exp\left[\frac{-g}{R_d} \int_{z=0}^{z} \frac{dz}{T(z)}\right]
\end{aligned}$$

Note that : $\int_a^b \frac{dx}{x} = \ln x \Big|_a^b$ and $\ln a - \ln b = \ln \frac{a}{b}$

Frame 2.6: The vertical pressure distribution.

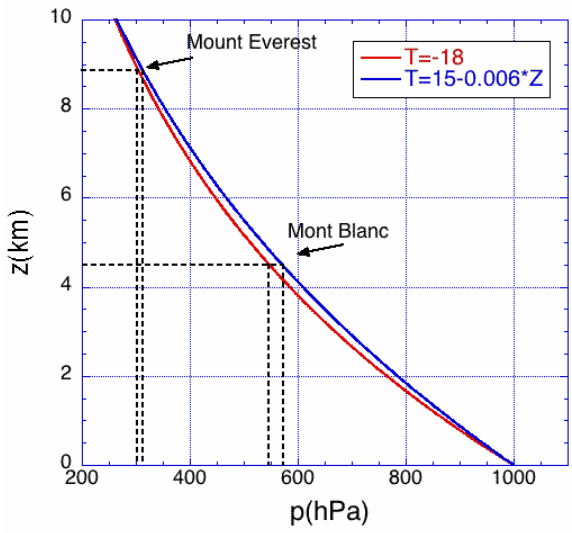

Figure 2.11: Vertical pressure distribution assuming a constant atmospheric temperature of -18°C (red curve) and assuming a surface temperature of 15°C and a constant lapse rate of -0.006 $\mathrm{K\,m^{-1}}$(blue) (see exercises).

There are two general restrictions in the use of the dry-adiabatic lapse rate: 1) no phase changes are allowed that lead to internal heat production or loss, and 2) heat exchange with the surroundings must be small compared to heat loss or gain due to expansion or compression. Therefore, γ_d is only applicable for processes involving fast vertical displacements.

Using the dry-adiabatic lapse rate we can study the static stability of the unsaturated (dry) atmosphere. To do so, we compare the observed atmospheric lapse rate $\gamma = \frac{\delta T}{\delta z}$ with the dry-adiabatic lapse rate of γ_d = -9.81 $\mathrm{K\,km^{-1}}$ of a fictitious air parcel that we move dry-adiabatically up or downwards. We can distinguish three different situations:

Use of the first law of thermodynamics (Eq. 2.8, Frame 2.3) and describe each term in the equation.

dW The work done by a parcel to expand is defined by the force used by the parcel to expand times the distance the parcel expanded, or pressure p times volume change dV. Assume that V is the volume of a unit mass of 1 kg, which is the specific volume α, and is per definition equal to the inverse of the density $\alpha = \rho^{-1}$.

$$dW = pd\alpha = pd\rho^{-1}$$

In the atmosphere $d\alpha$ or $d\rho^{-1}$ is difficult to determine, therefore we express dW in terms of parameters we can easily measure: temperature change dT and pressure change dp. Use the equation of state (Eq. 2.10) for a parcel with unit mass ($p\alpha = R_d T$). Partially differentiate:

$$\alpha dp + pd\alpha = R_d dT$$

and substitution in the above equation for dW results in:

$$dW = pd\alpha = R_d dT - \alpha dp$$

dIE is written in terms of the heat capacity (c_v) of the parcel, which is the amount of energy necessary to change the temperature of the parcel, or the change in internal energy with a change in temperature at constant volume:

$$c_v \equiv \left[\frac{dIE}{dT}\right]_{dV=0}$$

where c_v is the heat capacity at constant volume. Thus, the change in internal energy $d(IE) = c_v dT$. Substitute this, and dW in Eq. 2.8 results in:

$$dQ = c_v dT + R_d dT - \alpha dp = c_p dT - \alpha dp \,, \tag{2.11}$$

where $c_p = c_v + R_d$, the heat capacity of the air parcel at constant pressure (for air: $c_v = 717\,\mathrm{J\,kg^{-1}K^{-1}}$, $c_p = 1004\,\mathrm{J\,kg^{-1}K^{-1}}$).

dQ Assume the process is adiabatic, i.e. there is no heat exchange between parcel and surroundings, $dQ = 0$.

$$0 = c_p dT - \alpha dp \quad \rightarrow \quad \frac{dT}{dp} = \frac{\alpha}{c_p} = \frac{1}{\rho c_p}$$

The dry-adiabatic lapse rate (γ_d) of air is now given by:

$$\gamma_d = \left[\frac{dT}{dz}\right]_{dQ=0} = \left[\frac{dT}{dp}\frac{dp}{dz}\right]_{dQ=0} = -\frac{\rho g}{\rho c_p} = -\frac{g}{c_p} \,.$$

in which we make use of the hydrostatic balance, Eq. 2.10.

Frame 2.7: The dry adiabatic lapse rate.

$\gamma < \gamma_d$ unstable stratification
$\gamma = \gamma_d$ neutral stratification
$\gamma > \gamma_d$ stable stratification

In the stable case a parcel dry-adiabatically forced upwards wants to move back to its original position. In the unstable case a parcel forced upwards will accelerate even further upwards. In this case an air parcel also is able to spontaneously move upwards resulting in convection. In reality this happens mainly when the atmosphere is strongly heated from below so that $|\gamma|$ becomes larger than the dry-adiabatic lapse rate. Finally, in the neutral case, the initial movement will not change. The parcel will move further without being accelerated or decelerated. Figure 2.12 presents an example of a temperature profile and its corresponding lapse rate profile. In the example the observed lapse rate is over almost the complete profile larger than the dry-adiabatic lapse rate indicating stable conditions.

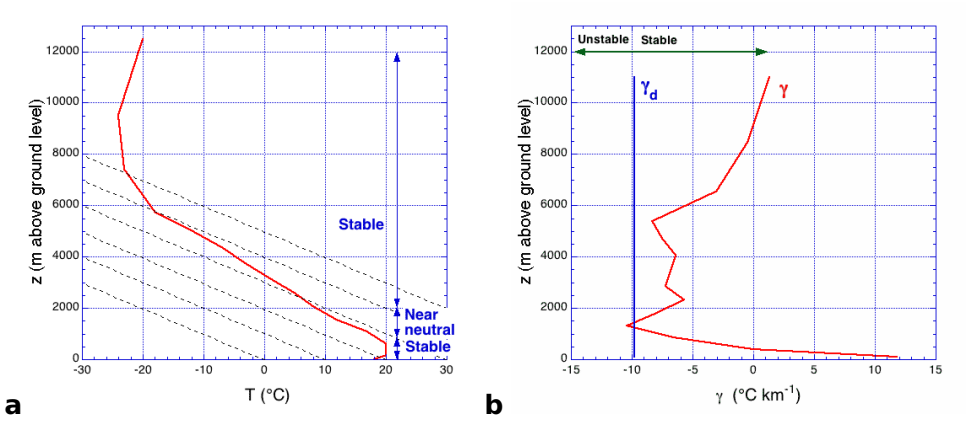

Figure 2.12: a) Temperature profile, and b) profile of the temperature lapse rate of the profile in a).

2.2.5 Potential temperature

We will now introduce a variable that is conserved under adiabatic motion, the potential temperature. The potential temperature θ can also be derived using the first law of thermodynamics (see Frame 2.8) and is defined as:

$$\theta = T\left(\frac{p_0}{p}\right)^{R_d/c_p} . \tag{2.12}$$

This equation calculates the temperature an air parcel would have when brought adiabatically from a location p with temperature T to a reference pressure p_0. p_0 is usually taken to be 1000 hPa or the surface pressure. Furthermore, θ is a conserved quantity for adiabatic processes, as is shown by taking the ratio of θ_1 when brought from p_1 to a reference level, to θ_2 when brought from p_2 to the same reference level:

$$\frac{\theta_1}{\theta_2} = \frac{T_1\left(\frac{p_0}{p_1}\right)^{R_d/c_p}}{T_2\left(\frac{p_0}{p_2}\right)^{R_d/c_p}} = \frac{T_1}{T_2}\left(\frac{p_2}{p_1}\right)^{R_d/c_p} = \left(\frac{p_1}{p_2}\right)^{R_d/c_p}\left(\frac{p_2}{p_1}\right)^{R_d/c_p} = 1 .$$

Because potential temperature is a conserved quantity for adiabatic processes it can be used as an indicator of air masses, because it is insensitive to vertical movements as long as no condensation or evaporation takes place.

The potential temperature can also be used to study the static stability of the atmosphere. The potential temperature lapse rate is defined as: $\gamma_\theta = \frac{\delta\theta}{\delta z}$. For dry-adiabatic movements the potential temperature lapse rate is 0. The static stability using potential

Use the first law of thermodynamics rewritten as Eq. 2.11, assuming adiabatic conditions ($dQ = 0$), and use the equation of state, then the specific volume can be eliminated from Eq. 2.11 resulting in an expression in which temperature and pressure are the only unknown quantities:

$$\frac{c_p}{R_d}\frac{dT}{T} = \frac{dp}{p}$$

Integration of this expression between T_1 at p_1 and T_2 at p_2 gives:

$$\frac{T_2}{T_1} = \left(\frac{p_2}{p_1}\right)^{R_d/c_p}$$

which can be used to define the potential temperature θ, Eq. 2.12.

Frame 2.8: The potential temperature.

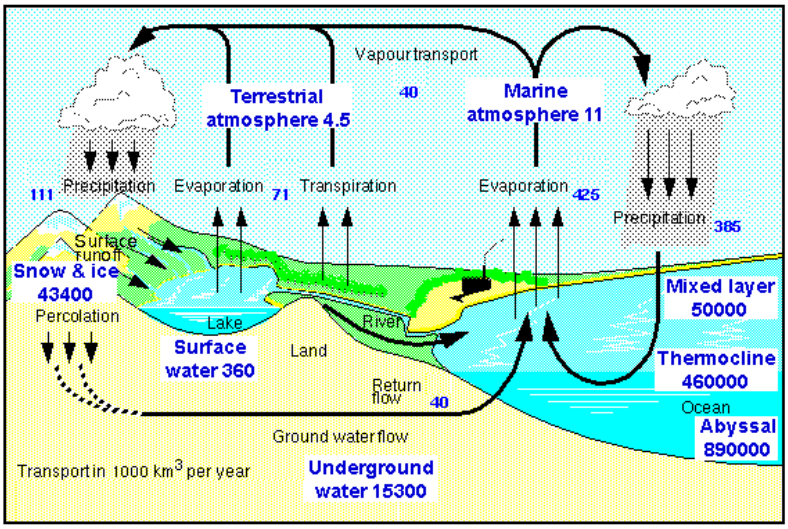

Figure 2.13: Global reservoirs and fluxes of water. Volumes are in $10^3\,m^3$ and fluxes in $10^3\,m^3\,yr^{-1}$.

temperature is then defined similarly to the temperature lapse rate with 3 different cases:

$\gamma_\theta < 0$ unstable stratification
$\gamma_\theta = 0$ neutral stratification
$\gamma_\theta > 0$ stable stratification

The next step is adding moisture to our atmosphere.

2.3 Atmospheric moisture

In the previous section the atmosphere was assumed to be dry. However, the atmosphere is mixture of dry air and water, in solid, liquid and vapour state. The concentration of water in the atmosphere is very variable in space and time, but seldom exceeds several %. Furthermore, compared to the oceans, the atmosphere is only a small water reservoir; only 0.001% of the total amount of water on Earth on average resides in the atmosphere (Figure 2.13). However, moisture in the atmosphere has a big influence on weather and climate through:

- Its ability to absorb shortwave and longwave radiation.
- Its ability to deplete heat through evaporation.
- Its ability to supply heat through condensation (on average 25% of $S_0/4$).
- Its ability to form clouds with their strong radiative properties.
- The transport of moisture and heat from one place to another.

2.3.1 Measures of humidity

There are several parameters that express the amount of moisture in the atmosphere, e.g. water vapor pressure, absolute humidity, mixing ratio, specific humidity and relative humidity. It depends on the application which ones are used.

The **water vapor pressure** (e, in Pa) is the partial atmospheric pressure which is exerted by water vapor. It results from the general fact that from a substance in liquid form, some of the molecules will escape into the vapor phase; evaporation occurs. The partial pressure due to these molecules per cubic metre is known as the vapor pressure, or in case of water, the water vapor pressure. From this follows that water vapor pressure is proportional to the number of water molecules in the atmosphere, and therefore, water vapor

pressure is a possible measure of humidity. Another possible measure of humidity is the **absolute humidity** (ρ_v, in $\mathrm{kg\,m^{-3}}$), which is the mass of water vapor per cubic meter, or the density of the water vapor.

As the other gasses in the atmosphere, water vapor behaves to a good approximation as an ideal gas, and using the definitions for water vapor pressure and absolute humidity, the equation of state for water vapor is defined as:

$$e = \rho_v R_v T \ , \tag{2.13}$$

where R_v is the specific gas constant for water vapor. The value of R_v follows from the specific gas constant for a single gas, which is defined by the universal gas constant divided by the molecular weight (M) of the gas, thus $R_v = R^*/M_{H_2O} \cong 462\,\mathrm{J\,kg^{-1}K^{-1}}$ where M_{H_2O} = 18. Note that since the water vapor is lighter than air (mass number 18 vs. 29), an equal-volume mixture of moist air is lighter than dry air.

The mixing ratio and the specific humidity are very similar measures of humidity. The **mixing ratio** (r, in $\mathrm{g\,kg^{-1}}$) is the ratio of the mass of water vapor to the mass of *dry* air. It can be written as:

$$r = \frac{m_v}{m_d} = \frac{\rho_v}{\rho_d} = \frac{\frac{e}{R_v T}}{\frac{p_d}{R_d T}} = \frac{R_d}{R_v}\frac{e}{p_d} = \varepsilon \frac{e}{p-e}$$

in which m_v is the mass of the water vapor and m_d is the mass of the dry air. Since the volume is the same for both masses, r also equals the ratio of the densities. Substituting the equations of state for water vapor (Eq. 2.13) and dry air (Eq. 2.9) then results in an expression in terms of the vapor pressure and total pressure of the volume, where ε is the ratio of the specific gas constant of dry air to the specific gas constant of water vapor ($\varepsilon = R_d/R_v \approx 0.62$). The **specific humidity** (q, in $\mathrm{g\,kg^{-1}}$) is defined similar to the mixing ratio, as the ratio of the mass of water vapor to the mass of air. It can similarly be written as:

$$q = \frac{m_v}{m_v + m_d} = \frac{m_v}{m_{tot}} = \frac{\rho_v}{\rho} = \frac{\rho_v}{\rho_d + \rho_v} = \frac{\frac{\rho_v}{\rho_d}}{1 + \frac{\rho_v}{\rho_d}} = \frac{r}{1+r} \approx r \ ,$$

in which m_{tot} is the total mass of the air package and ρ the density of the moist air. As a result the specific humidity can be written in terms of the mixing ratio and to a good approximation they are the same. However, we will use the specific humidity because the conservation equations are expressed in it. Note that the specific humidity can also be used in the equation of state for water vapor pressure: $e = \rho_v R_v T = q\rho R_v T$.

Since water vapor behaves to a good approximation as an ideal gas the equation of state for a moist atmosphere can now be derived. The moist atmosphere is a mixture of dry air and water vapor. Following Dalton's law the total pressure is the pressure for dry air plus the pressure for water vapor.

$$\begin{aligned} p = p_d + p_v &= \frac{m_d R_d}{V} T + \frac{m_v R_v}{V} T \\ &= \rho T \left(\frac{m_d R_d + m_v R_v}{m_d + m_v} \right) \\ &= \rho R_{mix} T \end{aligned} \tag{2.14}$$

Note that $\rho = (m_d + m_v)/V$. From this a specific gas constant for moist air can be derived

using the definition of specific humidity q in terms of mass m: $q = m_v/(m_v + m_d)$.

$$\begin{aligned} R_{mix} &= \frac{m_d R_d + m_v R_v}{m_d + m_v} \\ &= R_d \left(1 - q\left(1 - \frac{1}{\varepsilon}\right)\right) \\ &\approx R_d(1 + 0.61q) \end{aligned}$$

Substitution of this result into equation 2.14 gives:

$$p = \rho R_{mix} T = \rho R_d (1 + 0.61q) T = \rho R_d T_v \ ,$$

where $T_v = (1 + 0.61q)T$, the **virtual temperature**. The virtual temperature is a fictitious temperature at which a dry parcel, in the same conditions, would have the same density as the moist parcel. Furthermore, this also shows that the ideal gas law for the moist atmosphere is similar to that for the dry atmosphere if T is replaced by T_v as defined above.

Using the above result, a new expression for the specific humidity can be derived. Apply the ideal gas law to the wet and dry air fraction separately and use the definition of q in terms of density, $q = \rho_v/\rho = \rho_v/(\rho_v + \rho_d)$:

$$\begin{aligned} e &= \rho_v R_v T = \rho q R_v T \\ p_d &= \rho_d R_d T = (1 - q)\rho R_d T \end{aligned}$$

In the next step ρ is eliminated and q isolated:

$$\frac{q}{1-q} = \frac{eR_d}{p_d R_v} = \frac{\varepsilon e}{p_d} \ \rightarrow \ q \cong \frac{\varepsilon e}{p} \tag{2.15}$$

In the last step of this equation two assumptions are made: firstly $1 - q \approx 1$ and secondly $p_d \approx p$. The error this introduces to the estimated q does not exceed a few %. The problem with this expression is that partial water vapor pressure can not be readily measured. Therefore, moisture is often measured relative to saturation by determining e.g. the dew point temperature, the wet-bulb temperature or the relative humidity.

To explain what saturation actually is, consider an air parcel in which vapor molecules collide with each other. Some may stick to form tiny water droplets that are also constantly breaking apart. If enough vapor molecules are present, there may be enough collisions to form a stable population of liquid water droplets: this is called saturation and the vapor pressure at this point is the saturation vapor pressure (e_s). Note that the saying "warm air can hold more water vapor than cold air" is strictly speaking not correct. It is not the air that is holding the water vapor. It therefore does not matter what and if other gases are present, the saturation water vapor pressure would not change.

The above mentioned three parameters are defined as follows. The **dew point temperature** (T_d, in K) is the temperature at which after isobaric cooling (at constant pressure) condensation occurs; e reaches its saturation value e_s and $e(T) = e_s(T_d)$. Note that the specific humidity remains constant during cooling. The dew point temperature is in fact the minimum temperature that can be reached due to longwave radiative cooling. It can be determined by using a cooled mirror. Another temperature based on saturation is the **wet-bulb temperature** (T_w, in K), which is the temperature an air parcel can reach when moisture is added till saturation occurs. In other words, the wet-bulb temperature is the equilibrium temperature of a surface kept wet in a well ventilated environment. The specific humidity now increases to saturation point q_s. A graphic representation of T_d and T_w

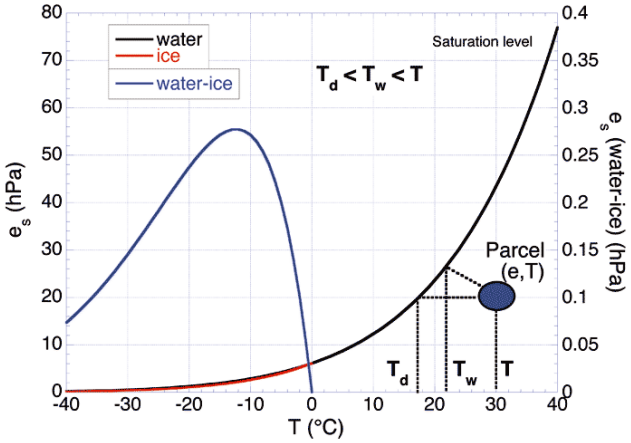

Figure 2.14: Saturated vapor pressure over water, ice and their difference as a function of temperature. Included is a graphic representation of the dew point temperature T_d, the wet-bulb temperature T_w and the absolute temperature of a parcel.

is given in Figure 2.14. Finally, the **relative humidity** (RH, in %) is the ratio of actual vapor pressure to saturation vapor pressure ($e/e_s \times 100\%$). Using the ideal gas law it can also be written as the ratio of vapor density to saturation vapor density ($\rho/\rho_s \times 100\%$) or as the ratio of specific humidity to saturation specific humidity ($q/q_s \times 100\%$). RH can be measured by using changing characteristics of materials.

To determine the actual moisture content from the above parameters knowledge of the saturation vapor pressure is necessary. The Clausius Clapeyron equation relates the saturated vapor pressure (e_s) to the absolute temperature (T). The relation follows from the first law of thermodynamics and the ideal gas law (see Frame 2.9) and reads:

$$e_s = e_0 \exp\left[\frac{L}{R_v}\left(\frac{1}{T_0} - \frac{1}{T}\right)\right] , \tag{2.16}$$

where e_0 is a known saturation vapor pressure e_s at given T_0. The value for e_s at melting point of ice is often taken for e_0 at T_0, $e_0 = 610.78\,\text{Pa}$ at $T_0 = 273.16\,\text{K}$. L is the phase change from state 1 to 2. Values of L for the phase change from ice to water to vapor are:

L_m	ice → water	$3.34\times10^5\,\text{J kg}^{-1}$	melt
L_s	ice → vapor	$2.84\times10^6\,\text{J kg}^{-1}$	sublimation
L_v	water → vapor	$2.51\times10^6\,\text{J kg}^{-1}$	evaporation

The Clausius Clapeyron equation shows that the saturation water vapor pressure e_s (and hence saturation specific humidity q_s) increases sharply with temperature (Figure 2.14). The Figure also shows that there is a significant difference between the saturation vapor pressure over water and over ice, which has implications for the formation of precipitation.

2.3.2 Global distribution of moisture

To explain variations, in specific humidity temperature is the dominating parameter. Figure 2.15a presents the annual average global distribution of the 2 m temperature. It shows very nicely the dependency of T on latitude and altitude, warm near the equator and cold near the poles and at higher elevations. Note also the lower temperatures over the South Pole compared to the North Pole which is due to the fact that the north pole is sea covered by sea ice and surrounded by land, while the south pole is land covered by km thick ice and surrounded by ocean. Figure 2.15b, shows the annual averaged global distribution of the 2 m saturation vapor pressure (e_s), and shows a very similar distribution as Figure 2.15a, high values in the tropics and low values in the polar regions and at high altitudes. This similarity is due to the higher moisture holding capacity of warm air.

Combine the first law of thermodynamics (Eq. 2.8) written as Eq. 2.11, and the ideal gas law for moist air (Eq. 2.13):

$$\begin{aligned} dQ &= c_v dT + p d\alpha \\ e &= \rho_v R_v T \ , \end{aligned}$$

Assume there is no change in internal energy of the parcel, $c_v dT = 0$. Eq. 2.11 reduces to $dQ = pd\alpha$, where in this case p is the vapor pressure e. Substituting the ideal gas law to eliminate vapor pressure and using the derivative of pressure to temperature from the ideal gas law ($de/dT = \rho_v R_v$) to eliminate density, results in:

$$\frac{dQ}{d\alpha} = T\frac{de}{dT}$$

The last step is to consider phase changes from state 1 to 2. dQ is then the heat necessary for the change and equals the latent heat for a phase change from 1 to 2, L_{12}. $d\alpha$ is the difference in specific volumes or densities between the two phases, $\alpha_2 - \alpha_1$. Furthermore, since the phase change occurs at saturated conditions e can be replaced by e_s, the saturated vapor pressure:

$$\frac{de_s}{dT} = \frac{1}{T}\frac{L_{12}}{\alpha_2 - \alpha_1} \cong \frac{L_{12} e_s}{R_v T^2} \ .$$

In the last step, the approximation is made that $\alpha_1 \ll \alpha_2$ and the ideal gas law is used again the remove density or specific volume from the equation. Integration of this expression between a known saturation vapor pressure e_s at given T, written as e_0 at T_0 results in the Clausius Clapeyron equation, Eq. 2.16.

Frame 2.9: The Clausius Clapeyron relation.

Figures 2.15c and d show the actual global moisture distribution in terms of the relative humidity RH and specific humidity q. The desert areas are clearly visible. Although T and e_s are high in these areas RH is extremely low, as well as q. Furthermore, the polar regions are in terms of q the dryest areas on earth, in terms of RH they are relatively wet, which is due to the low temperatures. Clearly the tropics are atmospheric moisture production regions. Part of the moisture is then transported to the poles. Owing to the strong dependence of e_s on T, nearly all water vapor is concentrated in the lowest few km of the troposphere. For example in summer most moisture resides in the lowest 2 km at mid-latitudes and in the lowest km in the polar regions. The distribution of the 2 m specific humidity is therefore very similar to the global distribution of the total precipitable water PW. PW is the vertically integrated water vapor:

$$PW = \int_0^\infty \rho_v dz = \int_0^\infty q\rho dz = \frac{1}{g}\int_0^{p_s} q dp \ .$$

Note that for PW to actual rain out, lifting of the air parcels is necessary. This either occurs by spontaneous convection or by frontal convection.

2.3.3 Stability of the moist atmosphere

The presence of moisture in the atmosphere has its effect on the stability of the atmosphere. It does so in two different ways:
1. Moisture decreases the mean molecular weight of air compared to dry air.
2. Upon condensation, moisture releases heat into the air (latent heat).
Both effects increase the bouyancy of moist air compared to dry air but because the latent heat of condensation L_c (= L_v) is considerable, the second effect is generally more important.

The release of heat during condensation changes the temperature lapse rate in the atmosphere. Consider an unsaturated moist air parcel that rises. It will cool according to the dry adiabatic lapse rate γ_d = -9.8 K km^{-1}. At a certain level the temperature reaches the

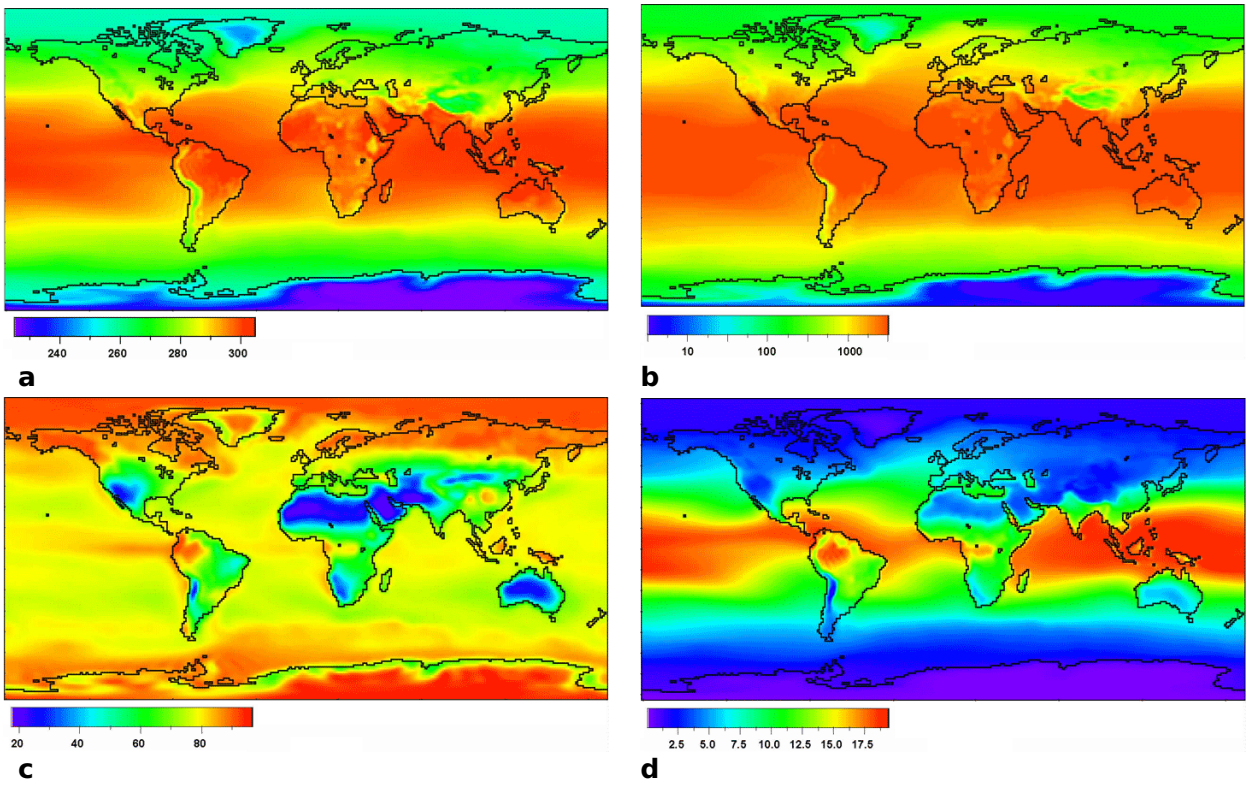

Figure 2.15: a) Annual mean 2 m temperature (in K). b) Annual mean 2 m saturation vapor pressure (in Pa). c) Annual mean 2 m relative humidity (in %). d) Annual mean 2 m specific humidity (in g kg^{-1}).

dew point temperature ($T = T_d$) where saturation ($e = e_s$) and thus condensation occurs. The level where this occurs is the Lifting Condensation Level (LCL). When the parcel is now lifted further the release of heat associated with condensation slows down the cooling of the parcel so that in general the moist (or pseudo) adiabatic lapse rate $\gamma_s > \gamma_d$ or since both lapse rates are negative $|\gamma_s| < |\gamma_d|$. The term pseudo is often used because a small part of the heat released during condensation is removed by rain. However, we will assume, all heat is added to the parcel.

The moist adiabatic lapse rate can be derived similarly to the dry adiabatic lapse rate by using the first law of thermodynamics and adding heat from condensation (Frame 2.10). When neglecting the pressure dependence of the change in saturation specific heat of the parcel (dq_s) we can write:

$$\gamma_s = \gamma_d \left(\frac{1}{1 + \frac{L_c}{c_p} \frac{dq_s}{dT}} \right) .$$

This relation shows that γ_s depends on temperature through dq_s/dT. This also results in γ_s not being constant with height as is γ_d. Furthermore, since $\frac{L_c}{c_p}\frac{dq_s}{dT}$ is larger than zero, $\gamma_s > \gamma_d$ (or $|\gamma_s| < |\gamma_d|$). Finally, γ_s asymptotically approaches γ_d with height because of the decrease of temperature with height in combination with the decrease in pressure becoming important as well.

In terms of the stability of the vertical structure of the atmosphere we can now distinguish three cases:

		γ	$<$	γ_d	absolutely unstable
γ_d	$<$	γ	$<$	γ_s	conditionally unstable
γ_s	$<$	γ			absolutely stable

Combine the first law of thermodynamics (Eq. 2.8) rewritten as Eq. 2.11, with the hydrostatic equation (Eq. 2.10) in the form $-\alpha dp = gdz$. Add heat from condensation to the parcel, $dQ = -L_c dq_s$ where dq_s is the change in saturation specific humidity q_s when heat is added to the parcel.

$$dQ = c_p dT - \alpha dp \quad \rightarrow \quad -L_c dq_s = c_p dT + gdz$$

Now consider dq_s by twice using Eq. 2.15 and partially integrating:

$$dq_s = d\left(\frac{\varepsilon e_s}{p}\right) = \frac{\varepsilon}{p} de_s - \frac{\varepsilon e_s}{p^2} dp = q_s \left(\frac{de_s}{e_s} - \frac{dp}{p}\right)$$

Substitution of the hydrostatic equation in which density is eliminated using the ideal gas law results in:

$$\frac{dp}{p} = -\frac{g}{RT} dz \quad \rightarrow \quad -L_c dq_s = -L_c q_s \left(\frac{de_s}{e_s} + \frac{g}{RT} dz\right)$$

Substitution of this result in the rewritten form of the first law of thermodynamics and solving it for dT/dz results in the moist adiabatic lapse rate γ_s:

$$\begin{aligned}
-L_c dq_s &= c_p dT + gdz \\
-L_c q_s \left(\frac{de_s}{e_s} + \frac{g}{RT} dz\right) &= c_p dT + gdz \\
-\frac{L_c q_s}{e_s} \frac{de_s}{dT} \frac{dT}{dz} - \frac{L_c q_s g}{RT} &= c_p \frac{dT}{dz} + g \\
\frac{dT}{dz} &= -\frac{g}{c_p} \frac{\left(1 + \frac{L_c q_s}{RT}\right)}{\left(1 + \frac{L_c q_s}{c_p e_s} \frac{de_s}{dT}\right)}
\end{aligned}$$

If we neglect the pressure dependence of dq_s we can write:

$$\gamma_s = \frac{dT}{dz} = -\frac{g}{c_p} \left(\frac{1}{1 + \frac{L_c}{c_p} \frac{dq_s}{dT}}\right) = \gamma_d \left(\frac{1}{1 + \frac{L_c}{c_p} \frac{dq_s}{dT}}\right) .$$

Frame 2.10: The moist adiabatic lapse rate.

The addition of the word conditionally refers to that for unstability to occur enough moisture must be present. Figure 2.16 presents a schematic view of these three cases.

When condensation or evaporation occurs in an air parcel and heat is added to or extracted from the parcel, the potential temperature is no longer conserved. The potential temperature is therefore also no longer a sufficient parameter to determine atmospheric static stability. Again we can use the first law of thermodynamics to derive a parameter that is conserved under moist adiabatic motion (Frame 2.11). The result is the **equivalent potential temperature** (θ_e, in K) defined as the temperature of an air parcel when first lifted to the level were saturation occurs, then all water is condensed out, and the parcel is

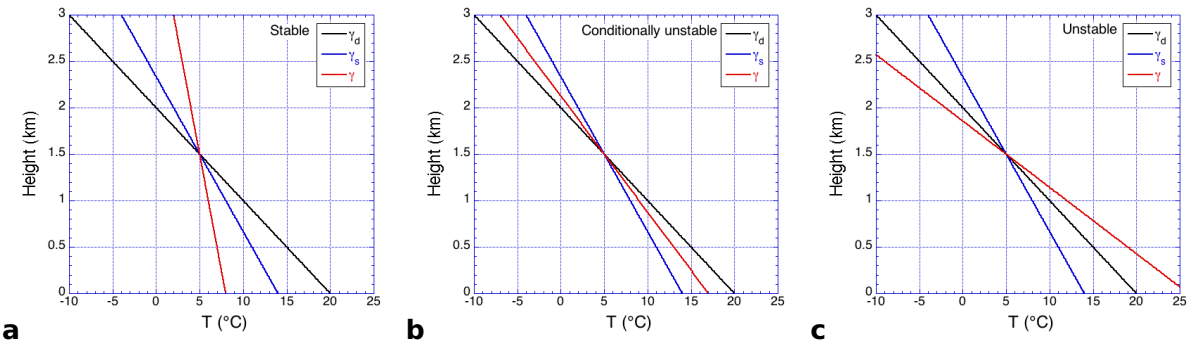

Figure 2.16: Illustration of stability in a moist atmosphere in terms of the dry, moist and actual lapse rate. a) absolutely stable, b) conditionally unstable, and c) absolutely unstable.

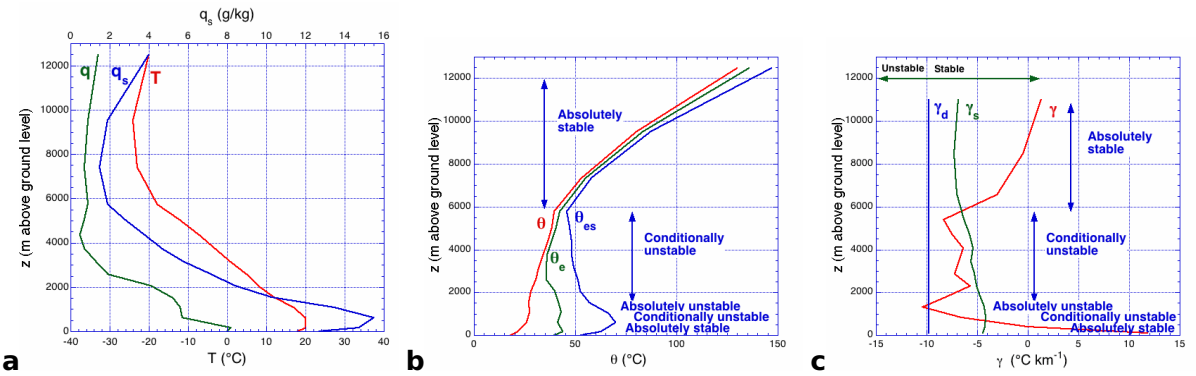

Figure 2.17: a) Measured profile of temperature and corresponding calculated saturation specific humidity. b) Potential en equivalent potential temperature lapse rate. c) Temperature lapse rate.

adiabatically lowered to a reference pressure level:

$$\theta_e = \theta \exp\left(\frac{L_c q_s}{c_p T}\right) = T_e \left(\frac{p_0}{p}\right)^{R_d/c_p} , \tag{2.17}$$

in which T_e is the corresponding equivalent temperature. Note that in this expression T is the temperature at saturation (at LCL). A good approximation of this equation is given by:

$$\theta_e = \theta + \frac{L_c}{c_p} q ,$$

where a Taylor expansion around 0 is taken from the exponent in equation 2.18, assuming the argument in the exponent is small. The equivalent potential temperature is a conserved quantity for moist adiabatic processes. Note that the equivalent potential temperature is always larger than or equal to the potential temperature, the presence of vapor in the atmosphere increases the potential temperature.

The atmospheric static stability can also be expressed in terms of the equivalent potential temperature. Again there are three cases:

$\gamma_{\theta_{e,s}} < 0$ conditionally unstable stratification
$\gamma_{\theta_{e,s}} = 0$ saturated neutral stratification
$\gamma_{\theta_{e,s}} > 0$ conditionally stable stratification

In combination with the potential temperature lapse rate (γ_θ) the stratification is said to be absolutely unstable when γ_θ and γ_{θ_e} are negative and absolute stable when both are positive. The term conditional refers to the fact that the stability or instability is conditional to the saturation of the air parcel.

An example of a vertical profile of temperature and moisture with corresponding lapse rates is plotted in Figure 2.17.

2.4 Aerosols and clouds

Besides air and moisture other particles are suspended in the atmosphere. These particles are called aerosols. They range in size between ~0.001 and 50 μm, and play an important role in the radiation budget of the atmosphere, and in the formation of fog, clouds and precipitation. Aerosols can directly be brought into the atmosphere by e.g. wind erosion, or they can be formed in the atmosphere when e.g. gas particles are changed into solid particles. An overview of the most important aerosols and their size is given in Figure 2.18.

Take the first law of thermodynamics (Eq. 2.8) rewritten as Eq. 2.11, substitute the gas law (Eq. 2.9) and add heat from condensation $dQ = -L_c dq_s$.

$$\begin{aligned} dQ &= c_p dT - \alpha dp \\ -L_c dq_s &= c_p dT - \frac{R_d T}{p} dp \\ -\frac{L_c dq_s}{c_p T} &= \frac{dT}{T} - \frac{R_d}{c_p}\frac{dp}{p} \\ -\frac{L_c dq_s}{c_p T} &= d\ln T - \frac{R_d}{c_p} d\ln p \end{aligned}$$

Substitute the total derivative of the potential temperature in the above result:

$$\theta = T\left(\frac{p_0}{p}\right)^{R_d/c_p} \quad \rightarrow \quad d\ln\theta = d\ln T - \frac{R_d}{c_p} d\ln p \ ,$$

results in an expression that gives the potential temperature change in a saturated displacement:

$$d\ln\theta = \frac{dQ}{c_p T} = -\frac{L_c dq_s}{c_p T} \ . \tag{2.18}$$

Now condensate all water vapor out by lifting the parcel to the level were saturation occurs, and then lower the parcel adiabatically to a reference pressure level:

$$\begin{aligned} \int_{\theta}^{\theta_e} d\ln\theta &= -\frac{L_c}{c_p T}\int_{q_s}^{0} \\ \ln\theta_e - \ln\theta &= -\frac{L_c}{c_p T}(0 - q_s) \\ \ln\frac{\theta_e}{\theta} &= \frac{L_c q_s}{c_p T} \\ \frac{\theta_e}{\theta} &= \exp\left(\frac{L_c q_s}{c_p T}\right) \\ \theta_e &= \theta\exp\left(\frac{L_c q_s}{c_p T}\right) \\ &= T\exp\left(\frac{L_c q_s}{c_p T}\right)\left(\frac{p_0}{p}\right)^{R_d/c_p} \\ &= T_e\left(\frac{p_0}{p}\right)^{R_d/c_p} \end{aligned}$$

where θ_e is the equivalent potential temperature and T_e is the equivalent temperature.

Frame 2.11: The equivalent potential temperature.

2.4.1 Characteristics

Aerosols can be classified based on their size or origin. Based on their origin the following classification can be made:

Continental aerosols are aerosols produced over the continents. They are generally small and can be found in large numbers. Especially in cities and industrialized areas the number of particles can be orders of magnitude larger than the natural concentration. Examples are crustal species which enter the atmosphere through erosion processes of the Earth's surface. They are mainly produced in subtropical deserts in the USA and Asia and mainly consist of silicates and clay particles of a relatively large radius. Furthermore, combustion and secondary products related to anthropogenic activities. Main production areas of these industrial particles are the industrialized regions of Europe and USA and the main type of aerosol produced is SO_2 (acid rain) which has a small radius. And finally, carbon dioxide, a product of forest fires and agricultural burning in the tropics.

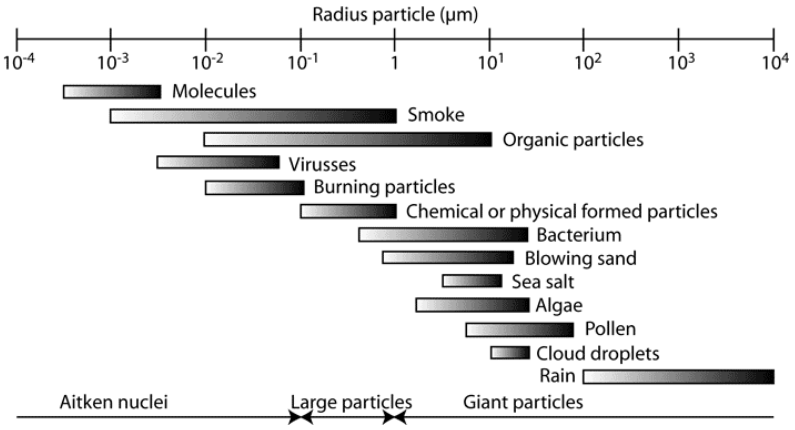

Figure 2.18: Different type of aerosols and their average sizes. Molecules and rain droplets are also included in this spectrum for comparison.

Marine aerosols are aerosols produced over the ocean, mainly sea salt produced from bursting ocean bubbles. These particles have generally a reasonable large radius but are less numerous than continental aerosols.

Volcanic/stratospheric aerosols are aerosols that are found at higher altitude, in the stratosphere, and are produced by volcanic eruptions and chemical processes.

The naturally formed particles, such as blown sand or sea salt can be found in the higher part of the particle size spectrum, while industrial formed particles are mainly found in the lower end of the spectrum. Particles produced by the biosphere over the continents can be found in all sizes. The smallest particles, radius $r < 0.1\,\mu$m are named Aitken nuclei, $0.1\,\mu\text{m} < r < 1\,\mu$m are large particles and $r > 1\,\mu$m are giant particles.

The residence time of particles in the atmosphere very much depends on their size and altitude above the surface. For the larger aerosols, their own fall speed is important, this process is called dry deposition, while for smaller particles the formation of rain droplets and collision with other droplets are the most important processes for the removal of particles from the atmosphere. The stability of the atmosphere also plays a role in the residence time of aerosols. The larger the stability, the longer the residence time, and values up to years are possible.

Figure 2.19 presents a normalized distribution of the number of particles, their volume and their surface area. Although the maximum of the number of particles is at small particle radius, the largest impact on the radiation budget in the atmosphere and droplet formation is from particles with radius around $0.1\,\mu$m, where the maximum in volume and surface area lies. The particle distribution varies over the continent and over the oceans and with altitude. Concentrations vary from $10^3\,\text{cm}^{-3}$ over the oceans to $> 10^5\,\text{cm}^{-3}$ over industri-

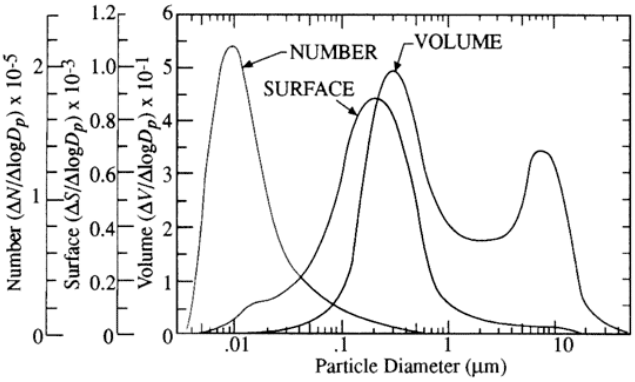

Figure 2.19: Normalized spectra of number, surface and volume of tropospheric aerosols.

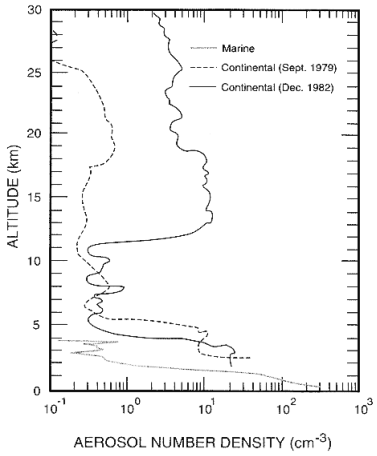

Figure 2.20: Vertical distribution of aerosol concentration over a ocean area, a continental area before and after the eruption of El Chicon (Mexico, 1982).

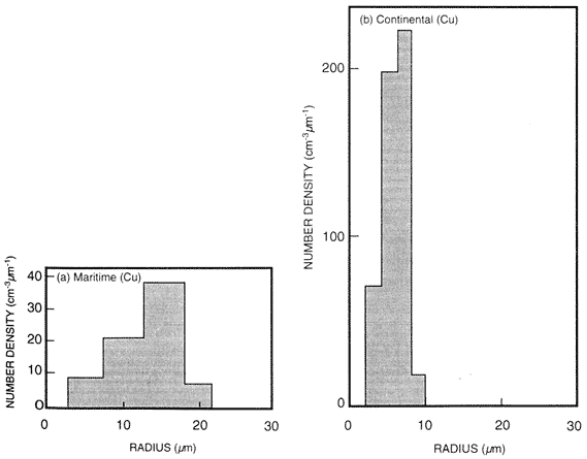

Figure 2.21: Cloud droplets number density in a cumulus cloud as a function of droplet radius over a) the ocean and b) the continent.

alized areas. Over the oceans most aerosols are found in the lower few km, while over the continent aerosols are also found in the stratosphere.

Figure 2.20 presents the vertical distribution of aerosols over the ocean and over the continent. The profile over the continent is taken over Mexico. To illustrate the effect of a volcanic eruption on aerosol concentrations a profile taken before and after the eruption of El Chicon in 1982 is presented. Especially the aerosol concentration in the stratosphere is increased.

Aerosols act as a surface for condensation and the size of the developed water droplet depends among others on the abundance of aerosols in the atmosphere. The larger the amount of aerosols the more cloud droplets are formed and the smaller these droplets are. Figure 2.21 presents the number of cloud droplets as a function of droplet radius in a cumulus cloud over the ocean and over the continent. It shows clearly how the scarcity of aerosols in the atmosphere over the ocean results in larger size but smaller number cloud droplets.

The effect of stratospheric aerosols on climate is twofold, it affects the shortwave and the longwave radiation flux. Aerosols scatter solar radiation. As a result the path length of photons through the atmosphere increases, increasing the chance of absorption. In regions of a low surface albedo (<0.3) aerosols tend to enhance atmospheric reflectivity while in regions of high surface albedo the dominating effect is absorption due to multiple scattering of photons. The impact of aerosols on radiation is radius dependent. Marine aerosols, which are relatively large, mainly scatter solar light while carbon, a smaller continental aerosol, mainly absorbs light. Note that all aerosols attenuate light. The effect on climate is a cooling below the layer with increased aerosol content and a warming above. Aerosols absorb longwave radiation and an increase in atmospheric aerosol content therefore increases temperature. To summarize, aerosols reflect or absorb radiation depending on size of the aerosols and wavelength of the radiation. The cooling effect due to reflection of shortwave radiation is dominant for smaller particles, the warming effect due to absorption of longwave radiation is dominant for larger particles with a critical radius marking the transition point. The critical radius is $\sim 2.3\,\mu$m.

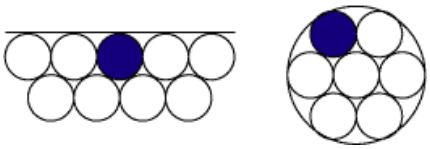

Figure 2.22: Illustration of the difference between e_s over a flat surface and a droplet.

2.4.2 Cloud formation

Water droplets can be viewed as a type of aerosol but are generally considered separately from other aerosols, and are also called hydrometeors. There are several processes that cause droplets to grow; homogeneous nucleation, heterogeneous nucleation and by collision.

Homogeneous nucleation describes cloud droplet growth on a cluster of water molecules. Such a cluster of water molecules form by chance collisions of water molecules. A typical size of such a cluster is 0.6×10^{-9} m. Growth then takes place by condensation for which the air must be supersaturated with water vapor. Supersaturation occurs when the air is saturated with moisture, with e_s larger than saturation over a flat surface. The saturation vapor pressure e_s is defined with respect to a flat surface. However, it is easier for a water molecule to escape a surface when the surface is curved, as in a droplet (Figure 2.22). The vapor pressure then necessary to maintain a curved surface or result in condensation on the surface must be larger than the vapor pressure for a flat surface, and the term supersaturation is used. The amount of supersaturation necessary for condensation depends on the size of the particles due to this curvature effect. The smaller the particle or droplet the larger the equilibrium supersaturation necessary for condensation to occur. The effect of curvature of a surface on the saturation vapor pressure e_s over that surface is described as follows:

$$\ln\left(\frac{e_{s,r}}{e_{s,\infty}}\right) = \left(\frac{2\gamma}{R_v\rho_w T}\right)\frac{1}{r}\,, \tag{2.19}$$

where γ is the surface tension ($\approx 0.075\,\mathrm{Nm}^{-1}$) and r is the droplet radius. It describes the larger e_s over a curved water surface compared to a flat surface. The equation is illustrated in Figure 2.23a. The curve describes an unstable equilibrium and can therefore not be maintained. It also shows the higher equilibrium supersaturation necessary for smaller droplets and that the curvature effect becomes small for larger droplets ($r > 1\mu$m). For a typical water molecule cluster size of $r = 0.6\times10^{-9}$ m a supersaturation of 700% is needed for condensation and growth to occur. Supersaturation exceeding 101% is seldom observed in the atmosphere and therefore homogeneous nucleation cannot explain initial cloud droplet formation.

Cloud droplets generally form due to heterogeneous nucleation in which aerosols act as a condensation nuclei for water vapor (Cloud Condensation Nuclei, CCN). The larger the nucleus, the lower the equilibrium supersaturation, and the more droplet growth by condensation is favored. Conditions for further growth are then equal to the homogeneous nucleation case, although growth is more likely because larger particles activate sooner than smaller.

An even more effective process is condensation on hygroscopic particles like sea salt (NaCl) or ammonium sulfate ($(NH_4)_2SO_4$). Hygroscopic particles absorb moisture and readily dissolve. The dissolved substance (solute) then lowers e_s of water vapor, the solute effect, because e_s is proportional to the absolute concentration of water molecules on the surface of the droplet. Therefore, a droplet containing salt favors condensation more than a

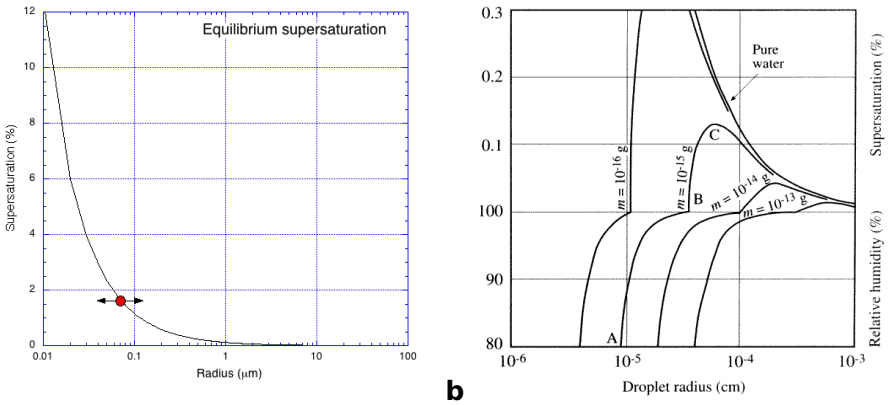

a **b**

Figure 2.23: a) Equilibrium supersaturation ε_c in % as a function of droplet radius ($\varepsilon_c = 100 * ((e_{s,r}/e_{s,\infty}) - 1.)$). Based on equation 2.19, pure water, for $T = 8°C$. b) Equilibrium supersaturation for solutions containing specific amounts of solute, Köhler curves.

pure water droplet of the same size. The equilibrium supersaturation curves resulting from solutions with specific amounts of solute are described by Köhler curves (Figure 2.23b). The curves describe how a droplet, which developes on a soluble nucleus, evolves along the curve corresponding to the fixed mass of that soluble. The presence of the soluble sharply reduces the equilibrium supersaturation and can eventually become negative, i.e. droplet formation below $RH = 100\%$.

The nature (stable or unstable) of the equilibrium depends on whether the radius is smaller or larger than a critical radius r_c. In the case $r < r_c$ (path A-C in Figure 2.23b) the equilibrium is stable. In this case adding (removing) a water molecule will drive the droplet to higher (lower) equilibrium supersaturation, so that forced evaporation (condensation) occurs until the particle has its original size. An example of this process is the formation of haze. In haze the droplets grow to a size dictated by the environmental humidity, but not larger. In maritime haze the availability of salt nuclei is necessary while continental haze developes through pollutants. In case $r > r_c$ the equilibrium is unstable. Adding (removing) a water molecule in this case drives a droplet to lower (higher) equilibrium supersaturation, so that forced condensation (evaporation) drives the droplet to even greater (smaller) size. This case is equivalent to pure water, but without the presence of a critical radius. In the growing branch, these droplets can grow into cloud droplets, and are said to be activated. The effect becomes weaker for larger radius when the curved surface approaches a plane surface. As a result the droplet population becomes more and more homogeneous.

The process of condensation is, however, too slow for droplets to reach precipitation size. When $r >\sim 20\,\mu$m collision takes over as the main growth mechanism. Growth by collision is a strongly non-linear process, it increases with increasing droplet size and fall speed. This favors the growth of only the larger droplets, and as a result the spectrum of condensation droplets broadens. The speed of growth depends on the size of the colliding droplets. Figure 2.24 illustrates the difference in growth rate between the process of condensation and collision.

Owing to the altitude of clouds, temperatures below 0°C often occur in clouds. Cold clouds are defined as clouds situated (in part) in altitude above the freezing level in the atmosphere, while warm clouds are situated totally below the freezing level. Homogeneous nucleation can also occur for ice but only occurs below -35°C to -40°C, which is only in very high clouds. At higher temperatures the formation of ice crystals indicate the presence of ice or freezing nuclei. An ice or freezing nucleus is a particle on which super cooled water

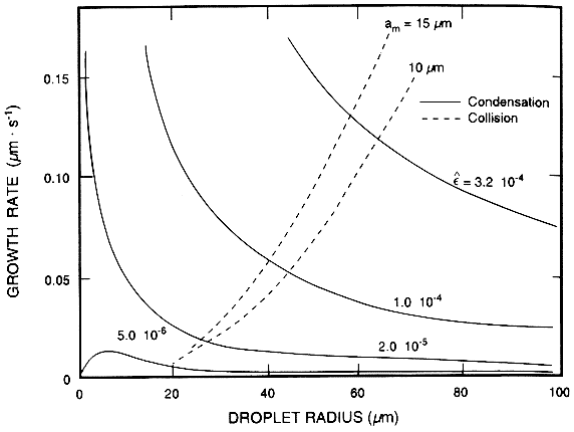

Figure 2.24: Droplet growth rate as a function of droplet radius for the process of condensation and collision.

vapor can freeze when temperatures are above -35°C. At which temperature the ice particle will grow depends on the type of freezing nucleus, i.e. its crystal structure. The more the freezing nucleus resembles ice, the higher the temperature for possible ice particle growth.

Most clouds are mixed water and ice clouds. Clouds that are saturated with respect to water are supersaturated with respect to ice (see the Clausius Clapeyron relation, Figure 2.14). As a result, growth through deposition is accelerated when the particle is frozen. This process, called the Bergeron process, is most effective in clouds between -10°C and -30°C, and can result in large ice crystals. Other processes for ice crystal growth are aggregation, which is the attachment of supercooled water films to the particle. This is an effective process between -0°C and -10°C. Furthermore riming or accretion which is the freezing of supercooled droplets on the ice particle upon impact. Owing to the reasonably large effective radius of an ice crystals this can be an effective process. Because of the effectiveness of ice crystal growth precipitation generally starts as ice crystals and clouds that produce large amounts of precipitation generally have a large vertical depth. An extreme example of accretion is the formation of hail for which very strong updraughts in the cloud are necessary.

When ice particles fall through the 0°C level they will start to melt. This takes some time, few minutes, and wet snow can be found at temperatures as high as 0°C. Often the 0°C level will drop after precipitation has started owing to the evaporation of droplets in dryer air below the cloud.

2.4.3 Cloud classification

Most clouds form through vertical motion, either forced or spontaneous, so that air can reach the lifting condensation level (LCL). Clouds can be classified according to their microscopic or macroscopic properties. A microscopic property is e.g. the contents type in combination with temperature: ice clouds, which are cold, below -40°C, mixed clouds, with temperatures between -40°C and 0°C, and water or warm clouds with temperatures above 0°C. Macroscopic quantities of clouds are e.g. height of the cloud base, vertical depth of the cloud and horizontal size. In terms of vertical depth a distinction is made between layered and piled clouds. In terms of altitude a distinction is made between low, mid and high level clouds. Layered or stratiform clouds form in a locally stable environment, forcing the clouds to spread horizontally. Another process in which stratiform clouds are formed is through surface or radiational cooling, e.g. fog. Piled or cumuliform clouds form in a locally unstable environment through heating at the surface or at certain level in the atmo-

Table 2.2: Cloud classification.

Level	Name	Contents
Low level	fog	water
(< 2500 m)	(S) Stratus	water
	(Ns) Nimbostratus	mixed
	(Sc) Stratocumulus	water
Mid level	(Ac) Altocumulus	water
(2500 - 6000 m)	(As) Altostratus	ice
High level	(Ci) Cirrus	ice
(> 6000 m)	(Cs) Cirrostratus	ice
	(Cc) Cirrocumulus	ice
Troposphere	(Cu) Cumulus	mixed
(Piled)	(Cb) Cumulonimbus	ice

sphere. Stratiform and cumuliform clouds occur at all levels. Cirriform (fibrous) clouds are thin high level clouds. The main families of clouds are presented in Table 2.2. The addition Alto refers to mid level, the addition Nimbo to precipitation bearing. Per family subdivisions are possible.

2.4.4 Precipitation

For the development of precipitation in clouds the atmosphere must satisfy by the following conditions: the atmosphere must be conditional or absolutely unstable, the unstable layer must be of significant depth and freezing nuclei must be available. Several types of showers can then be distinguished. Warm weather showers, which develope when the boundary layer is strongly heated. They mainly develope in spring and summer and time of formation is generally late in the afternoon. Showers can also develope in cold air masses. The instability is then caused by the advection of cold air at higher altitudes. Showers in cold front and squall-lines are also of this type. Furthermore, the showers in cold fronts and squall-lines often form in lines ordered perpendicular to the flow direction. The most severe storms occur in situations where the wind increases significantly with altitude. In such situations the precipitation is prevented from falling into the updraught, which would limit the strength of the storm.

Large scale precipitation is driven mainly by heating from below or advection of cold air at higher altitudes, and by forced rising of air along a front or due to orography. In the case of heating or cold air advection the precipitation is more intermediate in nature compared to frontal rain. Orographic precipitation is clearly visible in the higher average precipitation values at the outer chains of mountain ranges. The occurrence of föhn like winds is related to orographic precipitation, where through the release of latent heat the temperature at the luff side of the mountain rang is higher than at the lee side.

2.4.5 Brunt Väisälä frequency

A special type of clouds is Altocumulus lenticularis. This type of clouds is caused by wave trains around the lifting condensation level (LCL) in a stable atmosphere. In a stably stratified atmosphere the lapse rate $\gamma > \gamma_d$ and potential temperature θ increases with height. Adiabatic oscillations of an air parcel about its equilibrium level in a stably stratified atmosphere are referred to as bouyancy oscillations. The (angular) frequency of such oscillations

Consider the balance of forces of a parcel displaced vertically over a small distance δz without disturbing the environment (see Figure):

$$m\frac{d^2z}{dt^2} = pdA - (p+dp)dA - mg \ ,$$

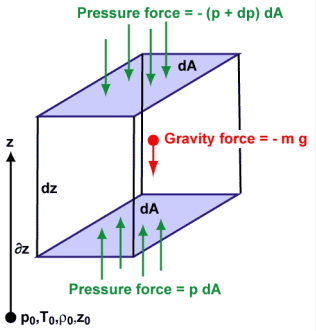

where p and m refer to the parcel. This expression is similar to the hydrostatic balance in section 2.2.3, but including vertical acceleration (d^2z/dt^2). Substitute $m = \rho dV = \rho dz dA$:

$$\begin{aligned} \rho dz dA\frac{d^2z}{dt^2} &= pdA - pdA + dpdA - \rho dz dA g \\ \rho\frac{d^2z}{dt^2} &= -\rho g - \frac{dp}{dz} \ . \end{aligned}$$

Assume that the atmosphere is in hydrostatic balance:

$$\frac{d\overline{p}}{dz} = -\overline{\rho}g \ ,$$

with $\overline{p}$ and $\overline{\rho}$ the environmental pressure and density. Assume that the parcel instantaneously adjusts to the environmental pressure during the displacement, $p = \overline{p}$. Then pressure can be eliminated from the equation:

$$\begin{aligned} \rho\frac{d^2z}{dt^2} &= -\rho g + \overline{\rho}g \\ \frac{d^2z}{dt^2} &= g\frac{\overline{\rho}-\rho}{\rho} = g\frac{T-\overline{T}}{\overline{T}} \ . \end{aligned}$$

In the last step the gas law is used to replace ρ by T. If the parcel is now displaced from location z_0 with p_0, T_0 and ρ_0 over distance dz, the temperature of the parcel can be expressed as $T(z) = T_0 + \gamma_d dz$ and the environmental temperature as $\overline{T}(z) = T_0 + \gamma dz$. Substitution in the above equation results in:

$$\frac{d^2z}{dt^2} = \frac{g}{T_0}\frac{(\gamma_d - \gamma)dz}{\left(1+\frac{\gamma dz}{T_0}\right)} = \frac{g}{T_0}(\gamma_d - \gamma)dz \ .$$

In the last step the assumption is made that $\gamma dz/T_0$ is very small. It can be shown (exercise) that:

$$\frac{T}{\theta}\frac{d\theta}{dz} = \gamma - \gamma_d \ .$$

Substitution then results in an harmonic oscillator:

$$\frac{d^2z}{dt^2} = -\frac{g}{\theta_0}\frac{d\theta}{dz}dz \ ,$$

with (angular) frequency $(g/\theta_0)(d\theta/dz) = N^2$ the square of the Bouyancy or Brunt Väisälä frequency, Eq. 2.20.

Frame 2.12: The Brunt Väisälä frequency.

is given by the Bouyancy or Brunt Väisälä frequency N (see Frame 2.12):

$$N^2 = \frac{g}{\theta_0}\frac{d\theta}{dz} \ , \tag{2.20}$$

derived in Frame 2.12. In the case $N^2 > 0$, i.e. the potential temperature increases with height, the parcel will oscillate about its initial level with a period $\tau = 2\pi/N$. In average tropospheric conditions $N \approx 1.2\times10^{-2}\,\mathrm{s}^{-1}$. In the case $N = 0$, no acceleration force exists and the parcel will be in neutral equilibrium at its new level. In case $N^2 < 0$, i.e. the potential temperature decreases with height, the displacement will increase exponentially in time. Note that the definition of N presents the familiar static stability criteria for dry air.

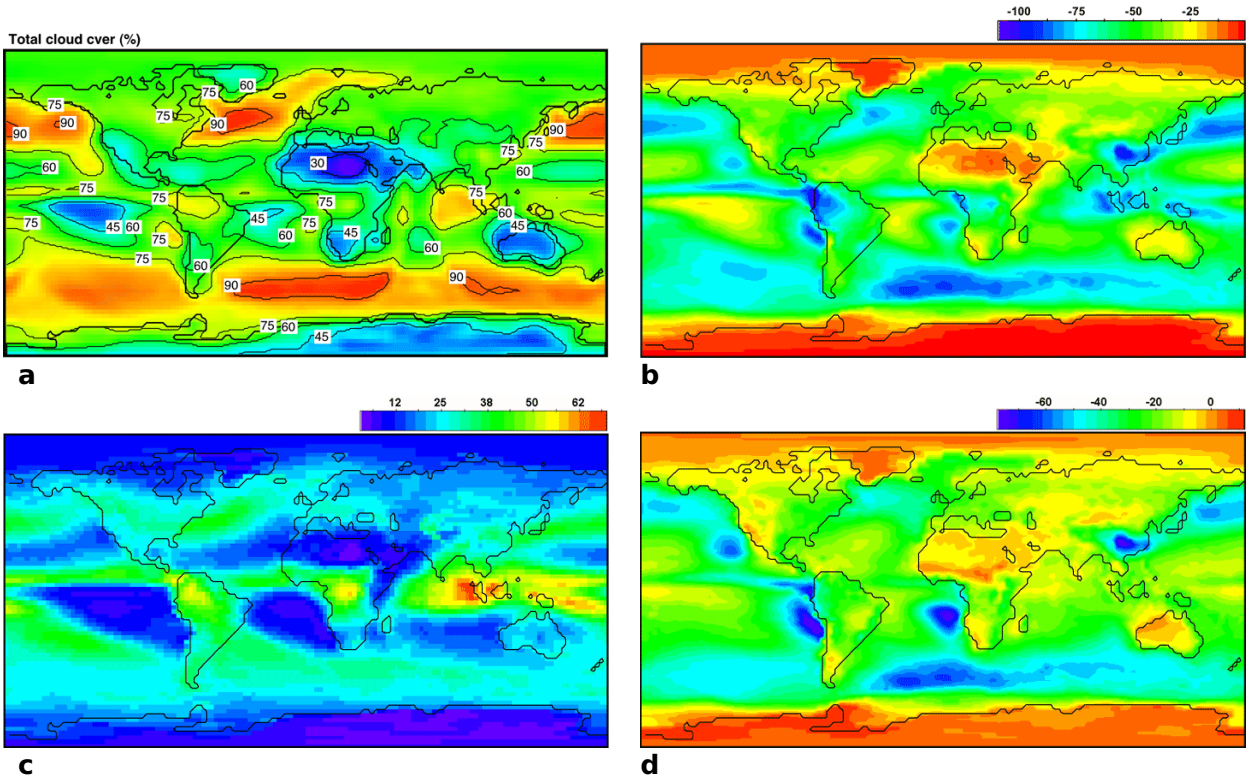

Figure 2.25: a) Annual mean cloud cover (in %). Annual mean effect of clouds on top of the atmosphere b) net shortwave radiation c) net longwave radiation, and d) net radiation, expressed as the difference between the case with and without clouds (in $\mathrm{W\,m^{-2}}$, cloud minus clear sky, fluxes towards the surface are defined positive).

2.4.6 Clouds and radiation

In section 2.4.1 the effect of aerosols on radiation is discussed. Clouds also have a significant impact on the radiation budget of the atmosphere. This impact is illustrated in Figure 2.25. The Figure shows that cloud cover reduces the top of the atmosphere net shortwave radiation with respect to clear sky conditions Figure 2.25b. In other words, clouds increase the amount of shortwave radiation reflected, i.e. the planetary albedo increases. Top of the atmosphere net longwave radiation increases, is less negative, in the presence of cloud cover. This is due to the fact that clouds reduce the radiation temperature of the total Earth atmosphere system. The net effect on the top of the atmosphere radiation budget is an increase in net radiation over areas with small values of cloud cover, the longwave radiation effect dominates, while in areas with large cloud cover the shortwave budget dominates and net radiation is reduced.

The role of clouds in the shortwave radiation flux is schematically illustrated in Figure 2.26a. Shortwave radiation is mainly scattered by cloud particles, only little absorption takes place. The scattering of cloud particles is Mie type of scattering. Mie scattering is scattering of radiation by particles whose size are comparable to or larger than the wave length of the radiation. Scattering then mainly occurs in the forward direction. The total effect of clouds on radiation then depends on cloud type, i.e. thickness, droplet spectrum, ice/water content, sun angle. The main effect, however, is the increase in planetary albedo due to the backscattering. In this illustration the cloud albedo is 0.68 and $52\,\mathrm{W\,m^{-2}}$ is absorbed by the cloud. The surface in this case is sea surface with a surface albedo of less than 0.1. Since not much radiation is reflected by the surface, heating by shortwave

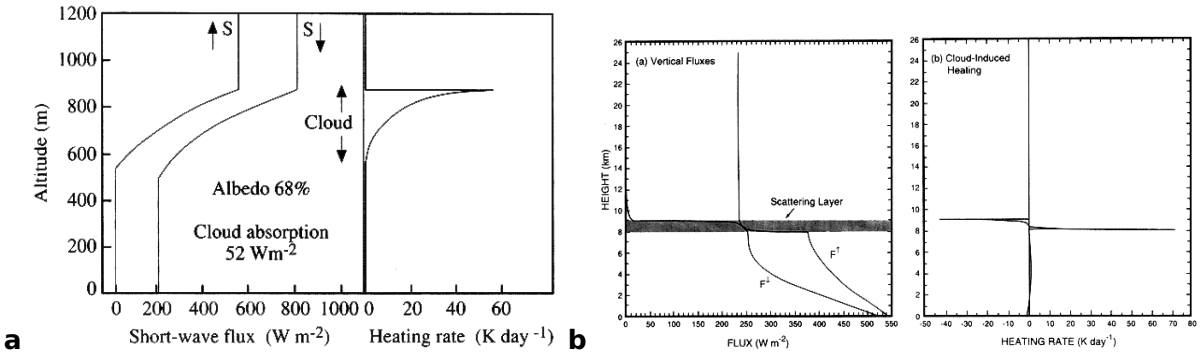

Figure 2.26: Vertical profiles of a) shortwave and b) longwave radiation including vertical profiles of the heating rates due to absorption of the type of radiation plotted.

radiation mainly occurs at the top of the cloud layer.

Clouds consist of water vapor and water vapor is a very efficient absorber of longwave radiation. Figure 2.26b illustrates the effect of clouds on the vertical distribution of longwave radiation fluxes in the atmosphere. Clouds very efficiently absorb the longwave radiation emitted by the Earth surface. They then transmit longwave radiation both up and downwards. The clouds emit more longwave radiation than they absorb, the clouds cool, especially at the top of the cloud where incoming longwave radiation is minimal.

2.5 Temperature and radiation in the clear atmosphere

2.5.1 The vertical structure of the atmosphere

The total atmosphere extends to ~32,000 km above the Earth surface. There are several different criteria that can be used to divide the atmosphere in different regimes e.g. temperature and composition (Figure 2.27a). The layer definitions given in section 2.2 are based on the atmospheric temperature structure and can be seen as a subdivision of the different layers defined based on composition. Based on composition the atmosphere is divided in the homosphere, heterosphere and exosphere.

The exosphere

The exosphere is the uppermost part of the atmosphere, ranging from ~500 km above the surface to ~32,000 km. The base of the exosphere is called the exobase or the critical level of escape. At this level a particle that moves rapidly upward will have a probability of $1/e$ of colliding with another particle on its way out of the atmosphere. The altitude of this level strongly depends on the temperature and ranges between ~500 and 1000 km. In the exosphere the molecular collisions are so rare that molecules can move out into space if their velocity exceeds the escape velocity. The escape velocity is the minimum speed a particle must have in order to escape the Earth's gravitational attraction. The gravitational force exerted by the Earth with mass M on a particle with mass m equals:

$$F_g = \frac{GMm}{r^2} = mg_0\frac{r_E^2}{r^2},$$

where G is the gravitational constant (6.673×10^{-11} N m^2 kg^{-2}) and r the distance between the centers of the two elements. In the second step the acceleration due to gravity at the

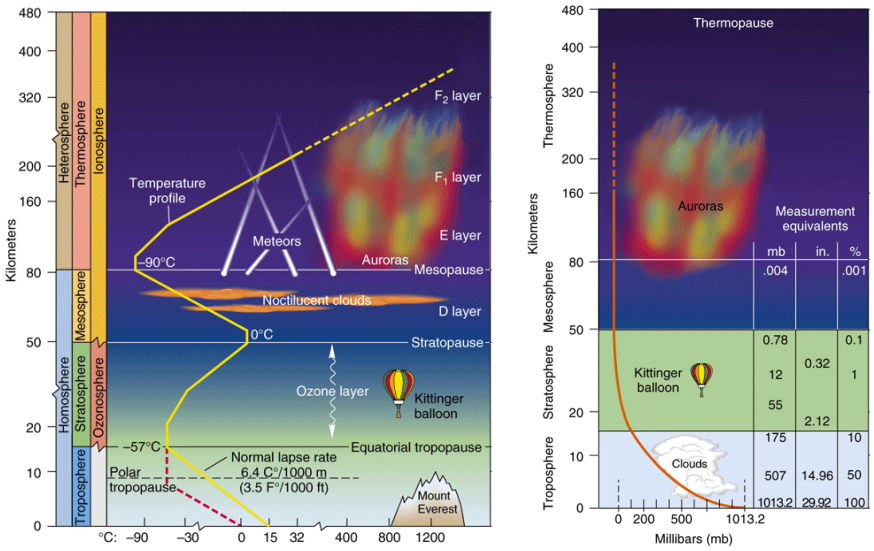

a **b**

Figure 2.27: Vertical structure of the atmosphere illustrating a) the different regions based on composition, temperature and function, respectively, the average temperature profile and the occurrence of certain phenomena at different altitudes, and b) the vertical pressure distribution.

Earth's surface $g_0 = F_g/m = GM/r_E^2 \approx 9.81\,\mathrm{m\,s^{-2}}$ is substituted, where r_E is the radius of the Earth (6.37×10^6 m). To escape the Earth's gravitational field the parcel must have greater energy than its gravitational binding energy:

$$\frac{1}{2}mv_e^2 = \int_{r_E}^{\infty} mg_0 \left(\frac{r_E}{r}\right)^2 dr\,,$$

where the left hand side of the equation is the kinetic energy of the parcel and the right hand side the graviational binding energy. This defines the escape velocity:

$$v_e = \sqrt{2g_0 r_E} \approx 11.2\ \mathrm{km\,s^{-1}}\,,$$

which is independent of the molecular mass.

The temperature at the critical level of escape is under normal conditions ∼1000 K but can fluctuate considerable due to changes in solar and geomagnetic activity, increasing temperature up to 2000 K under disturbed conditions. The speed of the molecules depend on the temperature and their mass. As a result the heavier species (like O) are contained by the Earth's gravitational field, while lighter species (like H) can escape quite easily and are therefore absent in the Earth's atmosphere, despite continual production by photodissociation of H_2O. Figure 2.28 illustrates the velocity distributions of O and H including the escape velocity.

In the exosphere less than 0.001% of the total air mass resides. Air pressure is less than 0.004 hPa and goes to 0 hPa (Figure 2.27b). Of the different type of molecules in the air, the lighter species are most abundant, and the air mainly constitutes of He and H.

The vertical variation of the atmospheric constituents is determined by two processes: molecular diffusion or gravitational settling, and turbulent diffusion by eddies (whirls) in the air. The molecular diffusion is defined by the product of molecule velocity and mean free path, which is the distance travelled by molecules without collision (10^{-7} m at surface, 1 m at 100 km). It depends on pressure, temperature and molecular mass. In the absence of external mixing the hydrostatic equation would describe the partial pressure profile for

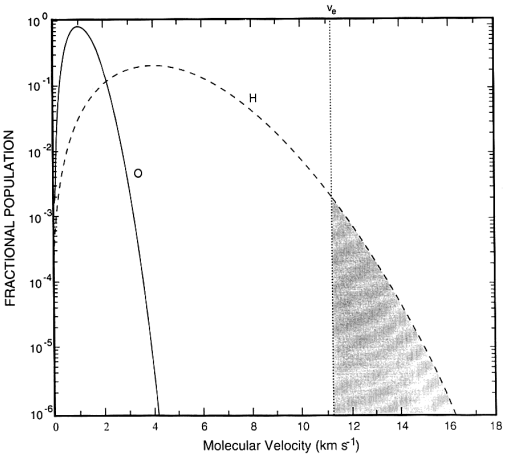

Figure 2.28: Velocity distribution of oxygen (O) and hydrogen (H) for a temperature of 1000 K. The fractional population is the fraction of the total population of a certain molecule having the same velocity.

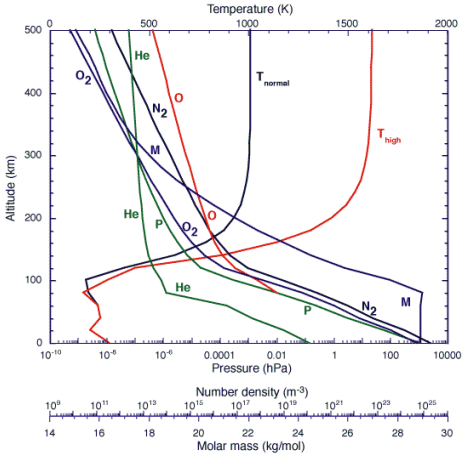

Figure 2.29: Vertical profiles of temperature (T_{normal}, T_{high}, K), total pressure (P, hPa), molecular mass of air (m, kg mol^{-1}), and concentration of several atmospheric components (He, O_2, O, N_2, m^{-3}). Temperature profiles of normal and high solar activity are plotted. Note that pressure and number density are plotted on a logaritmic scale.

each gas component.

$$\frac{dp_i}{dz} = -\rho_i g = -\frac{p_i M_i g}{R^* T} \ ,$$

where p_i is the partial pressure for each gas component i with molecular mass M_i. This implies gravitational settling of species and a changing atmospheric composition with height. This is clear in Figure 2.29 above ∼100 km altitude. Below about 100 km, the mean free path becomes so small that turbulent mixing is always much more important than molecular diffusion (gravitational settling). As a result, the inert gases, gases that do not undergo chemical reactions in the atmosphere, have constant mass mixing ratio r_i, i.e. $r_i = m_i/m_d$ and m_d are constant. Some species, e.g. O, O_2 and O_3, interact with (solar) radiation (dissociation and consequent re-combination by collision), which influences their vertical profiles.

The heterosphere

The heterosphere is the layer below the exosphere, and ranges between ∼100 km to the exobase or critical level at ∼500 km altitude. The base of this layer is called the turbopause, which marks the transition between the well mixed homosphere and the heterosphere where constituents adopt their individual distributions with height as the result of molecular diffusion (gravitational settling). In the heterosphere the mean free path exceeds turbulent displacements; diffusion becomes the main vertical mixing process, turbulence is suppressed and the flow becomes laminar.

Molecular diffusion acts on gases according to their molar mass as expressed in the hydrostatic equation for a single gas, and heavy species (like O_2) decrease more rapidly with height than lighter species (like O and He). As a result, the atmospheric composition (and hence mean molar mass) changes with height in the heterosphere (Figure 2.29). An additional process important in the heterosphere, apart from molecular diffusion, is photodissociation, which is the fragmentation of a molecule into two or more components as a

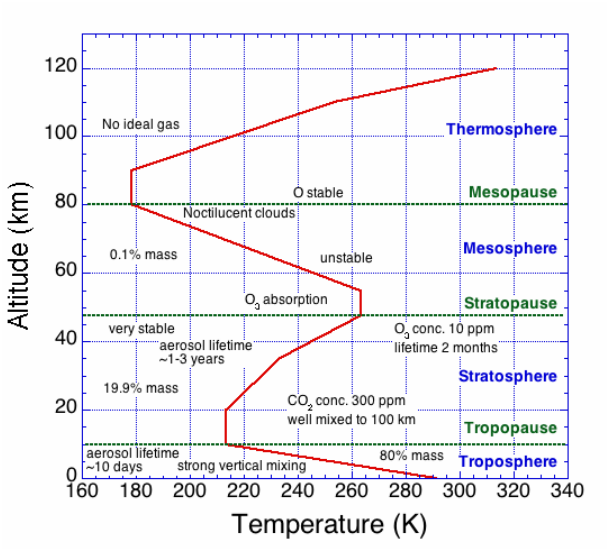

Figure 2.30: Schematic view of the atmospheric temperature structure in the homosphere. The Figure includes information on the atmospheric composition.

consequence of absorption of a photon (interaction with electromagnetic radiation). For example, not far above the turbopause atomic oxygen O becomes the dominant form of oxygen. Photo-dissociation is an important process for life on Earth because it filters the very energetic and damaging UV radiation out of the solar spectrum.

The homosphere

The homosphere is the lowest layer in the atmosphere, ranging from the surface up to the turbopause at ∼100 km. In this layer the mean free path is small enough for turbulent eddies in the circulation to be only weakly damped by molecular diffusion, i.e. turbulent diffusion dominates vertical mixing. Turbulence stirs different gases with equal efficiency, so that the mass mixing ration of a gas i, $r_i = m_i/m_d$ is constant in the homosphere. For example, $r_{N_2} = 0.78$ and $r_{O_2} = 0.21$. As a result, atmospheric composition is constant in the homosphere and the constant gas properties apply: the gas constant of dry air $R_d = 287\,\mathrm{J\,kg\,K^{-1}}$ and the average molecular mass for dry air $M_d = 28.96\,\mathrm{kg\,kmol^{-1}}$. In the homosphere the vertical profiles of O, O_2 and O_3 are determined by photo-dissociation of O_2 and subsequent recombination. This has a strong impact on the vertical temperature profile of the homosphere. Based on the temperature profile the homosphere can be sub-divided in 4 layers: the thermosphere (80-100 km), the mesosphere (50-80 km), the stratosphere (10-50 km) and the troposphere (0-10 km) (see section 2.2 and Figure 2.30).

2.5.2 Transport of radiation in the atmosphere

There are three main processes that affect radiation transport in the atmosphere: scattering, absorption, together they attenuate radiation, and emission. Short (solar) and long-wave (terrestrial / atmospheric) radiation have very different scattering, absorption and emission characteristics. Solar radiation is absorbed and scattered. Re-emission takes place in a different wavelength interval. Terrestrial radiation is absorbed and re-emitted in the same wavelength interval. Its profiles are therefore more difficult to understand.

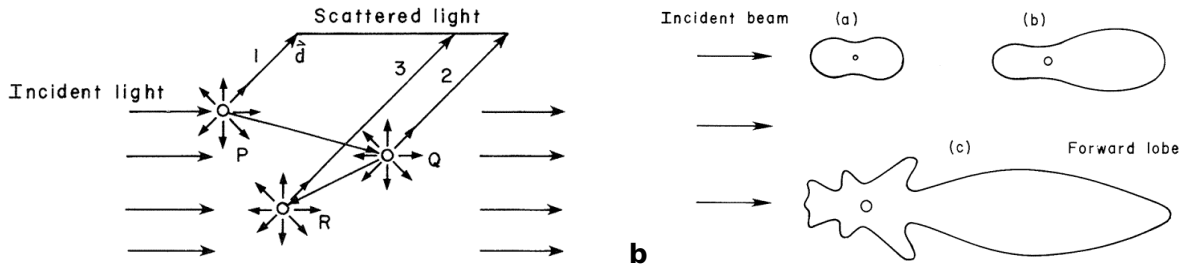

Figure 2.31: Illustration of the process of scattering. a) Scattering and multiple scattering, b) single scattering distributions as a function of particle size, small to large (a-c) particles.

Scattering

Scattering occurs when particles interact and as a result change in direction. It can also be described as the process by which a particle in the path of an electromagnetic wave continuously abstracts energy from the incident wave and re-radiates that energy in all directions. Most of the light that reaches our eyes does not come directly from its sources but indirectly by scattering. For example, the objects surrounding us are visible through the light that they scatter and the color of the object is then determined by the wavelength it scatters the radiation most effectively. In a scattering volume which contains many particles, each particle is exposed, and also scatters, light which has already been scattered, a process called multiple scattering (Figure 2.31. The main importance of multiple scattering is that it increases the chance of absorption.

The relative intensity of the scattering pattern is found to depend strongly on the size of the scattering particle in relation to the wavelength of the incident wave: the size wavelength ratio. When particles are much smaller than the incident wavelength (e.g. air molecules) the scattering is called Rayleigh scattering. When particles are much larger than the incident wavelength (aerosols, cloud droplets) the scattering is called Mie scattering in which scattering is more strongly in the forward direction. Molecular or Rayleigh scattering is proportional to λ^{-4}, so that blue light ($\lambda = 0.425\,\mu$m) scatters 5.5 times more than red light ($\lambda = 0.650\,\mu$m). This means that the solar beam looses a significant fraction of its shorter wavelengths (blue light), which reaches the surface as diffuse radiation coming from all directions. This is also why the sky, viewed away from the sun's disk, appears blue. As the sun approaches the horizon, sunlight travels through more air molecules, so that more and more of shorter wavelengths are scattered out of the solar beam. The sun's disk appears red. Larger particles in the atmosphere (like cloud droplets) also scatter sunlight (Mie scattering), but proportional to λ^{-1}. This process is therefore much less wavelength selective, and clouds appear white instead of blue.

Absorption

When absorption occurs the incident radiant energy is retained in the substance. Scattering is often accompanied by absorption, e.g. grass looks green because it scatters green light more effectively than red and blue light. These are absorbed and converted in another form of energy (heat). Scattering and absorption both remove energy from a beam of light traversing a medium, and their combined effect is called extinction or attenuation.

Absorption depends on the medium in combination with wavelength. Along a finite path length in the atmosphere absorption may be large at some wavelengths and small in others. In general, absorption in the visible spectrum is nearly absent but is very strong in the

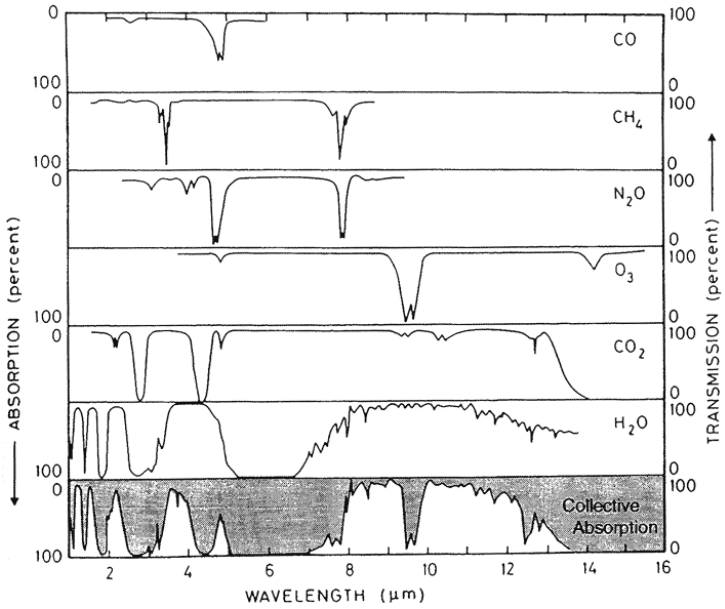

Figure 2.32: Absorption spectra for near infra red and longwave radiation for different gasses in the atmosphere in percentage of incident radiation.

infrared. All optically active gases contribute to the absorption spectrum in separate wavelength intervals. This is illustrated in Figure 2.32. For different gasses in the atmosphere it illustrates the percentage of incident radiation that is absorbed / transmitted.

Emission

Finally emission is defined as the generation and sending out of radiant energy. According to Kirchhoff's Law, under thermodynamic equilibrium, absorptivity at a given wavelength equals emissivity at a certain wavelength, $\alpha_\lambda = \varepsilon_\lambda$. The basis for describing thermal emission is blackbody radiation as described in section 2.1.1. Planck's law, Wien's Displacement Law and Stefan-Boltzmann's Law then describe the flux intensity as a function of wavelength for a given emission temperature, the wavelength at which the maximum occurs in this distribution, and the total radiation flux integrated over all wavelengths as a function of temperature.

2.5.3 Short and longwave radiation in the atmosphere: clear sky

After scattering and absorption the shortwave radiation spectrum at the surface is different from that at ToA and illustrated in Figure 2.2 for clear sky conditions. It is clear that the atmosphere is reasonably transparent for shortwave radiation. The energetic part of the solar radiation ($< 0.3\,\mu$m) is absorbed at high levels by photo-dissociation and photo-ionization of O_2 and O_3. Only 2% of the solar radiation reaching the surface of the Earth originates from wavelengths $< 0.32\,\mu$m. This part is responsible for sunburn. The spectrum shows several substantial absorption bands of H_2O and CO_2, this mainly occurs in passing from tropopause to ground. Note that at the surface, the shortwave spectrum peaks in middle of visible spectrum ($0.5\,\mu$m), which is the wavelength interval that our eyes are most sensitive to.

The longwave radiation spectrum at ToA is illustrated in Figure 2.33. It also shows several absorption bands, mainly from H_2O, CO_2 and O_3. In the band between 8 and $13\,\mu$m (770 - $1250\,\text{cm}^{-1}$) radiation emitted at the surface passes freely to space. This band is called

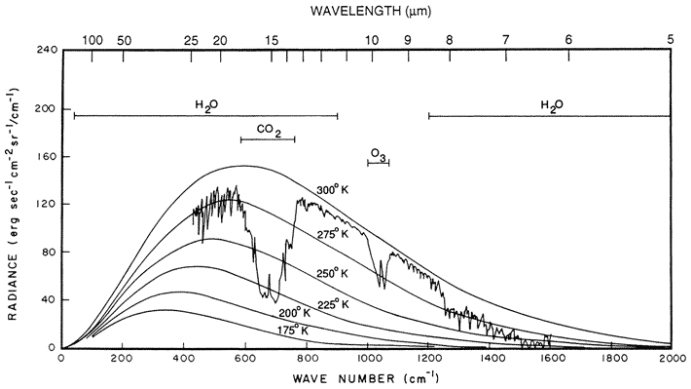

Figure 2.33: Terrestrial emission spectra for several different emission temperatures and observed at the top of the atmosphere.

the atmospheric window. From 13 μm onwards, absorption by water occurs. The terrestrial longwave spectrum also resembles blackbody curves, as does the solar spectrum. In the atmospheric window, 8 - 13 μm, the spectrum corresponds to a blackbody curve for a surface temperature of 288 K. At other wavelengths radiation is absorbed and re-emitted in the overlying atmosphere by water vapour and clouds, producing outgoing radiation that corresponds to lower temperatures. That is why the strong absorption bands of CO_2 (15 μm) and O_3 (9.6 μm) radiate from 220 K, representative for the upper troposphere, and 270 K, representative for the upper stratosphere.

Combining the short and longwave spectra results a bulk atmospheric absorption spectra (Figure 2.34). When evaluated at different altitudes, the spectra differ. From the Figure it is clear that between the tropopause and the surface radiation of longer wavelengths is effectively absorbed. Especially H_2O and CO_2 are very effective in the lowest part of the atmosphere. The vertical distribution of species in the atmosphere is clearly important in the radiation budget at the surface, and it will also influence the vertical temperature distribution.

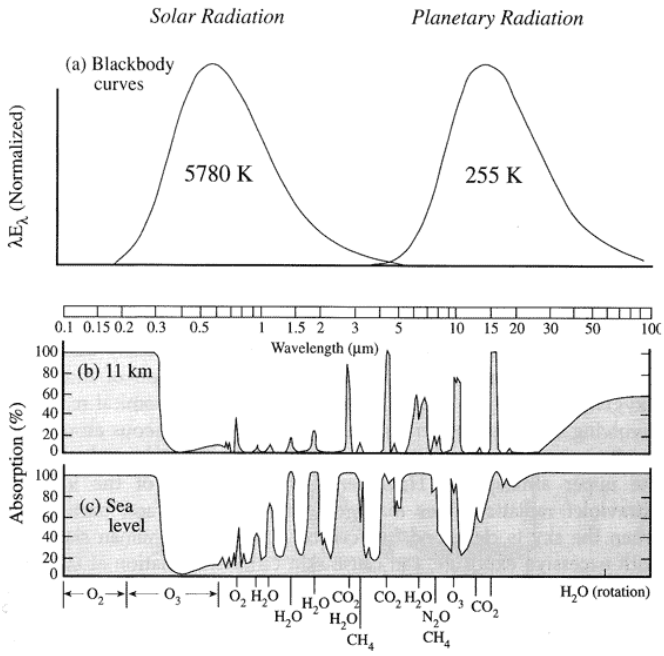

Figure 2.34: a) Blackbody spectra for T = 5780 K (solar) and T = 255 K (terrestrial). Radiation absorption in the atmosphere at b) the tropopause and c) the surface.

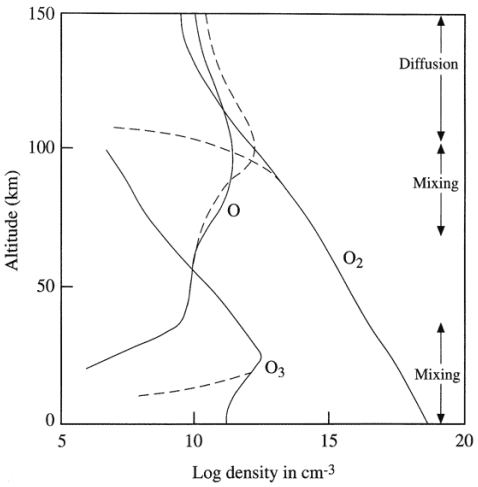

Figure 2.35: Vertical profiles of atomic oxygen O, molecular oxygen O_2 and ozone O_3.

2.5.4 Vertical distribution of atmospheric oxygen

Oxygen occurs in the atmosphere in three different forms: atomic oxygen O, molecular oxygen O_2, and ozone O_3. Atomic oxygen is formed by photo-dissociation of molecular oxygen:

$$O_2 + h\nu \rightarrow O + O \qquad \lambda < 0.24\,\mu m\ .$$

This process depends on the availability of photons having the required energy, i.e. high in the atmosphere, and the availability of O_2 molecules. The atomic oxygen will recombine into O_2 by collision. This process is more effective at higher pressures. Destruction of O also occurs by formation of ozone:

$$O + O_2 + M \rightarrow O_3 + M\ .$$

M is any third atom or molecule. For this process many O and O_2 are necessary and high pressure. The combination of these two processes result in a maximum of atomic oxygen O ∼100 km altitude.

The destruction of O results in the formation of ozone O_3. The amount of ozone formed depends on the availability of O, which has its maximum relatively high in the atmosphere, the availability of O_2, which is more abundant lower in the atmosphere, and the number of collisions, which is larger lower in the atmosphere. This results in a maximum production of ozone between 30 and 70 km. Ozone is destroyed by photo-dissociation:

$$O_3 + h\nu \rightarrow O_2 + O \quad \lambda \leq 11\,\mu m,\ \text{max at } 0.25\,\mu m\ ,$$

and recombination:

$$O_3 + O \rightarrow 2O_2\ ,$$

for which many O_3 and O are necessary, and high pressure. Destruction of ozone also occurs by oxidation in which ozone reacts with any species that includes an oxygen atom to produce O_2. This mainly takes place near the surface. In total these processes lead to an ozone maximum around 20 km altitude, the ozone layer. The resulting vertical profiles of O, O_2 and O_3 are plotted in Figure 2.35.

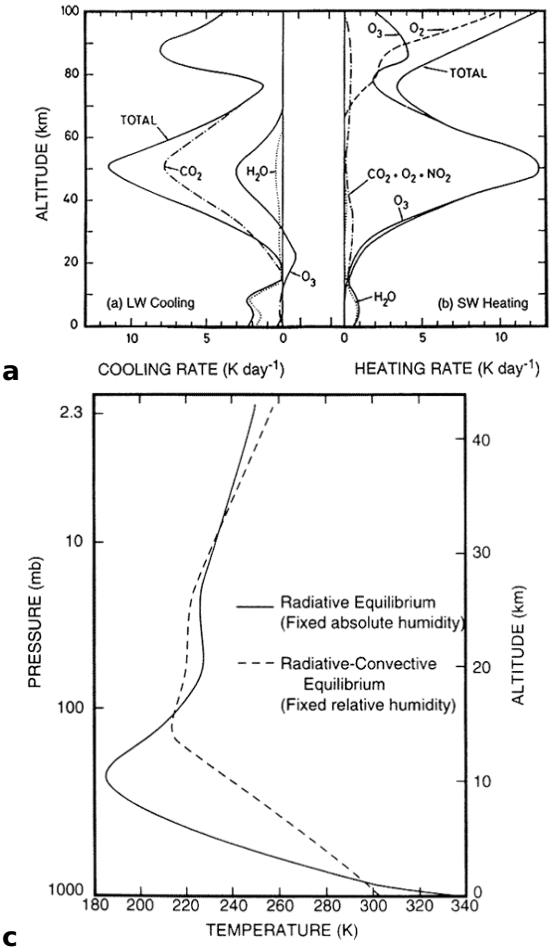

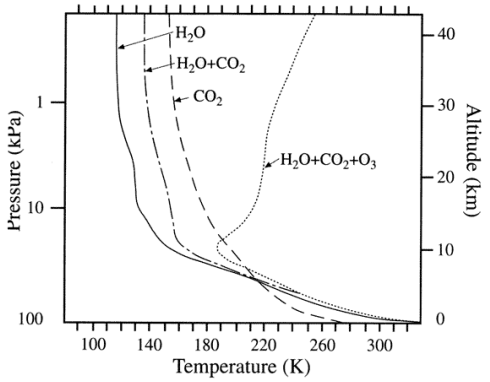

Figure 2.36: (a) Vertical profiles of heating/cooling rates for different atmospheric constituents for long (left) and short (right) wave radiation. b) Radiative equilibrium temperature profiles for a cloudless atmosphere consisting of H_2O, CO_2, H_2O + CO_2, and H_2O + CO_2 + O_3. c) Calculated temperature profiles for radiative equilibrium and thermal or radiative-convective equilibrium.

2.5.5 Radiation transport and the atmospheric temperature profile

From the above it is clear that the atmospheric constituents change the short and longwave radiation budgets. In changing the radiation budget, the heat budget of the atmosphere also changes. Adding radiative energy results in warming and removing it results in cooling.

The rate of heating or cooling depends on the atmospheric constituents. Figure 2.36 illustrates the vertical distribution of heating and cooling rates in the atmosphere due to the presence of different gasses. The primary longwave radiation absorbers (CO_2, O_3 and H_2O) are responsible for cooling of the atmosphere through so called "cooling to space". An exception is O_3 in the lower stratosphere, where it absorbs upwelling longwave radiation in the 9.6 μm band, in the atmospheric window. Water vapor (H_2O) dominates cooling in the troposphere (2 K day^{-1}), and in the stratosphere CO_2 (15 μm band) together with O_3 (9.6 μm band) dominates the cooling.

Shortwave radiation produces heating because the energy is not re-emitted at the same wavelength. Absorption by O_3 produces maximum heating near stratopause (±50 km). This is not the altitude with the highest concentration, but at this height radiation in the right wavelength is most abundant. In the troposphere, H_2O is the dominant shortwave absorber. However, heating rates of 1 K day^{-1} do not offset longwave cooling. Apparently, radiative transfer leads to net cooling of troposphere, which must be offset by heat transport from the surface. Note that the profiles presented in Figure 2.36a apply to clear sky conditions, the role of clouds on vertical radiation profile is not included and is considerable.

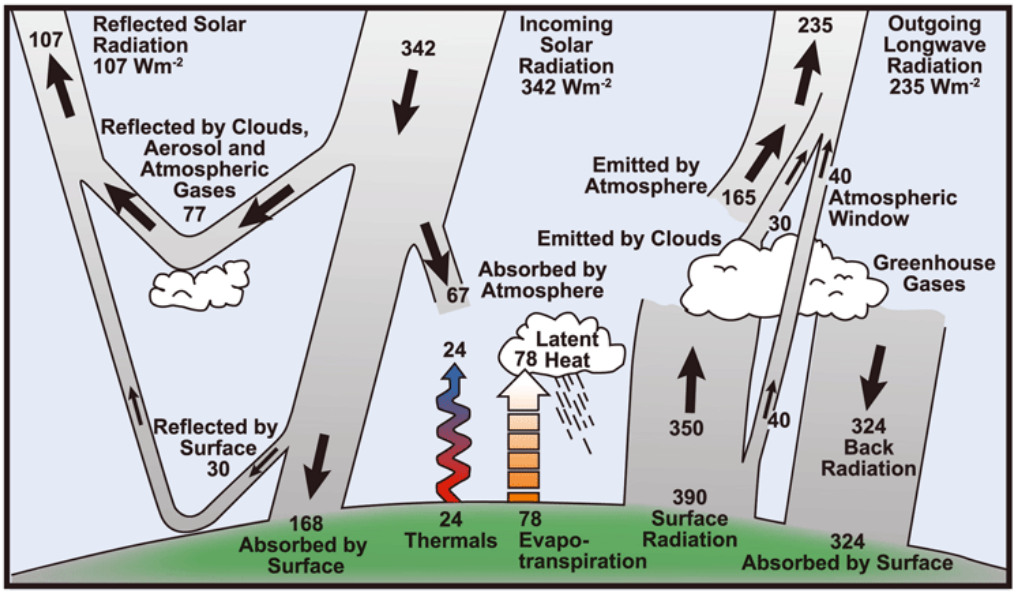

Figure 2.37: The heat balance of the Earth-atmosphere system, globally and annually averaged.

To illustrate the impact of the presence of certain atmospheric constituents Figure 2.36b presents theoretical temperature profiles for a cloudless atmosphere consisting of only the given gasses in radiative equilibrium. With only water vapor present the temperature profile in the troposphere already reasonably resembles the measurements. Only CO_2 results in too low temperatures. Adding CO_2 to the water vapor atmosphere increases the temperature by 10 to 20 K. However, only H_2O and/or CO_2 in the atmosphere is not enough to represent the observed temperature increase in the stratosphere. Shortwave absorption by O_3 is necessary to obtain this temperature increase.

An atmosphere in radiative equilibrium, especially the troposphere, is not stable. To include the vertical energy exchange by atmospheric motions Figure 2.36c presents the vertical temperature profiles for radiative equilibrium and radiative-convective equilibrium. In the troposphere, convection increases temperature, except near the surface. The result of the total of the processes presented here is the temperature profile presented in Figure 2.29b.

The total (global and annual mean) energy budget of the atmosphere is illustrated in Figure 2.37. At the top of the atmosphere radiative equilibrium exists, but not at the surface. The surface receives more energy in shortwave radiation than it looses in longwave radiation. The surface energy balance is closed by the surface turbulent fluxes of sensible and latent heat. They will be discussed in more detail later in this course. The global and annual averaged $Shw\downarrow$ at ToA equals $S_0/4 = 343\,\mathrm{W\,m^{-2}}$. 30% is reflected back to space by the atmosphere, clouds, and the surface (planetary albedo = 0.3). About 55% reaches the surface, where most is absorbed. The rest is absorbed by the atmosphere and clouds.

The absorbed Shw heats the surface and is radiated by Lw to the atmosphere ($390\,\mathrm{W\,m^{-2}}$). Most of the emitted Lw is absorbed in the atmosphere which in turn emits Lw to space and to the surface. As a result the net Lw loss at the surface is small and does not balance the absorbed Shw. The turbulent fluxes restore the balance.

Chapter 3

The dynamic atmosphere

3.1 Introduction

This chapter is concerned with motions in the atmosphere that are associated with weather and climate. We describe the motions with a set of partial differential equations, but because the motions in the atmosphere are extremely complex no general solutions to these equations are known to exist. To understand the role of atmospheric motions in observed weather and climate, it is therefore necessary to make simplifications of the fundamental governing equations. In this chapter we derive the equations, explain them and discuss simplifications for different cases. For more detailed information on the dynamics of the atmosphere see e.g. Holton (1992); Hartmann (1994); Wallace and Hobbs (2006).

3.2 Motion in the atmosphere

Wind is the motion of air in the atmosphere. The wind varies on various different time scales from seconds and minutes (turbulence), to hours and days (fronts, depressions), to years (annual cycle). Most energy in the spectral distribution of the wind variability is contained in the large scale fluctuations of days and in the small scale fluctuations of seconds.

Wind is induced by differential heating of the atmosphere by differences in solar input. This process is illustrated in Figure 3.1a. When evaluating two columns of air of which one is heated by solar radiation, the heated one expands compared to the colder one. At higher altitudes air will flow to the smaller, colder column to restore balance at this altitude. At the surface the colder column now contains more air, i.e. higher pressure, and the surplus flows back to the warmer column resulting in a cell circulation (Figure 3.1b).

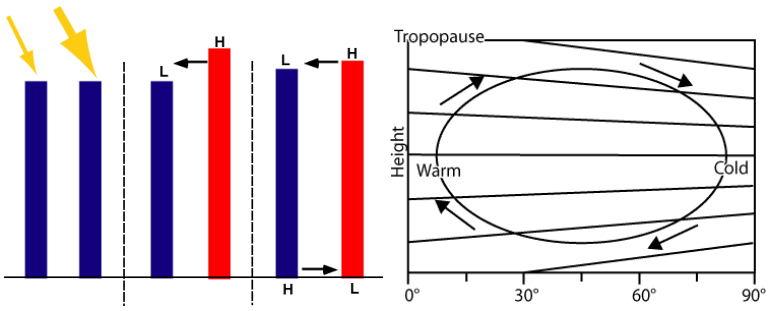

Figure 3.1: Left, differential heating resulting in atmospheric motion. Right, the resulting cell circulation.

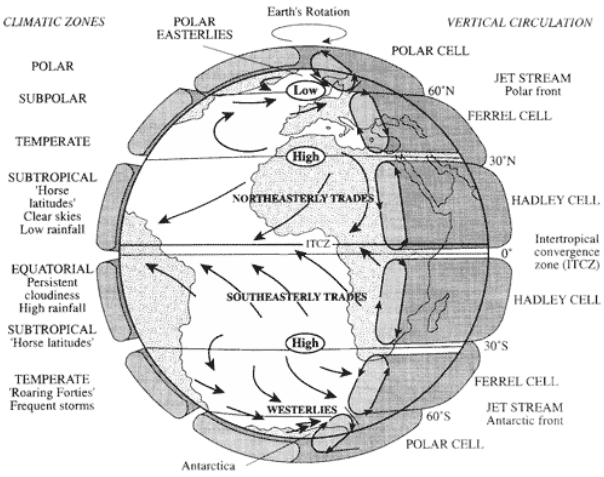

Figure 3.2: The general circulation patterns on Earth.

In the atmosphere the solar input decreases from equator to pole due to the declining Sun elevation. In addition, less solar radiation is absorbed due to increased reflection of solar radiation on clouds and aerosols, and the (snow covered) surface. To restore the balance, heat is transported through the atmosphere (and ocean) towards the poles. The rotation of the Earth complicates matters, and no single cell structure exists in the Earth's atmosphere but a three cell structure (Figure 3.2). Due to the rotation the air will obtain a eastward component near the surface and a westward component at high altitudes (this will be explained later). These zonal wind components will restrict the pole-ward energy transport and the temperature difference is enhanced instead of removed. Eventually this results in an unstable situation, and depressions start to form in the mid latitudes. They are effective transporters of heat towards the poles. In the tropics the Hadley cell is very effective in transporting heat pole-wards. The Hadley circulation manifests itself as a semi-permanent high pressure in the sub-tropics (e.g. the Azore High) and a low pressure around the equator. In the rising part of the circulation tropical rain storms are very effective in transporting heat.

The dynamics of the atmosphere is obviously very important for the transport of heat, on a global and regional scale. Pole-ward transport determines to a large extend the temperature difference between equator and pole. Changes in the transport also will change this temperature difference. For example, a smaller pole-ward heat transport means a cooling at higher latitudes and an increase in the extend of the snow and ice covered area. The albedo of the surface increases, decreasing the absorption of solar radiation and increasing the equator - pole temperature gradient, i.e. the albedo feedback. This will affect the global radiation budget. It is clear that the dynamics of the atmosphere is very important to understand weather and climate.

3.2.1 Coordinate systems

Cartesian vs natural (local) coordinates

In general we use the Cartesian reference frame where x and y are horizontal coordinates and z a vertical coordinate (Figure 3.3). However, for some phenomena it is convenient to use natural (or local) coordinates (s, n, z). In the natural coordinate system s is the direction parallel to the horizontal velocity in every point, n is the direction normal to the horizontal velocity in every point, and z is directed vertical upwards (Figure 3.3), as in the cartesian

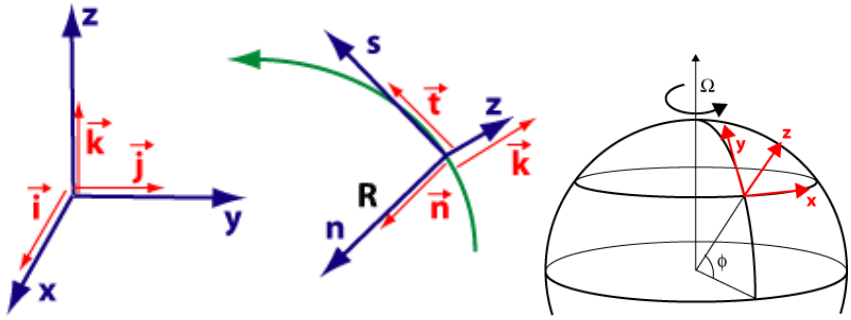

Figure 3.3: Left, Cartesian coordinates: x, y are horizontal coordinates, z the vertical, i, j and k are the corresponding unit vectors. Middle, natural (local) coordinates: s directed parallel to the motion in the horizontal plane, positive in the direction of motion, n directed normal to the motion in the horizontal plane, positive to the left, z the vertical. t, n and k are the corresponding unit vectors. R is the radius of curvature of the motion, positive in positive n direction. Right: Eulerian reference frame fixed to Earth. x points to the east, y points to the north, and z points locally vertical upward.

system. The radius of the curvature of the flow is given by R and is defined positive when directed in the positive n direction.

Eulerian vs Lagrangian reference frame

In the Eulerian reference frame motion is described with respect to a fixed reference frame, while in the Lagrangian description the reference frame moves with the motion. In general we will use the Eulerian description in which we attach our reference frame to the Earth surface. In the cartesian form of this frame x points to the east, y points to the north and z points along the local vertical (Figure 3.3). The velocity components are defined along these axes as well with u the x-component pointing to the east, v the y-component pointing to the north and w the vertical (z-)component of the velocity. In the meteorology a wind blowing from west to east is called a westerly wind.

3.2.2 Apparent forces

To describe motion in the atmosphere we use Newton's second law. This law states that the sum of the forces acting on a parcel determine the acceleration of the parcel (Frame 3.1). Forces in the atmosphere are e.g. gravity, pressure gradient, friction, etc. In addition to

Newton's first law of motion pertains to the behavior of objects for which the forces acting on it are balanced. It states that an object at rest tends to stay at rest and an object in motion tends to stay in motion with the same speed and in the same direction unless acted upon by an unbalanced force.

$$\sum \vec{F}_i = 0$$

Newton's second law of motion pertains to the behavior of objects for which the forces acting on it are NOT balanced. It states that the object on which an unbalanced force acts is accelerated. The acceleration depends on the unbalanced force itself and the mass of the object.

$$\sum \vec{F}_i = m\frac{d\vec{V}}{dt}, \quad \text{or in unit mass} \quad \sum \frac{\vec{F}_i}{m} = \frac{d\vec{V}}{dt}$$

In case $d\vec{V}/dt = 0$ a steady state exists and the second law reduces to the first law.

Frame 3.1: Newton's first and second laws.

Ω is the angular speed, the change in angle ($\delta\Psi$) per unit time (δt), or 2π angle change in one period of rotation (P):

$$\Omega = \frac{\delta\Psi}{\delta t} = \frac{2\pi}{P} = \frac{2\pi|\vec{V}|}{2\pi|\vec{r}|} \quad \Rightarrow \quad |\vec{V}| = \Omega|\vec{r}|$$

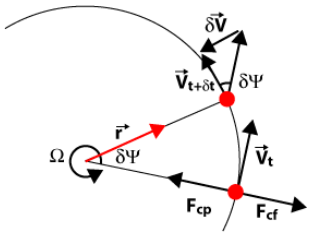

P is the distance over the circle divided by the speed of the parcel. The magnitude of the velocity change is:

$$|\delta\vec{V}| = |\vec{V}|\,\delta\Psi \; .$$

Note that for small values of $\delta\Psi$:

$$\sin(\delta\Psi) = \frac{|\delta\vec{V}|}{|\vec{V}|} \quad \Rightarrow \quad \delta\Psi \approx \frac{|\delta\vec{V}|}{|\vec{V}|} \; .$$

Based on the direction of the rotation, the ratio of the velocity change over speed change equals the ratio of direction of the string to the length of the string:

$$\frac{\delta\vec{V}}{|\delta\vec{V}|} = -\frac{\vec{r}}{|\vec{r}|} \quad \Rightarrow \quad \delta\vec{V} = -|\delta\vec{V}|\,\frac{\vec{r}}{|\vec{r}|}$$

With $\vec{r}$ directed opposite to $\delta\vec{V}$. Substitution of $|\delta\vec{V}|$ and the definition of Ω results in:

$$\delta\vec{V} = -\Omega\vec{r}\delta\Psi = -\Omega^2\vec{r}\delta t \; .$$

Division by δt and taking the limit of δ to 0 results in Eq. 3.1.

Frame 3.2: The centripetal acceleration Eq. 3.1.

these forces two *apparent* forces act on the parcel: the coriolis force and the centrifugal force. These forces are introduced to fulfill Newton's second law in a reference frame fixed to the Earth surface and therefore rotating with the Earth surface.

The centrifugal force

Let us look at the case in which an object is **not moving** in a reference frame fixed to the Earth surface. First imagine a parcel with mass m attached to a string and whirled through a circle with radius r at a constant angular velocity Ω. Observing from a fixed reference frame the speed of the parcel is constant but the direction it travels changes continuously so that its velocity is not constant. The velocity of the parcel can be written in terms of the angular velocity and length of the string (see Frame 3.2):

$$\frac{\partial\vec{V}}{\partial t} = -\Omega^2\vec{r} \tag{3.1}$$

This accelaration is called the centripetal acceleration (or centripetal force per unit of mass, F_{cp}) and is caused by the force of the string pulling the parcel. If we now observe this motion in a reference frame rotating with the parcel, the parcel is stationary, but F_{cp} still acts on it. In order to apply Newton's second law we now must include an *apparent* force, the centrifugal force (F_{cf}), which balances F_{cp}, and is equal in size and opposite in direction: $F_{cf} = \Omega^2\vec{r}$.

Gravity

The effect of the centrifugal force on Earth for non moving objects is illustrated in Figure 3.4. On Earth, the radius of a latitude circle is $|\vec{r}| = r_e \cos\phi$, with r_e the Earth radius (~6371 km), and ϕ the latitude. If the Earth did not rotate the gravitational force g^* would be directed

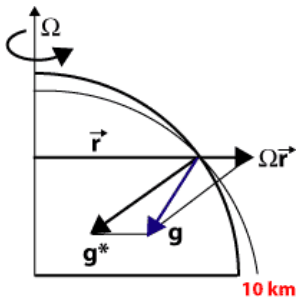

Figure 3.4: The effect of the centrifugal force on a non moving object on Earth, and gravity.

to the center of the Earth. The gravity we experience (the effective gravity g) is the sum of this gravitational force and the centrifugal force due to the rotation of the Earth.

$$\vec{g} = \vec{g^*} + \Omega^2 \vec{r}$$

Since F_{cf} is directed perpendicular to the axis of rotation, the effective gravity g is not directed towards the center of the Earth. The angle between $\vec{g}$ and $\vec{g^*}$ is about 0.1°. The Earth has adjusted its shape to the horizontal component of F_{cf} to assure that the effective gravity is directed perpendicular to the surface and no resultant force acts in the horizontal. As a consequence, the equatorial radius of the Earth is about 21 km larger than the polar radius. With $\Omega = 2\pi$ rad / 24 h $\cong 7.3\times10^{-5}$ rad s^{-1}, the component of F_{cf} has a maximum magnitude of 0.034 m s^{-2} at the equator and is 0 on the poles. g decreases with about 0.5% from the equator to the pole and is on average 9.81 m s^{-2} at sea level. Note that g also varies with altitude, about 0.23% per 10 km from sea level.

The geopotential

Gravity can also be represented in terms of the gradient of a potential function Φ, called the geopotential: $\nabla\Phi = -\vec{g}$. Note that $\vec{g} = -gk$ with k the unit vector directed upward perpendicular to the surface and g the length of $\vec{g}$ ($g = |\vec{g}|$). From this it follows that Φ is only a function of altitude ($\Phi(z)$) and the gradient of Φ is the gravity: $d\Phi/dz = g$. If $\Phi(z = 0) = 0$, then $\Phi(z)$ is the work required to raise a unit mass to height z from mean sea level.

$$\Phi = \int_0^z g\, dz$$

For many applications in the meteorology we assume that $g(z) = g(z = 0) = g_0$ and therefore $\Phi(z) = g_0 z$.

The coriolis force

For a parcel **moving** in a reference frame fixed to the Earth surface, a second *apparent* force becomes important, the coriolis force. Figure 3.5 illustrates the effect the apparent path of a moving parcel in a fixed and rotating reference frame. Viewed in a fixed reference frame the parcel moves in a straight line and the disk rotates underneath it. Viewed from the rotating disk the parcel path is deflected to the right and moves on a curve.

In the case of the Earth atmosphere system in which our reference frame is fixed to the Earth, this effect results in a deflection of the parcel path to the right on the Northern Hemisphere and to the left on the Southern Hemisphere. The apparent force responsible is called the coriolis force F_{co}. F_{co} acts perpendicular to the direction of motion. The effect

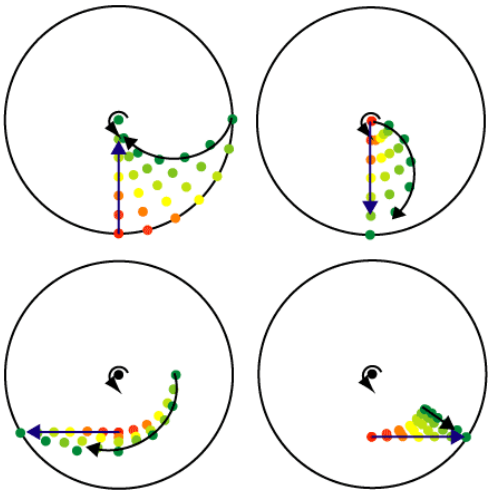

Figure 3.5: The apparent path of a moving parcel in a fixed and rotating reference frame for four different directions of movement with respect to the rotating disk. The straight arrow indicates the path in the fixed frame, the curved arrow in the rotating frame. The dots represent the location of the parcel at a certain time and the movement of those locations in time.

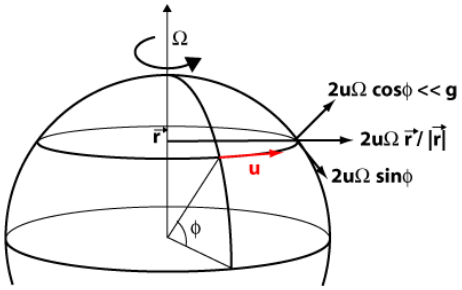

Figure 3.6: Coriolis deflection of an eastward moving parcel.

of F_{co} on a parcel depends on latitude and is largest near the pole and 0 on the equator. It acts only on moving parcels and is stronger for faster moving parcels.

Consider a parcel that moves along a latitude circle in easterly direction ($u > 0$, $v = 0$) (Figure 3.6). This introduces an additional centrifugal force F_{cf} through an additional angular velocity: $\delta\Omega = u/r$:

$$\vec{F}_{fc} = \left(\Omega + \frac{u}{r}\right)^2 \vec{r} = \Omega^2 \vec{r} + 2u\Omega\frac{\vec{r}}{r} + \left(\frac{u}{r}\right)^2 \vec{r} \tag{3.2}$$

The first term on the right hand site represents the centrifugal force due to the rotation of the earth, which is included in the effective gravity. The other two terms are the deflection terms which act outward along vector $\vec{r}$, i.e. perpendicular to the axis of rotation. For synoptic scale motions in the atmosphere $|u| \ll \Omega\vec{r}$ and the last term may be neglected. The second term is the coriolis force (F_{co}). The equation shows that for an easterly moving parcel F_{co} results in a horizontal acceleration in the north-south direction and a vertical acceleration (Figure 3.6).

We can repeat this exercise for a parcel moving in north-south direction and in the vertical direction (see Holton (1992); Wallace and Hobbs (2006)). The total result is a north-south acceleration (dv/dt) resulting from an east-west displacement (u), and an east-west acceleration (du/dt) resulting from a north-south displacement (v):

$$\begin{aligned} \frac{du}{dt} &= +2\Omega \sin\phi\ v \quad \equiv +fv \\ \frac{dv}{dt} &= -2\Omega \sin\phi\ u \quad \equiv -fu\ . \end{aligned} \tag{3.3}$$

f is the Coriolis parameter, which depends on latitude. On the Northern Hemisphere $f > 0$ and Coriolis acceleration deflects flow to the right. On the Southern Hemisphere $f < 0$ and

Examples From integration of Eq. 3.3 it follows that:

$$\frac{\partial u}{\partial t} = \frac{\partial^2 x}{\partial t^2} = +fv \quad \Rightarrow \quad x(t) - x(0) = +\frac{1}{2} fvt^2$$
$$\frac{\partial v}{\partial t} = \frac{\partial^2 y}{\partial t^2} = -fu \quad \Rightarrow \quad y(t) - y(0) = -\frac{1}{2} fut^2$$

where f is assumed to be constant. $\Omega = 7.3{\times}10^{-5}\,\mathrm{rad\,s^{-1}}$.

Question A soccer player in the Netherlands (50°N) kicks a free kick towards the goal. He is standing 40 m from the goal and the ball travels with a speed of $20\,\mathrm{m\,s^{-1}}$. How much is the ball deflected when it reaches the goal?

Answer The ball reaches the goal after 2 s. Assume that the ball was kicked in the x-direction then: $y(t) - y(0) = -\frac{1}{2} fut^2$ = -0.5 * 2*7.3×10^{-5}*sin(50) * 20 * 2^2 = -0.0044 m. Thus, the deflection of the ball after 2 s at 50°N is 4 mm, which is much less than the effect wind will have on the ball or spin. Spin on the ball can easily deflect the ball 100 times as much!

Question A missile travels at 50°N with a speed of $1000\,\mathrm{m\,s^{-1}}$. How much is the deflection of the missile after 30 minutes?

Answer Assume that the missile was fired in the x-direction then: $y(t) - y(0) = -\frac{1}{2} fut^2$ = 0.5 * 2*7.3×10^{-5}*sin(50) * 1000 * (30*60)^2 = -181184.8 m. Thus the deflection of the missile after 30 minutes at 50°N is 181.2 km, which is significant. Note also that ballistic missiles travel largely outside the atmosphere where no wind is present!

Frame 3.3: The effect of Coriolis deflection on a moving object.

Coriolis acceleration deflects flow to the left. Owing to the Coriolis acceleration, maintaining a steady flow on Earth is not possible. Note also that the Coriolis force is negligible for motions with time scales that are very short compared to the period of the Earth's rotation. Frame 3.3 illustrates the coriolis force by giving two examples.

Inertial oscillation

In the absence of any other force, the Coriolis force results in an inertial oscillation of the object. This can be seen by combining $du/dt = +fv$ with $dv/dt = -fu$ to form one equation in terms of u:

$$\frac{d^2 u}{dt^2} + f^2 u = 0\ ,$$

which is the equation of an harmonic oscillator with frequency f. Similarly an equation in terms of v can be derived. The period P of the oscillations described by this equation is:

$$P = \frac{2\pi}{|f|} = \frac{2\pi}{2\Omega|\sin\phi|} = \frac{\pi}{\frac{2\pi}{24h}|\sin\phi|} = \frac{12h}{|\sin\phi|}$$

In the atmosphere these so-called inertial oscillations are difficult to observe because typical wind speeds are too large, but in the ocean they are well developed and observed (Figure 3.7).

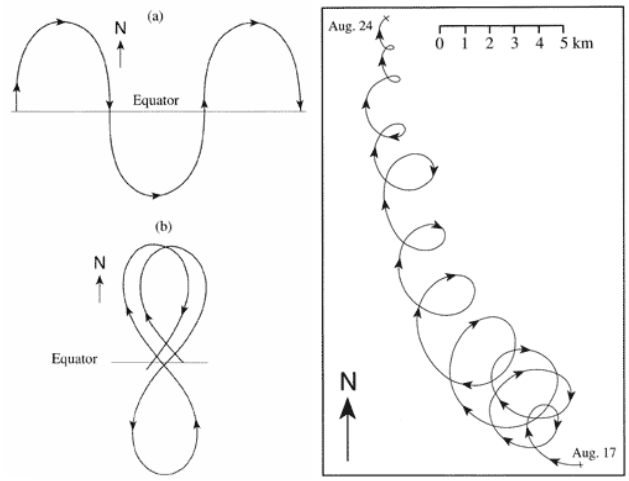

Figure 3.7: Inertial motion. Left top) a parcel moving initially away from the equator at a right angle. Left bottom) moving away under a different angle. Right In the ocean, based on buoy observations showing coriolis deflection on top of a background current.

3.2.3 The pressure gradient force

We now consider a real force acting on a parcel in the atmosphere, the (horizontal) pressure gradient force, which is a force that appears due to differences in air pressure. Consider a cube with sides δx, δy and δz, filled with air with mass M. The cube is located in a horizontal pressure field with pressure gradient $\partial p/\partial x$ (Figure 3.8). Consider the balance of forces in the x-direction. The pressure force on the left side of the cube (PF_A) is:

$$PF_A = p_A \delta y \delta z \ ,$$

and the pressure force on the right side of the cube (PF_B) is:

$$PF_B = -p_B \delta y \delta z = -(p_A + \frac{\partial p}{\partial x}\delta x + ...)\delta y \delta z \ ,$$

where p_B is written as a Taylor series of $p_A(x_A + \delta x)$. The pressure gradient force PGF is the sum of PF_A and PF_B:

$$PGF = PF_A + PF_B = -\frac{\partial p}{\partial x}\delta x \delta y \delta z \ .$$

Then the acceleration in the x-direction is:

$$\left(\frac{\partial u}{\partial t}\right)_{PGF} = \frac{PGF}{M} = \frac{PGF}{\rho \delta x \delta y \delta z} = -\frac{1}{\rho}\frac{\partial p}{\partial x} \ .$$

Similarly a pressure gradient force in the y-direction can be derived:

$$\left(\frac{\partial v}{\partial t}\right)_{PGF} = -\frac{1}{\rho}\frac{\partial p}{\partial y}$$

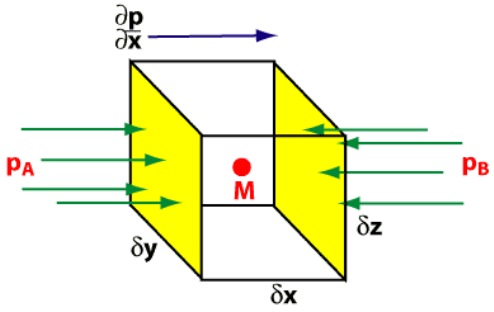

Figure 3.8: Pressure gradient force acting on a parcel.

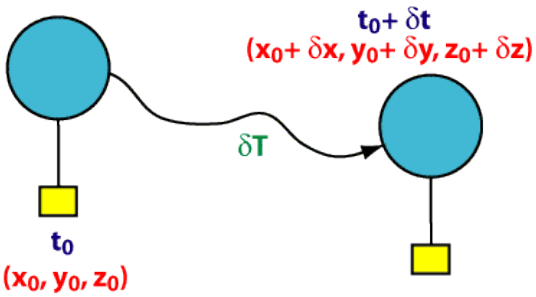

Figure 3.9: Total and local temperature derivative.

Suppose there is no other force acting on an air parcel (no coriolis or friction) to balance the pressure gradient force. In that case, giving an air density of 1.2 kg m^{-3} and a horizontal pressure gradient of $\partial p/\partial x$ = -10 hPa/100 km (typical in a low pressure area) the air parcel will be accelerated by $\partial u/\partial x = 0.0082\,\mathrm{m\,s^{-2}} = 3.0\,\mathrm{m\,s^{-1}\,h^{-1}}$. Note however, on our rotating Earth, there will always be the coriolis force acting on the air parcel once it has started to move.

3.2.4 The momentum equations

Including the pressure gradient force the balance of forces in the horizontal, per unit mass, result in the equations of motion (or momentum conservation):

$$\begin{aligned} \frac{du}{dt} &= -\frac{1}{\rho}\frac{\partial p}{\partial x} + fv + \text{friction} \\ \frac{dv}{dt} &= -\frac{1}{\rho}\frac{\partial p}{\partial y} - fu + \text{friction} \end{aligned} \tag{3.4}$$

Or in vector notation:

$$\frac{d\vec{V}}{dt} = -\frac{1}{\rho}\vec{\nabla}p - f\vec{k}\times\vec{V} + \text{friction}\ . \tag{3.5}$$

The equations describe the acceleration in the x-direction (east-west, eq. 3.4a) and y-direction (south-north, eq. 3.4b), respectively. These conservation laws express the rate of change for momentum following the motion, i.e. the total derivative. Furthermore, the first term on the right hand side is the pressure gradient force and the second term is the coriolis force. An expression for the friction term will be derived in the section on the atmospheric boundary layer. For now it will be neglected, which is a reasonable assumption far away from surface.

3.2.5 Total and local derivatives

In general conservation laws in the atmosphere describe the rate of change for e.g. momentum, heat or moisture. To apply these laws in an Eulerian (fixed) frame of reference, we must derive a relationship between the total derivative following the motion and the local derivative, which is the partial derivative with respect to time at a fixed location. To explain the difference between the two imagine a balloon carrying a temperature sensor and traveling through a temperature field (Figure 3.9). The temperature change measured by the balloon is the sum of the local heating/cooling rate and the change of environment

Question A balloon carries a temperature sensor through a temperature field. Calculate the rate of temperature change measured by the balloon (i.e. the total rate of change dT/dt).

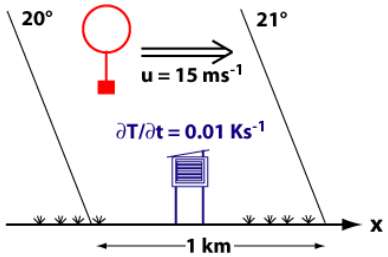

Answer

$$\frac{dT}{dt} = \frac{\partial T}{\partial t} + u\frac{\partial T}{\partial x} + v\frac{\partial T}{\partial y} + w\frac{\partial T}{\partial z} .$$

From the figure, $u = 15\,\mathrm{m\,s^{-1}}$, $v = w = 0\,\mathrm{m\,s^{-1}}$, $\partial T/\partial t = 0.01\,\mathrm{K\,s^{-1}}$.

$$\frac{\partial T}{\partial x} = \frac{21-20}{1000} = 0.001\,\mathrm{K\,m^{-1}} .$$

Substitution gives: dT/dt = 0.01 + 15*0.001 + 0 + 0 = $0.025\,\mathrm{K\,s^{-1}}$ = $90\,\mathrm{K\,h^{-1}}$

Frame 3.4: Total and local temperature derivative.

owing to its displacement:

$$\delta T = \frac{\partial T}{\partial t}\delta t + \frac{\partial T}{\partial x}\delta x + \frac{\partial T}{\partial y}\delta y + \frac{\partial T}{\partial z}\delta z .$$

To obtain the total derivative divide this equation by δt and take the limit of δ to 0. Note that:

$$\lim_{\delta t \to 0} \frac{\delta}{\delta t} = \frac{d}{dt} , \frac{dx}{dt} = u , \frac{dy}{dt} = v , \text{and } \frac{dz}{dt} = w \ :$$

$$\frac{dT}{dt} = \frac{\partial T}{\partial t} + u\frac{\partial T}{\partial x} + v\frac{\partial T}{\partial y} + w\frac{\partial T}{\partial z} .$$

The first term is the total derivative, which is equal to the sum of the local derivative (first term on the right hand side) and the advection terms (the last three terms on the right hand side). An example is given in Frame 3.4.

The momentum equations

The total derivative can be generalized:

$$\frac{d}{dt} = \frac{\partial}{\partial t} + u\frac{\partial}{\partial x} + v\frac{\partial}{\partial y} + w\frac{\partial}{\partial z} ,$$

and applied on the momentum equations:

$$\frac{du}{dt} = \frac{\partial u}{\partial t} + u\frac{\partial u}{\partial x} + v\frac{\partial u}{\partial y} + w\frac{\partial u}{\partial z} = -\frac{1}{\rho}\frac{\partial p}{\partial x} + fv$$

$$\frac{dv}{dt} = \frac{\partial v}{\partial t} + u\frac{\partial v}{\partial x} + v\frac{\partial v}{\partial y} + w\frac{\partial v}{\partial z} = -\frac{1}{\rho}\frac{\partial p}{\partial y} - fu$$

The equations now comprise non-linear terms and can only be solved analytically for special cases.

The momentum equations in natural coordinates

For some applications it is convenient to write the momentum equations in natural coordinates. The horizontal components (s, n) of the momentum equations neglecting friction

In natural coordinates $\vec{V} = V\vec{t}$, and the acceleration is:

$$\frac{d\vec{V}}{dt} = \vec{t}\frac{dV}{dt} + V\frac{d\vec{t}}{dt}$$

Write $d\vec{V}/dt$ in terms of a component along and normal to the trajectory (s and n-direction) (see Figure). Thus, the second term on the right hand side must be rewritten. Note that from geometrical considerations, assuming $\delta\Psi$ is small, $\delta s = R\delta\Psi$ and $|\delta\vec{t}| = |\vec{t}|\delta\Psi$. Combining results in $|\delta\vec{t}| = \delta s/R$. Again assuming small angles $\delta\Psi$, $\vec{\delta t}$ is directed parallel to $\vec{n}$, $\vec{\delta t} = \vec{n}|\delta\vec{t}|$. Substitution results in:

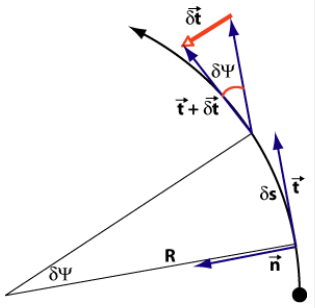

$$|\delta\vec{t}| = \frac{\vec{\delta t}}{\vec{n}} = \frac{\delta s}{R} \quad \Rightarrow \quad \frac{\vec{\delta t}}{\delta s} = \frac{\vec{n}}{R}\,.$$

Finally take the limit of δ to 0 and substitute:

$$\lim_{\delta\to 0}: \frac{d\vec{t}}{dt} = \frac{d\vec{t}}{ds}\frac{ds}{dt} = \frac{\vec{n}}{R}V \quad \Rightarrow \quad \frac{d\vec{V}}{dt} = \vec{t}\frac{dV}{dt} + \vec{n}\frac{V^2}{R}\,.$$

The different terms in the momentum equation (Eq. 3.5) neglecting friction, can now be written as:

$$\begin{aligned} \frac{d\vec{V}}{dt} &= \vec{t}\frac{dV}{dt} + \vec{n}\frac{V^2}{R} \\ -f\vec{k}\times\vec{V} &= -fV\vec{n} \\ -\frac{1}{\rho}\vec{\nabla}p &= -\left(\vec{t}\frac{\partial p}{\partial s} + \vec{n}\frac{\partial p}{\partial n}\right) \end{aligned}$$

resulting in Eq. 3.6.

Frame 3.5: The momentum equations in natural (local) coordinates.

become (see Frame 3.5):

$$\begin{aligned} \frac{dV}{dt} &= -\frac{1}{\rho}\frac{\partial p}{\partial s} \\ \frac{V^2}{R} + fV &= -\frac{1}{\rho}\frac{\partial p}{\partial n} \end{aligned} \tag{3.6}$$

Note that for motions parallel to the isobars $\partial p/\partial s = 0$, and the speed is constant following the motion.

Inertial flow in natural coordinates

As in the cartesian coordinate system we can evaluate the case in which we have no pressure gradients or other real forces acting on the parcel. The equation of motion (Eq. 3.6) than reduces to:

$$\frac{V^2}{R} + fV = 0 \quad \Rightarrow \quad R = -\frac{V}{f} = -\frac{V}{2\Omega\sin\phi}$$

Because in this case V is constant, R must be constant as well if we ignore the latitudinal dependency of f. The air parcels therefore follow circular paths with radius R and the direction of rotation is anticyclonic. This motion is again the inertial oscillation with period P:

$$P = \frac{2\pi|R|}{V} = \frac{2\pi}{|f|} = \frac{\pi}{\Omega|\sin\phi|} = \frac{12h}{|\sin\phi|}$$

The term *inertial* refers to the fact that the coriolis and centrifugal force appearing due to the relative motion of the flow, are caused by the inertia of the flow. Frame 3.6 provides an example.

Example The period of an inertial oscillation at a latitude close to Barbados (13 °N) is:

$$P = \frac{12}{|\sin\phi|} \quad \Rightarrow \quad P = 53h$$

In the atmosphere a typical wind speed is $10\,\mathrm{m\,s^{-1}}$. The radius of the oscillation than becomes:

$$R = -\frac{V}{f} = -\frac{v}{2\Omega\sin\phi} \quad \Rightarrow \quad R = 304.5 \text{ km}$$

In the ocean a typical flow speed is $0.1\,\mathrm{m\,s^{-1}}$. The radius of the oscillation than becomes:

$$R = -\frac{V}{f} = -\frac{V}{2\Omega\sin\phi} \quad \Rightarrow \quad R = 3.045 \text{ km}$$

The inertial oscillation is observed in the ocean (see figure). In the frequency spectrum two peaks are observed. One around the tidal frequency (12 hours), and one around the period of 53 h corresponding to the inertial oscillation.

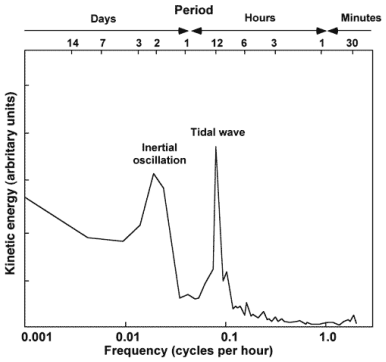

Frame 3.6: Inertial oscillation in the atmosphere and ocean.

3.3 Applications of the equations of motion

3.3.1 The Rossby number

Using the equations of motions different cases representing different phenomena in the atmosphere can be studies. To do so, the dominant processes involved must be identified. To that end, Eq. 3.6 is used to define a nondimensional parameter that represents the relative importance of the coriolis force with respect to the centrifugal force: the Rossby number. The Rossby number is the ratio of the centrifugal (or inertal) acceleration to the Coriolis acceleration:

$$\mathrm{Ro} \equiv \frac{V^2/R}{fV} = \frac{V}{fR}\,. \tag{3.7}$$

Using the Rossby numer three different situations described with Eq. 3.6 can be identified:
Ro $\gg 1$: The coriolis acceleration can be neglected compared to centrifugal acceleration, the flow is referred to as cyclostrophic.
Ro = O(1): Both coriolis and centrifugal acceleration cannot be neglected, the flow is referred to as gradient flow.
Ro $\ll 1$: The centrifugal acceleration can be neglected compared to Coriolis acceleration, the flow is referred to as geostrophic.

3.3.2 Geostrophic flow

In geostrophic flow Ro $\ll 1$ and a balance is struck between the Coriolis force (F_{co}) and the horizontal pressure gradient force (F_{pg}). This requires that the isobars are not curved but straight ($R \to \infty$). The geostrophic balance is a good approximation for almost all situations away from strong disturbances and the equator. Eq. 3.6 reduces to:

$$fV + \frac{1}{\rho}\frac{\partial p}{\partial n} = 0 \quad \Rightarrow \quad V_g = -\frac{1}{f\rho}\frac{\partial p}{\partial n}\,, \tag{3.8}$$

where V_g is the geostrophic wind This equations describes the famous rule of Buys Ballot (1857/1860): If you turn your back to the wind, the lower pressure will be on your left and

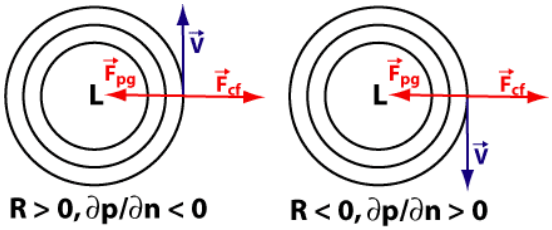

Figure 3.10: Possible solutions for cyclostrophic balance.

the higher pressure on your right on the Northern Hemisphere. Even though geostrophic balance is never exactly met, one can always define the geostrophic wind and study deviations from geostrophy.

3.3.3 Cyclostrophic flow

In cyclostrophic flow Ro $\gg$ 1 and a balance is struck between the Centrifugal force (F_{cf}) and the horizontal pressure gradient force (F_{pg}). In this case the horizontal scale of a disturbance is small and wind speeds are relatively high. The equations of motion then reduce to:

$$\frac{V^2}{R} = -\frac{1}{\rho}\frac{\partial p}{\partial n} \quad \Rightarrow \quad V = \left[-\frac{R}{\rho}\frac{\partial p}{\partial n}\right]^{1/2}, \tag{3.9}$$

where V is the cyclostrophic wind. Since $R\partial p/\partial n < 0$, there are two possible solutions. One in which $R < 0$ and $\partial p/\partial n > 0$, and one in which $R > 0$ and $\partial p/\partial n < 0$ (Figure 3.10).

A typical example of cyclostrophic balance is the tornado. For a typical tornado with radius R = 300 m, velocity V of 20 m s^{-1}, at about ∼45∘N were f is ∼10^{-4}s^{-1}, the Rossby number Ro becomes 1000, and Ro >> 0. So the coriolis force may be neglected, but most tornados are seen to rotate cyclonic in NH, so apparently coriolis force deflects air parcels in the initial stages of tornado formation. Another typical example is the water spout or dustdevil. They develop over warm land/ocean surfaces during unstable conditions or when a cold front passes. They have a typical radius R of 50 m and velocity V of 20 m s^{-1} giving for $f = 10^{-4}$ a Rossby number of Ro = 4000. They do not have a preferred direction of rotation.

3.3.4 Gradient flow

In a gradient flow Ro = O(1), and a three-way balance between the coriolis force (F_{co}), the centrifugal force (F_{cf}) and the horizontal pressure gradient force (F_{pg}) exists. The gradient

Table 3.1: Possible solutions for the gradient wind flow on the Northern Hemisphere ($f > 0$).

	$R > 0$	$R < 0$
$\frac{\partial p}{\partial n} > 0$	**A** - *Root:* $V < 0$ + *Root:* $V < 0$	**B** - *Root:* $V < 0$ + Root: anomalous (anticyclonic) low
$\frac{\partial p}{\partial n} < 0$	**C** - *Root:* $V < 0$ + Root: regular (cyclonic) low	**D** - Root: $V < -fR/2$, regular (anticyclonic) high + Root: $V > -fR/2$, anomalous (anticyclonic) high

Note that for a real solution of V the term in the root of Eq. 3.10 must be positive.

Case A The second term in the root is always negative,and therefore the root is always smaller than $fR/2$ or even negative. Since $R > 0$ the root must be larger than $fR/2$ to result in a positive V, and Case A does not give any physically realistic result.

Case B The term in the root is always positive and the root itself is always larger than $fR/2$. The negative root results in $V < 0$, which is not permitted, the positive root is physical realistic and results in an anomalous (anticyclonic) low. This low is very unstable and will not occur in reality.

Case C The term in the root is always positive and the root itself is always larger than $fR/2$. The negative root results in $V < 0$, which is not permitted, the positive root is physical realistic and results in a regular (cyclonic) low.

Case D This case only gives real results if $f^2R^2/4 > R/\rho\ \partial p/\partial n$. If the root is real it is always smaller than $fR/2$. The negative root results in $V < -fR/2$ and a regular (anticyclonic) high. The positive root results in $V > -fR/2$ and an anomalous (anticyclonic) high. In reality the anomalous case is very rare.

Exercise Derive Table 3.1 for the Southern Hemisphere.

Frame 3.7: Explanation of Table 3.1.

flow is valid for disturbances with strong, curved flow or close to the equator where F_{co} is small. For these cases Eq. 3.6 can be rearranged to:

$$V = -\frac{fR}{2} \pm \left(\frac{f^2R^2}{4} - \frac{R}{\rho}\frac{\partial p}{\partial n} \right)^{1/2} , \tag{3.10}$$

where V is the gradient wind. Not all solutions of this equation are physically realistic, i.e. V must be real and non-negative. Table 3.1 presents the possible solutions for the Northern Hemisphere. The table is explained in Frame 3.7. Figure 3.11 presents the four physically realistic solutions for the Northern Hemisphere.

Examples of the gradient wind balance are the extratropical cyclone and tropical cyclone. For a typical extratropical cyclone with radius $R = 500\,\mathrm{km}$, velocity $V = 15\,\mathrm{m\,s^{-1}}$, at ~60°N f is $\sim 1.25 \times 10^{-4}\,\mathrm{s^{-1}}$, the Rossby number Ro becomes 0.24, which is O(1). So the centrifugal acceleration may NOT be neglected. A tropical cyclone has a typical radius $R = 300\,\mathrm{km}$ and velocity $V = 30\,\mathrm{m\,s^{-1}}$ giving, at ~20°N f is $\sim 0.5 \times 10^{-4}\,\mathrm{s^{-1}}$, a Rossby number of Ro = 2.

For physically realistic solutions of Eq. 3.10 the term in the root must be larger than or equal to 0. As a result, we have a constraint for the horizontal pressure gradient:

$$\frac{f^2R^2}{4} > \frac{R}{\rho}\frac{\partial p}{\partial n} .$$

This constraint is always met for a low pressure area (Northern Hemisphere: $\partial p/\partial n < 0, R > 0$; Southern Hemisphere: $\partial p/\partial n > 0, R < 0$). There is only a constraint for the high pressure area, which must have a linear decrease of the pressure gradient towards the center (decreasing R), i.e. for $R \to 0$, $\partial p/\partial n \to 0$. For that reason the pressure distribution near the center of a high is always flat and the wind gentle compared to the region near the center of a low.

To illustrate the relation between the geostrophic wind and the actual wind we introduce the description of the geostrophic flow (Eq. 3.8) in Eq. 3.6:

$$\frac{V^2}{R} + fV + \frac{1}{\rho}\frac{\partial p}{\partial n} = 0 \;\Rightarrow\; \frac{V^2}{R} + fV - fV_g = 0 .$$

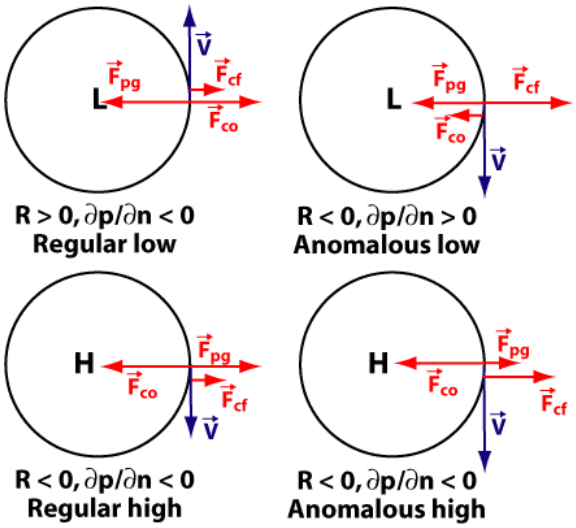

Figure 3.11: Possible solutions for the gradient balance. Upper left, case C, upper right, case B, lower two, case D of Table 3.1 and Frame 3.7.

or

$$\frac{V_g}{V} = 1 + \frac{V}{fR} \; .$$

This equation shows that for a regular low $fR > 0$ (always), and $V_g > V$ which means that the wind is subgeostrophic around a low pressure area. For a regular high $fR < 0$ (always), and $V_g < V$ which means that the wind is supergeostrophic around a high pressure area.

3.3.5 Geostrophic wind in cartesian coordinates

The geostrophic balance is a special case of the general flow described with eq. 3.6 in natural coordinates or eq. 3.4 in cartesian coordinates. We assume that the flow is frictionless and stationary ($d/dt = 0$, i.e. an uncurved flow). Eq. 3.4 than reduces to:

$$\begin{aligned} 0 &= -\frac{1}{\rho}\frac{\partial p}{\partial x} + fv \\ 0 &= -\frac{1}{\rho}\frac{\partial p}{\partial y} - fu \; . \end{aligned}$$

These can be solved for the geostrophic wind speed components $\vec{V}_g = (u_g, v_g)$:

$$u_g = -\frac{1}{f\rho}\frac{\partial p}{\partial y} \quad , \quad v_g = +\frac{1}{f\rho}\frac{\partial p}{\partial x} \; . \tag{3.11}$$

Note that these equations again show that the geostrophic wind blows parallel to the isobars.

Figure 3.12 illustrates the development of geostrophic motion in the atmosphere for the Northern Hemisphere. Consider a parcel at rest in a horizontal pressure gradient field. Friction can be neglected and the isobars are parallel. Under influence of the pressure gradient force F_{pg} the parcel will accelerate towards the lower pressure. Once motion has been initiated, the Coriolis force F_{co} will start to deflect the motion to the right (to the left on SH). F_{co} and F_{pg} balance when the parcel moves along the isobars and the acceleration has become zero. For the case illustrated in the figure the geostrophic motion is $v_g = 1/(f\rho)\ \partial p/\partial x$.

Write Eq. 3.11 in terms of motion along a constant pressure level instead of motion along a constant altitude level, thus replace z with p as the vertical coordinate. From the figure: a change in p in the x-direction at a fixed level z equals the gradient in p at that level times the horizontal distance along that level. The same change in p is derived when evaluating the vertical direction z at a fixed location x:

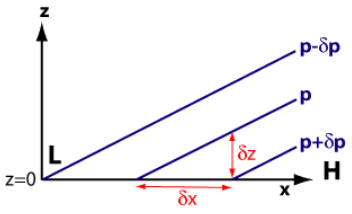

$$\delta p = \left[\frac{\delta p}{\delta x}\right]_z \delta x = -\left[\frac{\delta p}{\delta z}\right]_x \delta z \, .$$

The minus sign results from the decrease in p with increase in z. Division by δx results in:

$$\left[\frac{\delta p}{\delta x}\right]_z = -\left[\frac{\delta p}{\delta z}\right]_x \left[\frac{\delta z}{\delta x}\right]_p \, ,$$

where $\delta z/\delta x$ is the gradient of a pressure level. Now take the limit of δ to 0, make use of the hydrostatic balance (Eq. 2.10) and the definition of the geopotential ($\Phi(z) = gz$):

$$\lim_{\delta \to 0} : \left[\frac{\partial p}{\partial x}\right]_z = -\left[\frac{\partial p}{\partial z}\right]_x \left[\frac{\partial z}{\partial x}\right]_p = \rho g \left[\frac{\partial z}{\partial x}\right]_p = \rho \left[\frac{\partial \Phi}{\partial x}\right]_p \, .$$

Similarly the pressure gradient in the y-direction can be derived resulting in:

$$-\frac{1}{\rho}\left[\frac{\partial p}{\partial x}\right]_z = -\left[\frac{\partial \Phi}{\partial x}\right]_p$$
$$-\frac{1}{\rho}\left[\frac{\partial p}{\partial y}\right]_z = -\left[\frac{\partial \Phi}{\partial y}\right]_p \, .$$

Substitution in Eq. 3.11 results in Eq. 3.12.

Frame 3.8: Conversion to pressure coordinates.

Pressure coordinates

A disadvantage of the expression for the geostrophic wind in Eq. 3.11 is the fact that air density is needed for the calculation and the method is not easily applicable away from surfaces of constant height for which the equation is derived. When we analyze the atmosphere away from the surface, in meteorology it is customary to present the height of a constant pressure level instead of looking at levels of constant height (z). To that end, a number of standard pressure levels are defined: 1000, 925, 850, 700, 500, 400, 300 hPa etc. The geostrophic wind ($\vec{V}_g = (u_g, v_g)$) at the constant pressure level is a simple function of the slope of that particular pressure level:

$$u_g = -\frac{1}{f}\left[\frac{\partial \Phi}{\partial y}\right]_p \quad , \quad v_g = +\frac{1}{f}\left[\frac{\partial \Phi}{\partial x}\right]_p \, , \tag{3.12}$$

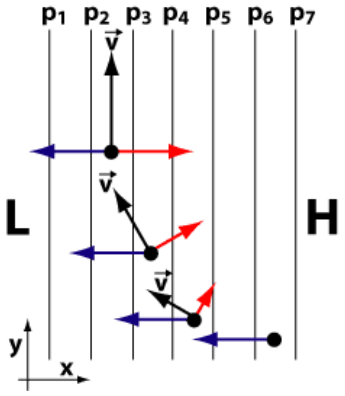

Figure 3.12: The development of geostrophic wind in the Northern Hemisphere.

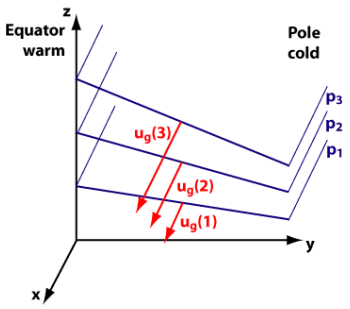

Figure 3.13: Changing layer thickness and geostrophic wind.

in which Φ is the geopotential. The derivation of these expressions is given in Frame 3.8. Note that the equations for motion also can be written in pressure coordinates.

$$\begin{aligned} \frac{du}{dt} &= -\left[\frac{\partial \Phi}{\partial x}\right]_p + fv + \text{friction} \\ \frac{dv}{dt} &= -\left[\frac{\partial \Phi}{\partial y}\right]_p - fu + \text{friction} \end{aligned} \tag{3.13}$$

3.3.6 Thermal wind

From the hydrostatic equation (Eq. 2.10) it is clear that the height of a pressure level depends on air density and therefore on air temperature. A result of this dependence of layer thickness on temperature is that the levels of constant pressure in the atmosphere are sloped from equator to the poles (Figure 3.13). Furthermore, because the mean atmospheric temperature decreases with latitude, the pole-equator slope of constant pressure levels also steepens with height. This causes the westerly wind to increase with height. This change of the geostrophic wind with height is called the thermal wind. The thermal wind explains the presence of the jet streams at the top of the troposphere (Figure 3.14). In the figure the slope in isotherms towards the poles is clear. In the region with the largest gradients, a maximum in wind speed is observed, the jet streams.

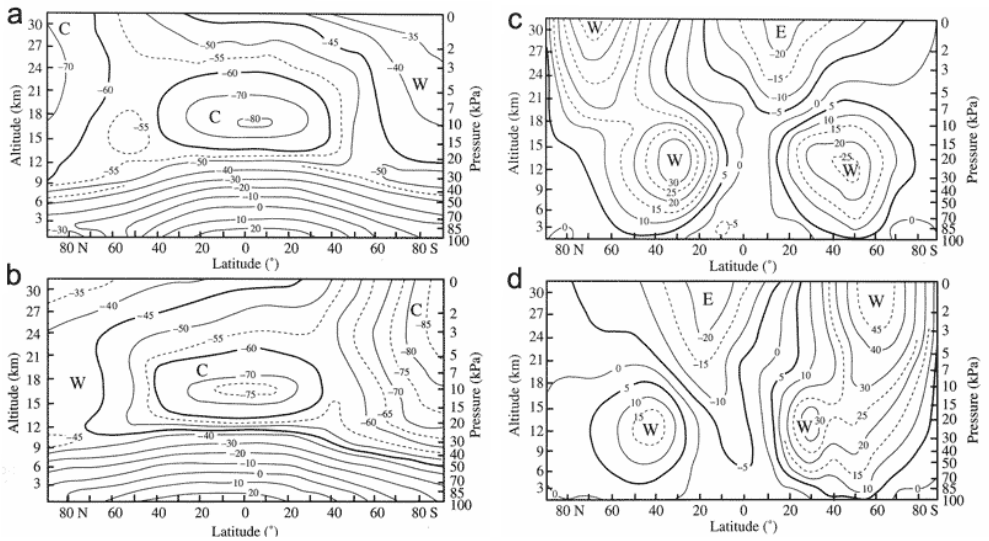

Figure 3.14: Zonal mean temperature (°C) (a and b) and mean zonal wind distribution ($m\,s^{-1}$) (c and d) for December January February (a and c) and June July August (b and d). Note that one of the vertical axes in the figures must be wrong.

Example Consider the layer between $p_1 = 850\,\text{hPa}$ and $p_2 = 700\,\text{hPa}$. For $\overline{T} = 270\,\text{K}$:

$$\Delta Z \cong \frac{\Phi_2 - \Phi_1}{g_0} = R_d \overline{T} \ln\left(\frac{p_1}{p_2}\right) \quad = \quad 287.05 * 270 * \ln\left(\frac{850}{700}\right) = 1505\,\text{m}$$

For $\overline{T} = 230\,\text{K}$:

$$\Delta Z \cong \frac{\Phi_2 - \Phi_1}{g_0} = R_d \overline{T} \ln\left(\frac{p_1}{p_2}\right) \quad = \quad 287.05 * 230 * \ln\left(\frac{850}{700}\right) = 1282\,\text{m}$$

Z is the geopotential height defined as $Z = \Phi(z)/g_0$. Note that Z is numerically almost identical to the height z, but incorporates the effect of temperature.

Frame 3.9: Effect of temperature on layer thickness.

To derive an expression for the thermal wind we first derive the hypsometric relation, which relates the layer thickness to the mean layer temperature. First combine the hydrostatic equation (Eq. 2.10), the gas law (Eq. 2.9) and the geopotential:

$$dp = -\rho g dz = -\frac{pg}{R_d T} dz = -\frac{p}{R_d T} d\Phi \ .$$

Rearange to form:

$$-R_d T d\ln p = d\Phi \ ,$$

and integrate between pressure levels p_1 and p_2 ($p_1 > p_2$). This results in the hypsometric relation:

$$\Phi_2 - \Phi_1 = R_d \overline{T} \ln\left(\frac{p_1}{p_2}\right) \ , \quad \text{where} \quad \overline{T} \equiv \frac{\int_{p_1}^{p_2} T d\ln p}{\int_{p_1}^{p_2} d\ln p} \tag{3.14}$$

$\overline{T}$ is the mean temperature of the level between p_1 and p_2. Frame 3.9 presents an example of the effect of different temperatures on layer thickness.

The thermal wind components can be written in terms of the average layer temperature $\overline{T}$ and upper and lower pressure level of the layer under consideration (see Frame 3.10 for derivation):

$$\begin{aligned} u_T \equiv \quad u_g(p_2) - u_g(p_1) = \quad & -\frac{R_d}{f}\left[\frac{\partial \overline{T}}{\partial y}\right]_p \ln\left(\frac{p_1}{p_2}\right) \\ v_T \equiv \quad v_g(p_2) - v_g(p_1) = \quad & +\frac{R_d}{f}\left[\frac{\partial \overline{T}}{\partial x}\right]_p \ln\left(\frac{p_1}{p_2}\right) \end{aligned} \tag{3.15}$$

or in terms of changing layer thickness by susbtitution of the hypsometric equation (Eq. 3.14):

$$\begin{aligned} u_T \quad &= \quad -\frac{1}{f}\frac{\partial}{\partial y}(\Phi_2 - \Phi_1) \\ v_T \quad &= \quad +\frac{1}{f}\frac{\partial}{\partial x}(\Phi_2 - \Phi_1) \end{aligned} \tag{3.16}$$

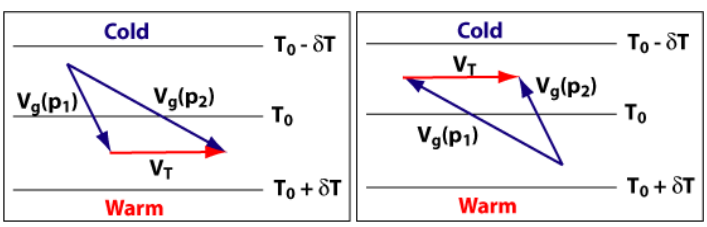

Figure 3.15: a) Backing (turning counterclockwise) of the wind with height in case of cold advection. b) Veering (turning clockwise) of the wind with height in case of warm advection. In the Northern Hemisphere.

The thermal wind is derived from the geostrophic wind by integration of Eq. 3.12 to p and making use of the hydrostatic balance (Eq. 2.10) and the gas law (Eq. 2.9). For the u_g-component, first integration to p:

$$u_g = -\frac{1}{f}\frac{\partial \Phi}{\partial y} \Rightarrow \frac{\partial u_g}{\partial p} = -\frac{1}{f}\frac{\partial}{\partial y}\frac{\partial \Phi}{\partial p},$$

and then substitution of $\partial p/\partial z = -\rho g$ and $p = \rho R_d T$:

$$\frac{\partial \Phi}{\partial p} = g\frac{\partial z}{\partial p} = -\frac{1}{\rho} = -\frac{R_d T}{p}.$$

The thermal wind relation for both components becomes:

$$\frac{\partial u_g}{\partial \ln p} = +\frac{R_d}{f}\left[\frac{\partial T}{\partial y}\right]_p$$

$$\frac{\partial v_g}{\partial \ln p} = -\frac{R_d}{f}\left[\frac{\partial T}{\partial x}\right]_p$$

Or in vector form: $$\frac{\partial \vec{V}_g}{\partial \ln p} = -\frac{R_d}{f}\vec{k} \times \nabla_p T$$

Integration between p_1 and p_2 gives the thermal wind components (Eq. 3.15) with $\overline{T}$ the mean layer temperature. Using the hypsometric equation (Eq. 3.14) the thermal wind can also be written in terms of the layer thickness. To that end substitute:

$$\overline{T} = \frac{\Phi_2 - \Phi_1}{R_d \ln\left(\frac{p_1}{p_2}\right)}.$$

Note that in Eq. 3.15 the horizontal differential is along a pressure level, i.e. p is constant. The result is Eq. 3.16, which can also be written in vector form:

$$\vec{V}_T = \frac{1}{f}\vec{k} \times \nabla(\Phi_2 - \Phi_1)$$

Frame 3.10: The thermal wind equation.

These equations show that the strength of the thermal wind is determined by the thickness of the layer and the horizontal temperature gradient.

With the thermal wind relation the pressure, temperature and geostrophic wind fields in the atmosphere are coupled. This has important diagnostic applications. The relation can be used to check the consistency of balloon soundings or in the initialization of Numerical Weather Prediction Models.

The thermal wind can also be used as a diagnostic tool. For example to observe cold or warm air advection. When the geostrophic wind blows under an angle with the isotherms, the wind will advect the colder or warmer air with it. The thermal wind blows parallel to the isotherms with the warm air to the right when facing down stream in the Northern Hemisphere (to the left in the southern Hemisphere). Thus, the geostrophic wind will turn with altitude (see Figure 3.15) in case of advection. A vertical wind profile can therefore give a reasonable estimate of horizontal advection.

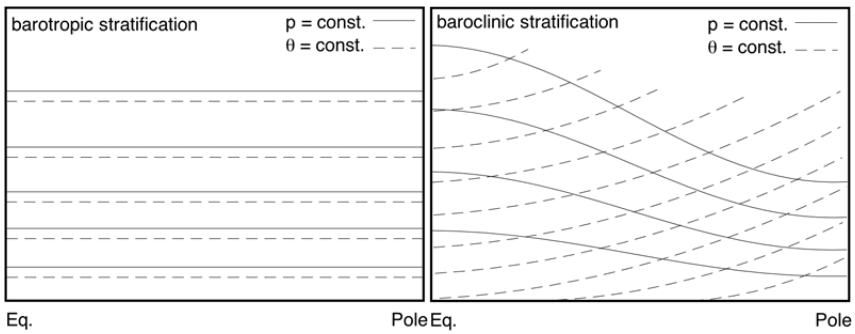

Figure 3.16: Different type of stratification in the atmosphere

Assume a purely zonal (East-West) geostrophic flow, which means a stationary flow with no friction effects or advection.

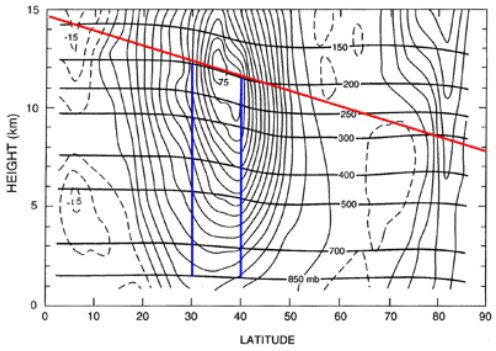

Question Calculate the strength of the jet stream, by calculating the zonal geostrophic wind (Eq. 3.12).

$$u_g = -\frac{1}{f}\left[\frac{\partial \Phi}{\partial y}\right]_p$$

Note that the figure is for the Northern Hemisphere.

Answer The maximum of the jet is at 35°N, so $f = 2\Omega\sin\phi = 2{*}7.3{\times}10^{-5}{*}\sin(35) = 0.84{\times}10^{-4}\,\mathrm{s}^{-1}$.
The change in layer thickness in the y-direction (south-north) is taken as the slope of the $p = 200\,\mathrm{hPa}$ level through the maximum in zonal wind:

$$\frac{\partial \Phi}{\partial y} \cong g_0 \frac{\Delta z}{\Delta y} = 9.81\,\mathrm{m\,s^{-2}}\,\frac{6.7\ \mathrm{km}}{10000\ \mathrm{km}} = 0.00657\,\mathrm{m\,s^{-2}}$$

Combining these results gives a geostrophic wind $u_g \cong 78\,\mathrm{m\,s^{-1}}$.

Question Calculate the zonal thermal wind between the 850 and 200 hPa levels.

Answer

$$u_T \equiv u_{g,200} - u_{g,850} = -\frac{1}{f}\frac{\partial}{\partial y}(\Phi_{200} - \Phi_{850}) \cong -\frac{1}{f}\frac{\Delta(\Phi_{200} - \Phi_{850})}{\Delta y}$$

At 30°N: $\Phi_{200} - \Phi_{850} \approx g_0(z_{200} - z_{850}) = g_0 * (12100 - 1500) = g_0 * 10600\,m^2\,s^{-2}$
At 40°N: $\Phi_{200} - \Phi_{850} \approx g_0(z_{200} - z_{850}) = g_0 * (11500 - 1450) = g_0 * 10050\,m^2\,s^{-2}$
Substitution results in:

$$u_T = -\frac{9.81\,m\,s^{-2}}{0.84\times10^{-4}\,s^{-1}}\,\frac{10050\,m - 10600\,m}{1110000\,m} = 58\,m\,s^{-1}$$

which is a reasonable number as can be seen in the figure. Contour line interval is $5\,\mathrm{m\,s^{-1}}$.

Frame 3.11: Example of the thermal wind, application to the jet stream

Barotropic vs baroclinic

A barotropic atmosphere is one in which the density depends only on the pressure ($\rho = \rho(p)$), so that the isobaric surfaces are also surfaces of constant density. For an ideal gas, the isobaric surfaces will also be isothermal. Since the thermal wind results from changes in temperature on an isobaric surface, in an barotropic atmosphere the thermal wind will be zero and the geostrophic wind does not change with height.

In a baroclinic atmosphere the density is also a function of temperature ($\rho = \rho(p, T)$), the thermal wind is therefore nonzero, and the geostrophic wind does change with height. Figure 3.16 illustrates a barotropic and baroclinic atmosphere. It shows that in a barotropic atmosphere, the temperature is constant along pressure levels so that θ and p levels coincide. In a baroclinic atmosphere, they do not.

3.4 Synoptic scale motions in mid-latitudes

In this section we apply the knowledge on motion in the atmosphere gained sofar on several synoptic scale phenomena observed at mid latitudes, e.g. polar fronts, Rossby waves and depression formation.

The u-component of the thermal wind:

$$u_T \equiv u_g(p_2) - u_g(p_1) = -\frac{R_d}{f}\left[\frac{\partial \overline{T}}{\partial y}\right]_p \ln\left(\frac{p_1}{p_2}\right)$$

$$\partial u_g = +\frac{R_d}{f}\left[\frac{\partial \overline{T}}{\partial y}\right]_p \partial \ln(p)$$

Substitute the hydrostatic equation ($\partial p/\partial z = -\rho g$) in which density ρ is replaced by $\rho = p/(R_d T)$, the gas law:

$$\partial \ln p = -\frac{g}{R_d T} dz \,,$$

results in:

$$\frac{\partial u_g}{\partial z} = -\frac{g}{f\overline{T}}\left[\frac{\partial \overline{T}}{\partial y}\right]_p \Rightarrow \frac{\Delta u_g}{\Delta z} = -\frac{g}{f\overline{T}}\frac{\Delta \overline{T}}{\Delta y}$$

In the last step the equation is made discrete to match front conditions. Rearranging the terms results in the given equation for the slope of an east-west orientated front (with a temperature gradient in the north-south direction).

Frame 3.12: The slope of a front.

3.4.1 The polar front

In the atmosphere we observe fronts, which are regions with a strong discontinuity in temperature, or the boundaries between two air masses. Fronts are produced by the rotation of the Earth through the thermal wind balance. The polar front is a special type of front, it demarcates the boundary between cold, polar air and mild, mid-latitude air. Across the polar front large temperature gradients exist. These large temperature gradients force the jet stream at approximate 10 km height via the thermal wind balance.

Fronts don't just exist at the surface of the earth, they have a vertical structure or slope. The slope of a front is dictated by the thermal wind balance. A vertical front (Figure 3.17a) does not obey the thermal wind relation because in that case the horizontal temperature gradients are NOT associated with vertical geostrophic wind gradients. In this configuration there are no vertical geostrophic wind gradients. In the case of a sloping front, there is a vertical geostrophic wind gradient. The slope of an east-west orientated front (with a temperature gradient in the north-south direction) can be calculated by:

$$\frac{\Delta z}{\Delta y} = -\frac{f\overline{T}}{g}\frac{\Delta u_g}{\Delta T} \,.$$

This relation is based on the u-component of the thermal wind in combination with the gas law and the hydrostatic equation (Frame 3.12).

For the polar front the greatest temperature contrasts are found between the continents and the oceans during winter. That is why in the winter period an outspoken longitudinal asymmetry shows up in the climatologies (Figure 3.18). Figure 3.18 presents the height of

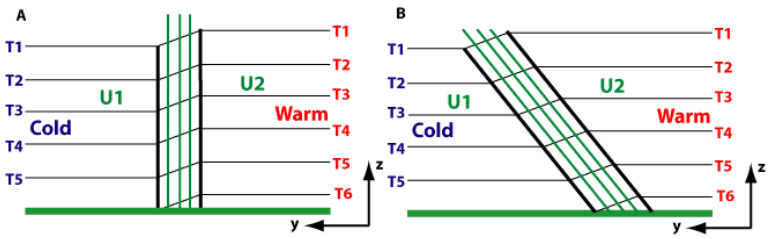

Figure 3.17: Schematic view of a front. a) unstable configuration, b) stable configuration.

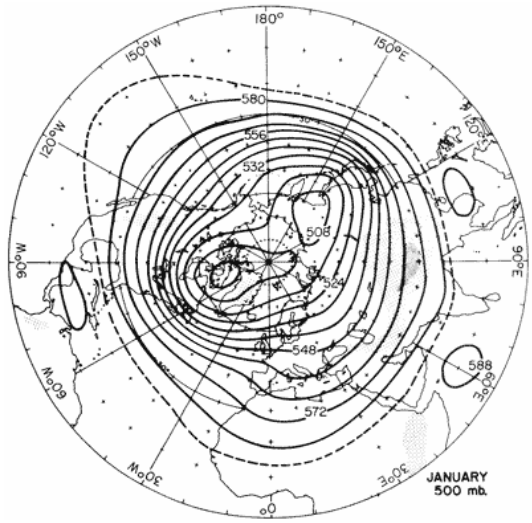

Figure 3.18: Height of the 500 hPa level for the Northern Hemisphere winter.

the 500 hPa level for the Northern Hemisphere winter. The height of the level is representative for the average temperature and strong changes in height therefore also denote strong temperature gradients. Furthermore, the flow is on average parallel to the isolines. Note the strong longitudinal asymmetry with stronger jets at the continental exit points. These form the starting points of the North Atlantic and Pacific storm tracks. Note that these are stationary features that show up in the climatologies, and are called standing Rossby waves. Rossby waves will be discussed later.

Heat is transported through the polar front. If this is not the case, the temperature gradients and strength of the jet stream would increase until the flow becomes dynamically unstable and mixing starts. This is called baroclinic instability. An expression of the dynamical instability of the polar front is its wavy character. These waves grow at the expense of the kinetic energy of the main circulation to form mid-latitude disturbances (depressions).

Warm and cold fronts

Besides the polar front, warm and cold fronts are typical features in the atmosphere. In general fronts are classified as to which type of air mass (cold or warm) is replacing the other. This means that a cold front demarcates the leading edge of a cold air mass displacing a warmer air mass, and a warm front is the leading edge of a warmer air mass replacing a colder air mass (Figure 3.19). If the front is essentially not moving (i.e. the air masses are not moving) it is called a stationary front.

The slope of warm and cold fronts differ. Warm fronts typically have a gentle slope so the air rising along the frontal surface is gradual. This usually favors the development of widespread layered or stratiform cloudiness and precipitation along and to the north of the

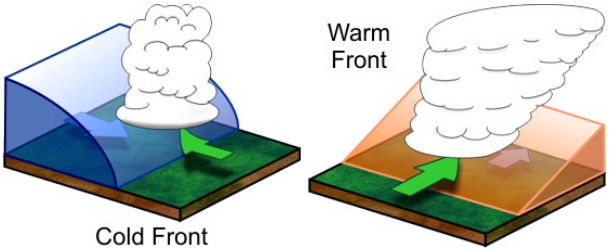

Figure 3.19: Illustration of a cold and warm front.

The continuity equation follows from considering an Eulerian control volume with mass inflow and outflow [$\mathrm{kg\,m^{-2}\,s^{-1}}$] (see figure). The center of the control volume is in x, y, z. Consider mass flow in the x-direction, with velocity component u:

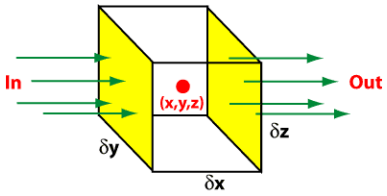

$$\text{In}: \quad \rho u \quad -\frac{\delta x}{2}\frac{\partial(\rho u)}{\partial x}$$
$$\text{Out}: \quad \rho u \quad +\frac{\delta x}{2}\frac{\partial(\rho u)}{\partial x}$$

The factor 2 results from the fact that x, y, z is the center of the volume. The net mass flow in/out the volume in the x-direction is the difference of the above fluxes times the area through which the flux flows:

$$(\text{In}-\text{Out})\delta y\delta z = -\frac{\partial(\rho u)}{\partial x}\delta x\delta y\delta z$$

Similar consideration lead to similar expressions for the y and z direction:

$$\begin{aligned} x&: -\tfrac{\partial(\rho u)}{\partial x}\delta x\delta y\delta z \\ y&: -\tfrac{\partial(\rho v)}{\partial y}\delta x\delta y\delta z \quad \Rightarrow -\left[\frac{\partial(\rho u)}{\partial x}+\frac{\partial(\rho v)}{\partial y}+\frac{\partial(\rho w)}{\partial z}\right]\delta x\delta y\delta z \\ z&: -\tfrac{\partial(\rho w)}{\partial z}\delta x\delta y\delta z \end{aligned}$$

The term to the right is the total net mass in/out the volume, which is the sum of the three separate terms. Per unit volume the mass change is then:

$$-\left[\frac{\partial(\rho u)}{\partial x}+\frac{\partial(\rho v)}{\partial y}+\frac{\partial(\rho w)}{\partial z}\right]$$

which must be equal to the local density change and results in Eq. 3.17, the mass divergence form of the continuity equation. If we write out Eq. 3.17:

$$\begin{aligned} \frac{\partial\rho}{\partial t}+\frac{\partial\rho u}{\partial x}+\frac{\partial\rho v}{\partial y}+\frac{\partial\rho w}{\partial z} &= \\ \frac{\partial\rho}{\partial t}+u\frac{\partial\rho}{\partial x}+v\frac{\partial\rho}{\partial y}+w\frac{\partial\rho}{\partial z}+\rho\left(\frac{\partial u}{\partial x}+\frac{\partial v}{\partial y}+\frac{\partial w}{\partial z}\right) &= \\ \frac{d\rho}{dt}+\rho\left(\frac{\partial u}{\partial x}+\frac{\partial v}{\partial y}+\frac{\partial w}{\partial z}\right) &= 0\,. \end{aligned}$$

The last part is Eq. 3.18, the velocity divergence form of the continuity equation.

Frame 3.13: Mass conservation equations.

front. The slope of cold fronts are more steep and air is forced upward more abruptly. This usually leads to a narrow band of showers and thunderstorms along or just ahead of the front, especially if the rising air is unstable.

The velocity of cold and warm fronts also differ. Cold fronts typically move faster than warm fronts, so in time they "catch up" to warm fronts. As the two fronts merge, an occluded front forms. In the occluded front, the cold air undercuts the cooler air mass associated with the warm front, further lifting the already rising warm air.

Fronts are usually detectable at the surface in a number of ways. Winds usually "converge" or come together at the fronts. Also, temperature differences can be quite noticeable from one side of the front to another. Finally, the pressure on either side of a front can vary significantly.

3.4.2 Mass conservation

The occurence of Rossby waves (Figure 3.18) is the result of conservation of vorticity. To derive the vorticity equation we first must derive the continuity equation, which describes

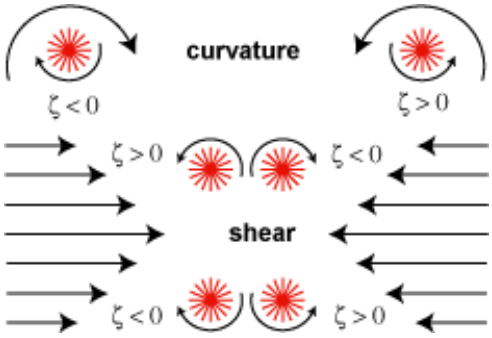

Figure 3.20: Curvature and shear vorticity. $\zeta = \frac{\partial v}{\partial x} - \frac{\partial u}{\partial y}$.

the conservation of mass. The derivation of the continuity equation is given in Frame 3.13. The mass divergence form of the continuity equation is:

$$\frac{\partial \rho}{\partial t} + \frac{\partial \rho u}{\partial x} + \frac{\partial \rho v}{\partial y} + \frac{\partial \rho w}{\partial z} = 0 \,, \tag{3.17}$$

which states that the mass change per unit volume equals the local density change. When you write this out and regroup the terms, the divergence of the velocity field emerges:

$$\frac{\partial u}{\partial x} + \frac{\partial v}{\partial y} + \frac{\partial w}{\partial z} \,,$$

and the continuity equation is written in its velocity divergence form:

$$\frac{1}{\rho}\frac{d\rho}{dt} + \frac{\partial u}{\partial x} + \frac{\partial v}{\partial y} + \frac{\partial w}{\partial z} = 0 \tag{3.18}$$

which states that the total rate of density change minus the divergence of the velocity field is 0. For an incompressible fluid $d\rho/dt = 0$ and the continuity equation reduces to:

$$\frac{\partial u}{\partial x} + \frac{\partial v}{\partial y} + \frac{\partial w}{\partial z} = 0 \,, \tag{3.19}$$

i.e. the divergence of the velocity field is 0 for an incompressible fluid.

3.4.3 Vorticity

The next step in studying large scale motions in the atmosphere is to derive the vorticity equation. We are interested in vorticity because it is highly correlated with with synoptic-scale weather disturbances. Vorticity is the microscopic measure of rotation in a fluid, it is the spin of an infinitesimal fluid element about its own axis. In mathematical form vorticity is defined as the curl of the fluid velocity:

$$\omega = \nabla \times \vec{V} = \begin{vmatrix} i & j & k \\ \frac{\partial}{\partial x} & \frac{\partial}{\partial y} & \frac{\partial}{\partial z} \\ u & v & w \end{vmatrix} = \begin{pmatrix} \frac{\partial w}{\partial y} - \frac{\partial v}{\partial z} \\ \frac{\partial u}{\partial z} - \frac{\partial w}{\partial x} \\ \frac{\partial v}{\partial x} - \frac{\partial u}{\partial y} \end{pmatrix} \,,$$

and is a vector quantity, directed along the axis of rotation perpendicular to the surface of the fluid element.

In both the atmosphere and ocean the large scale motion is predominantly horizontal because vertical velocities are in general much smaller than horizontal velocities. That is why the vertical component of vorticity is most useful for aiding an understanding of the large scale motions in the atmosphere:

$$\zeta = \frac{\partial v}{\partial x} - \frac{\partial u}{\partial y} \tag{3.20}$$

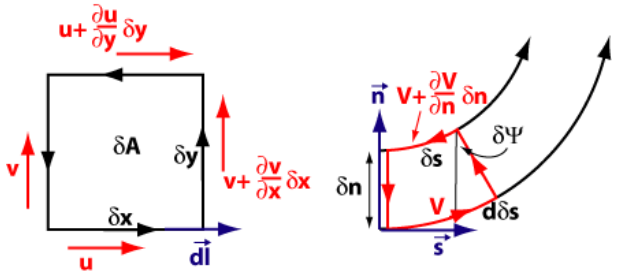

Figure 3.21: Circulation, a macroscopic measure of fluid rotation. a) Cartesian coordinates, b) natural coordinates.

We can distinguish two types of vorticity, curvature and shear vorticity. Curvature vorticity results from a curve in the flow pattern itself. Shear vorticity results from horizontal changes in the velocity field. Both are illustrated in Figure 3.20. Vorticity is said to be positive when the rotation is counterclockwise and negative for clockwise rotation.

To illustrate how to interpret vorticity consider circulation, which is a macroscopic measure of fluid rotation. Circulation is the integral of velocity V over a closed contour with length dl:

$$C = \oint V \bullet dl \; .$$

Vorticity is then the change in circulation per surface area δA in the limit of δA to 0: $\zeta \equiv \lim_{\delta A \to 0} \frac{\delta C}{\delta A}$. To determine δC consider the circulation about a rectangular element in the x, y plane as illustrated in Figure 3.21a. The rectangle is located in a field with a velocity gradient in the x and y-direction. The change in circulation δC is the sum of velocity times distance over each side of the rectangle:

$$\begin{aligned} \delta C &= u\delta x + \left(v + \frac{\partial v}{\partial x}\delta x\right)\delta y \\ &\quad - \left(v + \frac{\partial u}{\partial y}\delta y\right)\delta x - v\delta y \\ &= \left(\frac{\partial v}{\partial x} - \frac{\partial u}{\partial y}\right)\delta x \delta y \; . \end{aligned}$$

Therefore, with $\delta A = \delta x \delta y$, vorticity ζ becomes:

$$\zeta \equiv \lim_{\delta A \to 0} \frac{\delta C}{\delta A} = \left(\frac{\partial v}{\partial x} - \frac{\partial u}{\partial y}\right) \; ,$$

which equals Eq. 3.20.

Vorticity in natural coordinates

Similarly as in cartesian coordinates, vorticity in natural coordinates can be illustrated by looking at circulation. To determine δC consider circulation about an element as illustrated in Figure 3.21b. The element is located in a field with a velocity gradient. δC is again the sum of velocity times distance over each side of the element:

$$\delta C = V(\delta s + d\delta s) - (V + \frac{\partial V}{\partial n}\delta n)\delta s \; .$$

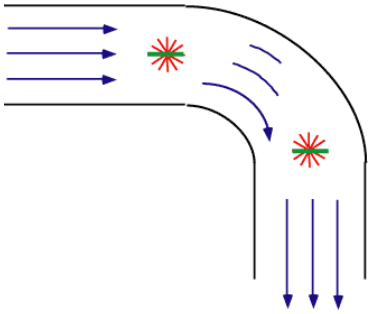

Figure 3.22: Shear and curvature vorticity in a frictionless pipe. Upstream of the bend the vorticity is zero.

Note that velocity is defined along $\vec{s}$ and therefore zero along $\vec{n}$. Assuming the angle $\delta\Psi$, made over the curve, is small, $d\delta s = \delta\Psi\delta n$. Then the circulation can be written as:

$$\begin{aligned}
\delta C &= V(\delta s + \delta\Psi\delta n) - (V + \frac{\partial V}{\partial n}\delta n)\delta s \\
&= V\delta s + V\delta\Psi\delta n - V\delta s - \frac{\partial V}{\partial n}\delta n\delta s \\
&= \left(V\frac{\delta\Psi}{\delta s} - \frac{\partial V}{\partial n}\right)\delta n\delta s
\end{aligned}$$

Now take the limit of δs and δn to 0:

$$\zeta \equiv \lim_{\delta s,\delta n\to 0}\frac{\delta C}{\delta n\delta s} = \left(V\frac{\delta\Psi}{\delta s} - \frac{\partial V}{\partial n}\right) .$$

Thus the vertical component of the vorticity is the result of the sum of two parts; curvature vorticity (first term on the right hand side) which represents in the atmosphere the turning of the wind along a streamline, and shear vorticity (second term on the right hand side) which represents the rate of change of wind speed normal to the direction flow. So straight-line motion has non-zero vorticity in the presence of shear (e.g. jet stream!) but curved flow may have zero vorticity if 1) and 2) cancel, for example in a frictionless pipe flow with zero vorticity upstream of a bend (Figure 3.22). Curvature vorticity rotates the fluid parcel clockwise ($V/R < 0$) while shear vorticity rotates the parcel counterclockwise ($\partial V/\partial n < 0$) as fluid along the inner boundary on the curve flows faster in just the right proportions so that the parcel does not turn.

Vorticity in the atmosphere

In dynamical meteorology we are chiefly interested in the vertical component of the vorticity (from now on just called vorticity), because it is highly correlated with with synoptic-scale weather disturbances. We define the vertical component of the *absolute* vorticity as:

$$\eta \equiv \vec{k}\cdot(\nabla\times\vec{V_a}) = \frac{\partial v_a}{\partial x} - \frac{\partial u_a}{\partial y} ,$$

with $\vec{V_a}$ the absolute velocity. The vertical component of the *relative* vorticity is given by:

$$\zeta \equiv \vec{k}\cdot(\nabla\times\vec{V}) = \frac{\partial v}{\partial x} - \frac{\partial u}{\partial y} ,$$

The difference between the absolute and relative vorticity is given by the vertical component of the vorticity of the Earth due to its rotation:

$$\vec{k}\cdot(\nabla\times\vec{V_{Earth}}) = 2\Omega\sin\phi = f ,$$

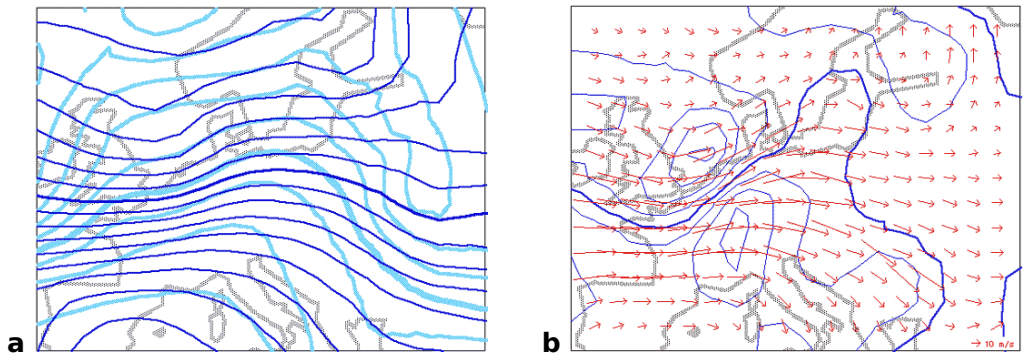

Figure 3.23: Analyses of the storm of 27 October 2002. a) Height of the 500 hPa surface (solid), contour interval is 50 m, thick line is 5500 m, and temperature at 500 hPa (grey), contour interval is 2.5°C, thick line is -20°C. b) Relative vorticity at 500 hPa, contour interval is $0.25\times10^{-4}\,s^{-1}$, thick line is $0\,s^{-1}$, and wind velocity vectors.

which is the coriolis parameter. Thus, absolute vorticity is relative vorticity plus the coriolis parameter representing the Earth vorticity:

$$\eta = \zeta + f \ .$$

As an example consider motion at mid latitudes. Typical scales then are wind speed $U = 10\,m\,s^{-1}$, and horizontal scale $L = 1000\,km$, which gives:

$$\zeta = \frac{\partial v}{\partial x} - \frac{\partial u}{\partial y} \leq \frac{U}{L} \approx \frac{10\ m\,s^{-1}}{1000\ km} = 10^{-5}\ s^{-1} \ .$$

The $\leq$ sign derives from the fact that the two terms will partially cancel: the above scale analysis thus provides a maximum value. Apparently relative vorticity is significantly smaller than the planetary vorticity, which at middle latitudes is an order of magnitude larger ($10^{-4}\,s^{-1}$). Figure 3.23 illustrates the connection between relative vorticity and meanders in the jet stream visualised as the height of the 500 hPa field for the storm that tracked over western Europe, 27 October 2002.

The vorticity equation

To describe the evolution of vorticity in the atmosphere we use the vorticity equation (Frame 3.14) for an incompressible fluid. At mid latitudes this equation reads:

$$\frac{d_h(\zeta+f)}{dt} = (\zeta+f)\frac{\partial w}{\partial z} \approx f\frac{\partial w}{\partial z} \ . \tag{3.21}$$

For a pure horizontal flow $w = 0$ and this equation reduces to:

$$\frac{d_h(\zeta+f)}{dt} = 0 \ , \tag{3.22}$$

the barotropic vorticity equation. This equation states that the absolute vorticity is conserved for a pure horizontal synoptic scale motions at mid latitudes.

Eq. 3.22 helps us to explain the meanders visible in the jet stream visualised by the height of the 500 hPa level (Figure 3.24). These meanders are the representation of Planetary or Rossby waves in the atmosphere. Planetary or Rossby waves are the wave type of most importance for large-scale meteorological processes. Three applications of the vorticity equation are given below; the free propagating Rossby wave, the topographic (stationary) Rossby wave, and thermal highs and lows.

From the equations of motion we derive an equation for the rate of change of vorticity by taking:

$$\frac{\partial}{\partial x}\frac{dv}{dt} - \frac{\partial}{\partial y}\frac{du}{dt}.$$

With: $\frac{\partial}{\partial y}\frac{du}{dt} = \frac{\partial}{\partial y}\left[\frac{\partial u}{\partial t} + u\frac{\partial u}{\partial x} + v\frac{\partial u}{\partial y} + w\frac{\partial u}{\partial z} = -\frac{1}{\rho}\frac{\partial p}{\partial x} + fv\right]$

$$= \left[\frac{\partial^2 u}{\partial t \partial y} + \frac{\partial u}{\partial y}\frac{\partial u}{\partial x} + u\frac{\partial^2 u}{\partial y \partial x} + \frac{\partial v}{\partial y}\frac{\partial u}{\partial y} + v\frac{\partial^2 u}{\partial y^2} + \frac{\partial w}{\partial y}\frac{\partial u}{\partial z} + w\frac{\partial^2 u}{\partial y \partial z} = -\frac{\partial \rho^{-1}}{\partial y}\frac{\partial p}{\partial x} - \rho^{-1}\frac{\partial^2 p}{\partial y \partial x} + f\frac{\partial v}{\partial y} + v\frac{\partial f}{\partial y}\right]$$

and: $\frac{\partial}{\partial x}\frac{dv}{dt} = \frac{\partial}{\partial x}\left[\frac{\partial v}{\partial t} + u\frac{\partial v}{\partial x} + v\frac{\partial v}{\partial y} + w\frac{\partial v}{\partial z} = -\frac{1}{\rho}\frac{\partial p}{\partial y} - fu\right]$

$$= \left[\frac{\partial^2 v}{\partial t \partial x} + \frac{\partial u}{\partial x}\frac{\partial v}{\partial x} + u\frac{\partial^2 v}{\partial x^2} + \frac{\partial v}{\partial x}\frac{\partial v}{\partial y} + v\frac{\partial^2 v}{\partial x \partial y} + \frac{\partial w}{\partial x}\frac{\partial v}{\partial z} + w\frac{\partial^2 v}{\partial x \partial z} = -\frac{\partial \rho^{-1}}{\partial x}\frac{\partial p}{\partial y} - \rho^{-1}\frac{\partial^2 p}{\partial x \partial y} - f\frac{\partial u}{\partial x} - u\frac{\partial f}{\partial x}\right]$$

Combining these and using $\frac{\partial}{\partial x}\rho^{-1} = -\rho^{-2}\frac{\partial \rho}{\partial x}$ results in:

$$\frac{\partial}{\partial t}\left(\frac{\partial v}{\partial x} - \frac{\partial u}{\partial y}\right) + \frac{\partial u}{\partial x}\left(\frac{\partial v}{\partial x} - \frac{\partial u}{\partial y}\right) + u\left[\frac{\partial}{\partial x}\left(\frac{\partial v}{\partial x} - \frac{\partial u}{\partial y}\right)\right] + \frac{\partial v}{\partial y}\left(\frac{\partial v}{\partial x} - \frac{\partial u}{\partial y}\right) + v\left[\frac{\partial}{\partial y}\left(\frac{\partial v}{\partial x} - \frac{\partial u}{\partial y}\right)\right]$$
$$+ \frac{\partial w}{\partial x}\frac{\partial v}{\partial z} - \frac{\partial w}{\partial y}\frac{\partial u}{\partial z} + w\left[\frac{\partial}{\partial z}\left(\frac{\partial v}{\partial x} - \frac{\partial u}{\partial y}\right)\right]$$
$$= \frac{1}{\rho^2}\left(\frac{\partial \rho}{\partial x}\frac{\partial p}{\partial y} - \frac{\partial \rho}{\partial y}\frac{\partial p}{\partial x}\right) - f\left(\frac{\partial u}{\partial x} + \frac{\partial v}{\partial y}\right) - u\frac{\partial f}{\partial x} - v\frac{\partial f}{\partial y}$$

The next step is to use the definition of $\zeta = \left(\frac{\partial v}{\partial x} - \frac{\partial u}{\partial y}\right)$ and the fact that f only varies in the y direction so that

$$\frac{df}{dt} = \frac{\partial f}{\partial t} + u\frac{\partial f}{\partial x} + v\frac{\partial f}{\partial y} + w\frac{\partial f}{\partial z} = v\frac{df}{dy} \quad \text{gives:}$$

$$\frac{\partial \zeta}{\partial t} + u\frac{\partial \zeta}{\partial x} + v\frac{\partial \zeta}{\partial y} + w\frac{\partial \zeta}{\partial z} + \zeta\left(\frac{\partial u}{\partial x} + \frac{\partial v}{\partial y}\right) + \frac{\partial w}{\partial x}\frac{\partial v}{\partial z} - \frac{\partial w}{\partial y}\frac{\partial u}{\partial z} = \frac{1}{\rho^2}\left(\frac{\partial \rho}{\partial x}\frac{\partial p}{\partial y} - \frac{\partial \rho}{\partial y}\frac{\partial p}{\partial x}\right) - f\left(\frac{\partial u}{\partial x} + \frac{\partial v}{\partial y}\right) - v\frac{df}{dy}$$

$$\frac{d\zeta}{dt} + \frac{df}{dt} = \frac{d(\zeta + f)}{dt} = -(\zeta + f)\left(\frac{\partial u}{\partial x} + \frac{\partial v}{\partial y}\right) + \left(\frac{\partial w}{\partial x}\frac{\partial v}{\partial z} - \frac{\partial w}{\partial y}\frac{\partial u}{\partial z}\right) + \frac{1}{\rho^2}\left(\frac{\partial \rho}{\partial x}\frac{\partial p}{\partial y} - \frac{\partial \rho}{\partial y}\frac{\partial p}{\partial x}\right)$$

The first term on the righthand side is the divergence term, the second term the twisting or tilting term and the third term the solenoidal term. Based on scale analyses, the vertical advection, the tilting term and the solenoidal term are neglected, resulting in:

$$\frac{d_h(\zeta + f)}{dt} = -(\zeta + f)\left(\frac{\partial u}{\partial x} + \frac{\partial v}{\partial y}\right) \cong -f\left(\frac{\partial u}{\partial x} + \frac{\partial v}{\partial y}\right)$$

with $\frac{d_h}{dt} = \frac{\partial}{\partial t} + u\frac{\partial}{\partial x} + v\frac{\partial}{\partial y}$ the total horizontal derivative. Using the incompressible form of the continuity equation: $\frac{\partial u}{\partial x} + \frac{\partial v}{\partial y} + \frac{\partial w}{\partial z} = 0$ results in Eq. 3.21.

Frame 3.14: The vorticity equation.

Free propagating Rossby waves

In a barotropic atmosphere the Rossby wave is an absolute vorticity conserving motion which owes its existence to the variation of the Coriolis force with latitude, the so-called β-effect ($\beta = df/dy$). Eq. 3.22 shows that if absolute vorticity is conserved, meridional (north-south) displacement of fluid particles, which will change f, will induce relative vorticity in order for the absolute vorticity to be conserved. This is illustrated in Figure 3.25. On the Norhtern Hemisphere, a displacement to the north results in an increase in f, therefore, ζ must be < 0 giving a clockwise rotation. A displacement to the south results in a decrease in f, therefore, ζ must be > 0 giving a counterclockwise rotation. Combined, the result is a wave around the latitude of its original location.

The Rossby wave described in Figure 3.25 propagates. This can be understood as follows: consider a closed chain of parcels aligned along a circle of latitude with $z = 0$ at time t_0. Suppose at t_1 a parcel is displaced a distance δy from the original latitude. Conservation of

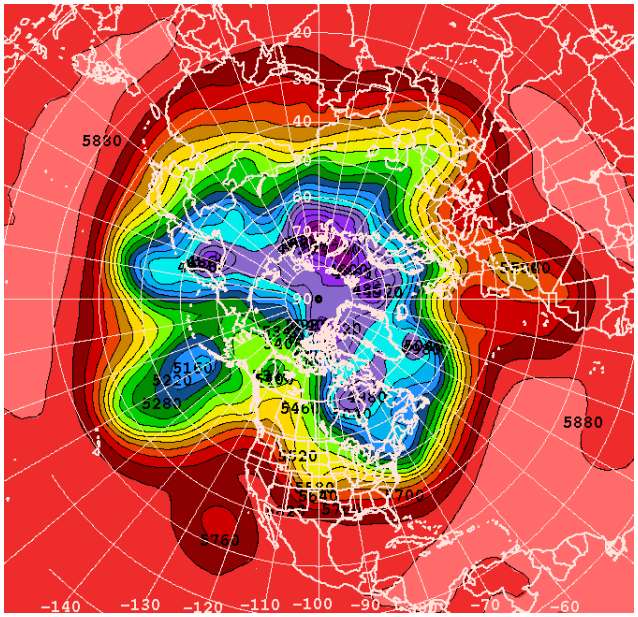

Figure 3.24: Height of the 500 hPa level in January 2003.

vorticity results in:

$$f_{t_0} = (\zeta + f)_{t_1} \quad \rightarrow \quad \zeta_{t_1} = f_{t_0} - f_{t_1} = -\frac{\partial f}{\partial y}\delta y = -\beta \delta y$$

Thus the change in relative vorticity equals the gradient in f times the displacement.

It is evident that if the chain of parcels is subjected to a sinusoidal meridional displacement then the induced perturbation in vorticity will be positive (cyclonic) for a southward displacement and negative (anticyclonic) for a northward displacement. Thus, the pattern of vorticity maxima and minima propagates to the west, which constitutes a free propagating Rossby wave (Figure 3.26).

It is possible to derive the dispersion relation for free propagating Rossby waves. A dispersion relation describes the relation between energy of the system, which is proportional to the frequency of the wave, and momentum, which is proportional to the wave number. The dispersion relation for the free propagating Rossby wave is derived in Frame 3.15 and reads:

$$\omega k + \beta = 0 \quad \rightarrow \quad \omega = -\frac{\beta}{k}\,, \tag{3.23}$$

with ω the frequency of the wave ($= 2\pi/P$) and k the wavenumber in the x-direction (=

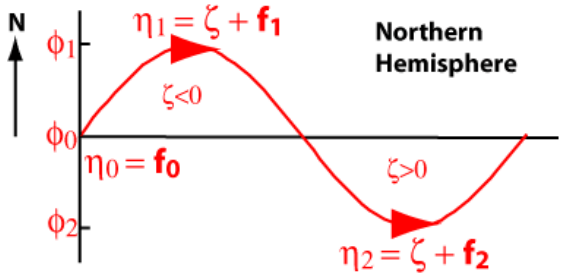

Figure 3.25: Conservation of absolute vorticity.

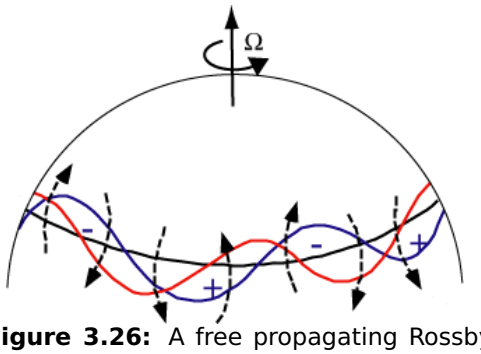

Figure 3.26: A free propagating Rossby wave.

The dispersion relation for Rossby waves follows from the conservation of absolute vorticity (barotropic vorticity equation):

$$\frac{d_h(\zeta+f)}{dt} = \frac{\partial\zeta}{\partial t} + u\frac{\partial\zeta}{\partial x} + v\frac{\partial\zeta}{\partial y} + \beta v = 0$$

Assume a simple distribution of meridional velocity given by:

$$v = v_0 \sin(\omega t - kx)$$

This results for the relative vorticity in:

$$\zeta = \frac{\partial v}{\partial x} - \frac{\partial u}{\partial y} = \frac{\partial v}{\partial x} = -k v_0 \cos(\omega t - kx)$$

with $\omega = 2\pi/P$ the frequency and $k = 2\pi/\lambda$ the wavenumber in the x-direction of the wave. λ is the wavelength. Substitute this in the barotropic vorticity equation results in the dispersion relation for Rossby waves, Eq. 3.23.

Examples of the relation between wavelength λ, period P and phase velocity c of Rossby waves:

λ (km)	P (days)	c (m s^{-1})
100	284	-0.004
1000	28	-0.41
5000	5.6	-10.3
10000	2.8	-41
20000	1.4	-164

Frame 3.15: The dispersion relation of the free propagating Rossby wave.

$2\pi/\lambda$, λ is the wave length). The phase velocity c of this wave is:

$$c \equiv \frac{\omega}{k} = -\frac{\beta}{k^2}$$

For Rossby waves c is always positive, i.e. always westwards, and it increases in magnitude with increasing wavelength. If the (westerly) tropospheric flow velocity is greater than the westward migration of the Rossby wave, the wave will move eastward relative to the surface. Very long Rossby waves therefore will tend to travel westward and shorter waves eastward. The most likely stationary wavelength is somewhere between 5000 and 10 000 km. In Figure 3.24 λ is ∼7000 km. Frame 3.15 presents some examples of the relation between wavelength λ, period P and phase velocity c of Rossby waves.

Topographic (stationary) Rossby waves

The topographic Rossby wave arrises when we allow for vertical motion in the vorticity equation (Eq. 3.21). Again we assume a barotropic atmosphere (no change of geostrophic wind with height). Integrating Eq. 3.21 between two levels results in:

$$\frac{d_h}{dt}\frac{(\zeta+f)}{H} = 0\ , \tag{3.24}$$

with H the thickness of the layer between the two levels (see Frame 3.16). This equation describes the conservation of *potential* vorticity for a barotropic fluid. The potential vorticity is a measure of the ratio of the absolute vorticity to the effective depth of the vortex.

Eq. 3.24 describes how a wave in the horizontal plane developes due to a flow over a topographic baries. This is illustrated in Figure 3.27 for the Northern Hemisphere. First look at the case where we have a westerly zonal flow. If this zonal flow encounters a topographical barrier, the depth of the column will decrease (Figure 3.27a). In order for potential vorticity to remain conserved, absolute vorticity must also decrease. If upstream $\zeta = 0$, this can only be achieved by ζ becoming negative, i.e. anticyclonic (southward)

Assume a barotropic atmosphere, integrate the vorticity equation (Eq. 3.21) between two levels D_1 and D_2:

$$\begin{aligned}
\int_{D_1}^{D_2} \frac{d_h(\zeta+f)}{dt}\partial z &= \int_{w(D_1)}^{w(D_2)} (\zeta+f)\partial w \\
z\frac{d_h(\zeta+f)}{dt}|_{D_1}^{D_2} &= (\zeta+f)w|_{w(D_1)}^{w(D_2)} \\
\frac{d_h(\zeta+f)}{dt}(D_2-D_1) &= (\zeta+f)(w(D_2)-w(D_1))
\end{aligned}$$

Note that:

$$w(D_1)=\frac{dD_1}{dt}\ ,\ w(D_2)=\frac{dD_2}{dt}\ ,$$

and write $H = D_2 - D_1$, the thickness of the layer between the two levels. This results in:

$$\begin{aligned}
\frac{1}{(\zeta+f)}\frac{d_h(\zeta+f)}{dt} &= \frac{(w(D_2)-w(D_1)}{(D_2-D_1)} \\
\frac{1}{(\zeta+f)}\frac{d_h(\zeta+f)}{dt} &= \frac{1}{(D_2-D_1)}\left(\frac{dD_2}{dt}-\frac{dD_1}{dt}\right) \\
\frac{1}{(\zeta+f)}\frac{d_h(\zeta+f)}{dt} &= \frac{1}{H}\frac{d_h H}{dt} \\
\frac{d_h \ln(\zeta+f)}{dt} &= \frac{d_h \ln H}{dt} \\
\frac{d_h}{dt}(\ln(\zeta+f)-\ln H &= \frac{d_h}{dt}\ln\left(\frac{(\zeta+f)}{H}\right)=0\ ,
\end{aligned}$$

which is equivalent to Eq. 3.24 and describes conservation of potential vorticity for a barotropic fluid.

Frame 3.16: Topographic (stationary) Rossby waves.

curvature and a leeside trough forms. When the column has passed the barrier and has attained its original depth, it is southward of its original position (thus f smaller) and must start curving in a cyclonic sense to balance this deficit. Steady westerly flow over a barrier apparently results in a wavelike trajectory in the horizontal plane (Figure 3.27b).

In case of an easterly flow over a topographic barries, the situation is different. Suppose the flow would remain undisturbed until it reached the barrier (Figure 3.27c). Conservation of potential vorticity would induce a northward motion (ζ negative). But f becomes larger to the north, and even stronger decrease of ζ would is needed resulting in a complete reversal of the flow. Therefore, no steady-state potential vorticity conserving flow is possible. What actually happens in this case is that instead, the flow starts to adjust before it meets the barrier, i.e. it begins to curve cyclonically before the mountain. This curvature is produced by the pressure field generated by the mountain forcing. When the flow descends the process is simply reversed, and no wavelike pattern is found on the leeside.

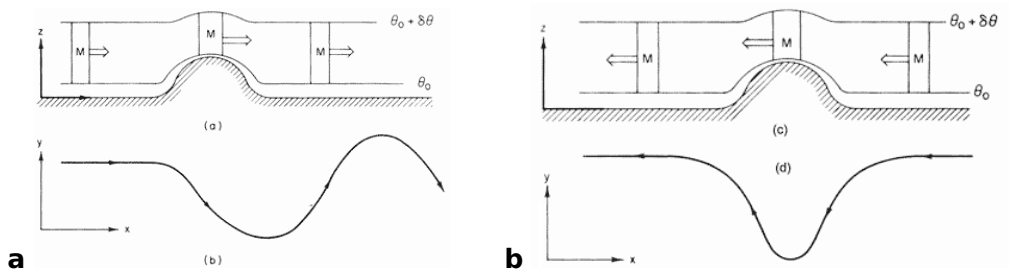

Figure 3.27: Topographic Rossby wave for a westerly (a,b) and easterly (c,d) flow on the Northern Hemisphere.

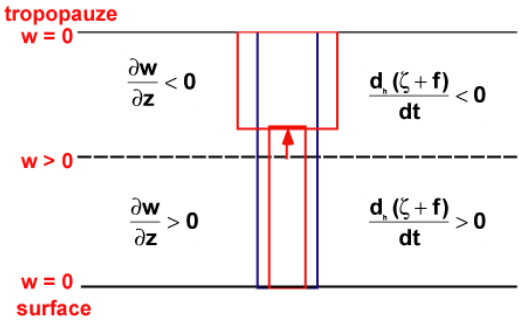

Figure 3.28: Development of a thermal high.

Thermal highs and lows

The third application of vorticity are thermal highs and lows. These may develop through local heating or cooling. Consider vertical troposheric motion where the latitudinal variation of f does not play a role. A column without relative vorticity becomes heated from below. The heated air starts to ris and accelerates upwards ($\partial w/\partial z > 0$). If the tropopauze acts as a lid to vertical motion the air is decelerated ($\partial w/\partial z < 0$). As a result (Eq. 3.21) cyclonic circulation (thermal low) is induced in the lower troposhere and anticyclonic circulation in the upper troposphere (Figure 3.28). The upward motion means inclusion of potentially very moist surrounding surface air which, upon condensation, could generate additional buoyancy. This is an important mechanism for tropical cyclone development. The reverse happens when the air is cooled from below.

Cyclogenesis

A final application is cyclogenesis, the growth of (mid-latitude) cyclones. First we look at baroclinic instability. The polar front in the atmosphere is not in equilibrium. If it were, it would not allow transport of heat and other properties across the frontal surface. If no heat were transported across the front, an $1\,\mathrm{K\,day^{-1}}$ cooling of the atmosphere poleward of 50°N would occur. The associated thermal wind would induce wind shear making the atmospheric flow hydrodynamically unstable and baroclinic instability occurs.

A depression generally developes east of a trough in the wave pattern of the jetstream. The cyclonic circulation of a depression advects warm air northwards and upwards east of the depression core, while west of it cold air is afvected southwards and downwards. Both movements enhance the wave pattern in the jet and release potential energy for further development of te baroclinic instability (Figure 3.29). Eventually warm air is completely undercut by the cold air (occluded front) and the depression will begin to decay as surface friction dissipates its kinetic energy. A typical cycle lasts 3-6 days, but this may also be just several hours!

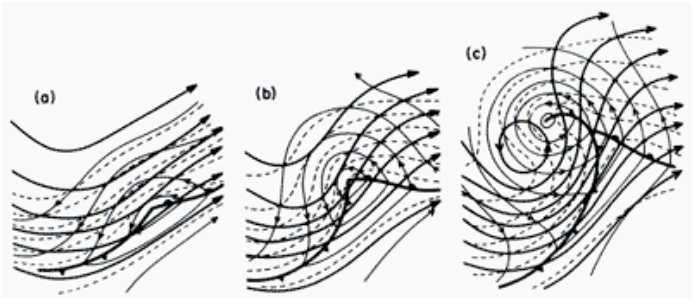

Figure 3.29: A developing baroclinic wave a three stages of development. Heavy solid lines: 500 hPa contours, thin lines: 1000 hPa contours, dashed: thickness 1000-500 hPa layer.

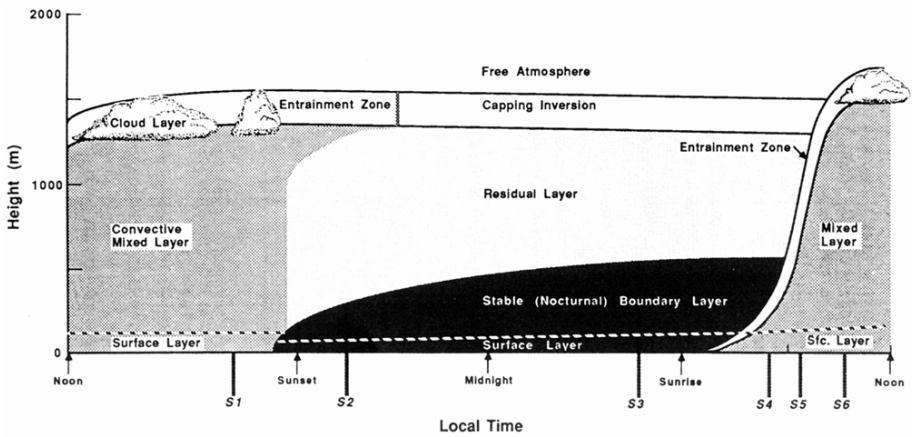

Figure 3.30: The daily cycle in the clear weather ABL over land.

The barotropic vorticity equation can be used to predict the changes in vorticity of a developing midlatitude disturbance. It assumes perfectly horizontal motion (w = 0). For a cyclonic disturbance ζ is negative. From the barotropic vorticity equation it follows that absolute vorticity is conserved, a small movement to the North therefore results in ζ to become more negative, developing the disturbance further.

3.5 The atmospheric boundary layer

The atmospheric boundary layer (ABL) is defined as that part of the atmosphere that exchanges information with the surface on short time scales (less than 1 hour). It is the part of the atmosphere in which we live.

A very important feature of the ABL is that close to the surface of the Earth, the atmospheric flow becomes turbulent and breaks up in eddies. These eddies effectively transport momentum, heat and moisture in the vertical. The main reasons for turbulence to develop in the ABL is vertical wind shear and negative buoyancy ($d\theta/dz < 0$). Through friction at the surface, the wind becomes zero at the surface, which makes the flow hydrodynamically unstable. This type of turbulence is denoted by mechanical produced turbulence. Negative buoyancy ($d\theta/\ dz < 0$) developes through heating of the Earth surface by absorption of solar radiation (Bouyancy turbulence).

Turbulence is destructed by a stable stratification (positive bouyancy, $d\theta/dz > 0$). This occurs in case of strong surface cooling, i.e. night-time and clear sky. These processes are referred to as mechanical production (shear production) of turbulence and buoyancy production/destruction of turbulence, respectively. Turbulence is dissipated at the smallest length scales through viscosity of the air.

There are several different types of boundary layers, characterised mainly by stability. We may distinguish:
1) the clear weather ABL over land,
2) neutral ABL over land (Ekman layer), and
3) the marine ABL.
The clear weather ABL over land is characterised by an outspoken daily cycle in temperature, wind speed and depth following absorption of solar radiation at the surface. Strong heat and moisture exchange occurs at the surface. The depth of this ABL varies from 200 m at night (Òstable ABLÓ) to 1500 m at day ("mixed layer"). The neutral ABL over land or "Ekman layer" is characterised by the fact that clouds and strong winds prevent strong

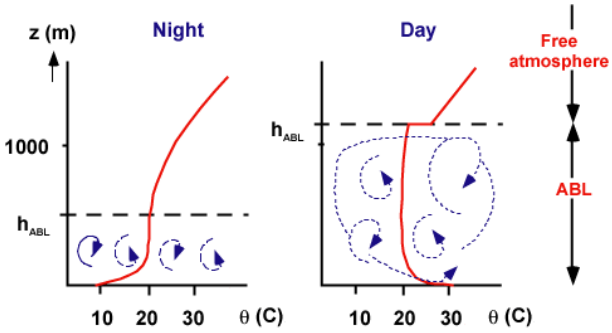

Figure 3.31: Potential temperature profile of the clear weather ABL over land during night and day.

daily cycle. Turbulent heat and moisture exchange at the surface is small. The Ekman ABL acts merely as a friction layer, exchange of momentum. The depth is typically 1000 m. The marine ABL is characterised by a small daily cycle, which is due to mixing in the upper ocean layers transporting absorbed solar energy away from the surface. In this ABL the roughness is variable (waves). Potentially strong advection effects may occur because of the long response time of the water surface temperature and because of the strong land-ocean temperature contrast. Otherwise this ABL is comparable to the Ekman ABL. We will not specifically treat this ABL in this course. More information on turbulence and different types of boundary layers can be found in Garratt (1992).

3.5.1 The clear weather ABL over land

Figure 3.30 illustrates the development of the clear weather ABL over land. From sunrise the Sun starts to heat the surface, and vigorous vertical mixing occurs through strong surface heating resulting in a daytime mixed ABL. The turbulence is bouyancy and mechanically produced. The maximum depth is ∼1500 m, topped by a capping surface inversion. After sunset the surface heating disapears and the nighttime stable ABL developes. The surface cools through longwave cooling resulting in a stable stratification. Turbulence is now only generated by wind shear and desctructed by bouyancy. The ABL only slowly grows in its depth is poorly defined.

Figure 3.31 illustrates the daily cycle in the potential temperature profile. During daytime the ABL is mixed. The potential temperature profile is constant except for the near surface layer, where it is absolutely unstable. From the surface layer air parcels may rise unimpeded to the ABL top where they meet potentially warmer air. During night the ABL is stably stratified. The surface layer is also stably stratified. Buoyancy destructs turbulence and wind shear must keep the mixing going. As a result the ABL is only slowly growing.

3.5.2 Exchange of heat and moisture: the surface energy balance

From the above it is clear that the structure of the ABL very much depends on what happens at the surface, heating by shortwave radiation, cooling by longwave radiation, heating or cooling by the turbulent heat fluxes. In principle, all energy fluxes through the surface should balance ($E = 0$), unless energy is used for phase changes of the surface (like melt). This energy balance can be written as:

$$E = Shw\downarrow(1-\alpha) + Lw\downarrow + Lw\uparrow + SHF + LHF + G\ ,$$

and is illustrated in Figure 3.32. Here, the fluxes are defined positive when directed towards the surface. The radiative fluxes are extensively described in section 2.1. The sensible heat

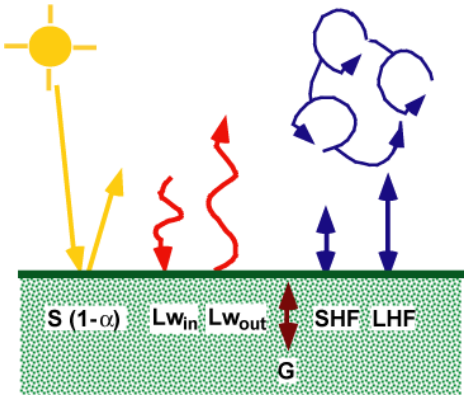

Figure 3.32: The surface energy balance.

flux (*SHF*) is the result of temperature difference between atmosphere and surface, while the latent heat flux (*LHF*) describes the heat flux though exchange of moisture between surface and atmosphere, i.e. condensation, evaporation. G is the sub surface energy flux describing transport of heat from or too deeper soil layers. The sensible (*SHF*) and latent (*LHF*) heat fluxes at the surface can be expressed as (in $\mathrm{W\,m^{-2}}$):

$$SHF = \rho c_p C_h V(\theta_a - \theta_{sur}) \tag{3.25}$$

$$LHF = \rho L_v C_h V(q_a - q_{sur})\,, \tag{3.26}$$

where ρ is the near-surface air density, c_p is the specific heat of air at constant pressure ($=1005\,\mathrm{J\,kg^{-1}\,K^{-1}}$) and L_v is the latent heat of vaporization ($2.5\times10^6\,\mathrm{J\,kg^{-1}}$). Furthermore, V is the absolute wind speed, which is a measure for wind shear near the surface, i.e. the mechanical turbulence production. In this expression the heat fluxes are proportional to the difference between atmospheric (subscript a) potential temperature (θ) or specific humidity (q), and surface (subscript *sur*) θ or q. The atmospheric value is usually a near surface value typically measured at 2 m in e.g. a Stevenson screen. Finally C_h is the bulk heat exchange coefficient for (sensible and latent) heat. It still depends on the bouyancy of the air and the roughness of the surface. A typical value is 0.001. Frame 3.17 present two examples for typical values of the heat fluxes in stable and unstable conditions.

The examples in frame 3.17 and Figure 3.33 show nighttime fluxes smaller and opposite of sign compared to daytime fluxes. This is often the case. In general the turbulent heat fluxes are smaller than the radiation fluxes. However, annually averaged, they represent a net energy loss for the surface and are therefore important (see Figure 2.37). In areas

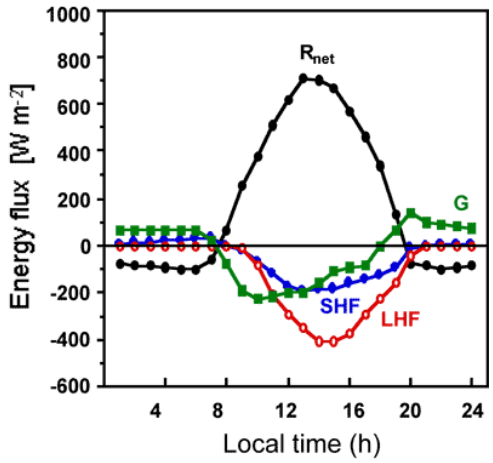

Figure 3.33: The diurnal cycle in the surface energy balance for a sunny summer day over a moist, dark land surface at middle latitudes.

Unstable stratification (daytime)

Use the following values in Eqs. 3.25 and 3.26:
$\rho = 1.\ \mathrm{kg\,m^{-3}}$
$V = 5\,\mathrm{m\,s^{-1}}$
$\theta_a = 295\,\mathrm{K}$, $\theta_{sur} = 300\,\mathrm{K}$
$q_a = 13\,\mathrm{g\,kg^{-1}}$, $q_{sur} = 21\,\mathrm{g\,kg^{-1}}$ (saturated)
$C_h = 0.001$.
SHF becomes -25 $\mathrm{W\,m^{-2}}$ and *LHF* becomes -120 $\mathrm{W\,m^{-2}}$. Note that q_{sur} is the saturation value at 300 K.

Stable stratification (nighttime)

Use the following values in Eqs. 3.25 and 3.26. Compared to the daytime case wind speed is lower and the surface is cooling:
$\rho = 1.2\,\mathrm{kg\,m^{-3}}$
$V = 3\,\mathrm{m\,s^{-1}}$
$\theta_a = 295\,\mathrm{K}$, $\theta_{sur} = 290\,\mathrm{K}$
$q_a = 13\,\mathrm{g\,kg^{-1}}$, $q_{sur} = 11\,\mathrm{g\,kg^{-1}}$ (saturated)
$C_h = 0.0005$.
SHF becomes +9 $\mathrm{W\,m^{-2}}$ and *LHF* becomes +9 $\mathrm{W\,m^{-2}}$. Note that q_{sur} is the saturation value at 290 K.

Frame 3.17: Turbulent fluxes in unstable (daytime) and stable (nighttime) stratification.

where rainfall exceeds evaporation, surface air is saturated and heat loss through *LHF* (evaporation) dominates the turbulent heat exchange.

The global distribution of *SHF* and *LHF* in summer and winter is illustrated in Figure 3.34. *LHF* is mostly negative in summer as well as in winter, i.e. evaporation occurs extracting heat from the surface. For evaporation to occur moisture must be available. *LHF* is therefore largest over the warm ocean in the tropics. Moisture is also available in the polar regions as snow and ice. Evaporation is however small due to the low temperatures. Desert regions are also clearly visible as regions with low amount of evaporation. Temperature is high enough for significant evaporation, there is however no moisture available. Over the large land masses a clear annual cycle is visible with higher vales in *LHF* in summer and lower values in winter.

SHF is positive in winter and negative in summer. Negative values indicate strong heating of the surface by solar radiation resulting in unstable conditions in which the surface heats the atmosphere. There is a strong annual cycle over land in areas with seasonal snow cover. In winter, when the surface is snow covered large part of the solar radiation is reflected by the surface and not used to heat the surface. The atmosphere is relatively warm and sensible heat transport is directed towards the surface. In summer, the snow has dissapeared and the surface warms up, heating the atmosphere from below.

3.5.3 Growth of the mixed layer

During daytime the clear weather ABL over land is well mixed resulting in the potential temperature profile in Figure 3.31b. After sunrise, the Sun starts to heat the surface and *SHF* will become negative, i.e. directed upwards, heating the atmosphere from below. The temperature increases and the mixed layer starts to grow. The growth of the mixed layer occurs at the top of the boundary layer and is described by entrainment and encroachment.

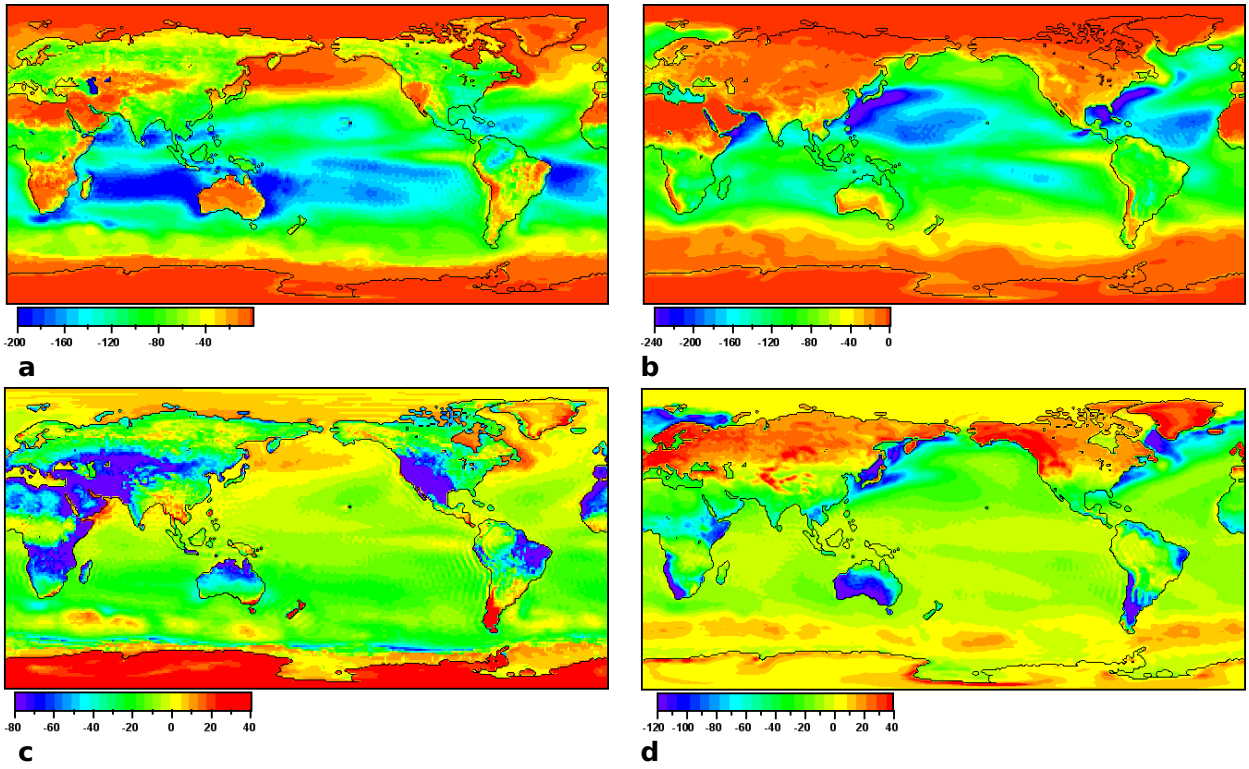

Figure 3.34: Global distribution of *LHF* (a,b) and *SHF* (c,d) for June, July, August (a,c) and December, January, February (b,d) (in $\mathrm{W\,m^{-2}}$).

Entrainment

Entrainment is the exchange of air over a capping inversion from above to within the boundary layer. This is usually the means by which an atmospheric boundary layer topped by a capping inversion increases its height. With the exchange of air over the capped inversion, heat is transported into the boundary layer. First assume no increase in height of the boundary layer. The heat transported into the layer by *SHF* is completely used to increase the temperature over the complete layer (conservation of energy):

$$\frac{d\theta_m}{dt} = \frac{SHF}{\rho c_p h_m}$$

This change of temperature decreases the temperature inversion by $-d\theta_m/dt$. Entrainment will add energy to the boundary layer which is not used to heat or cool but to increase its height. When h_m increases, the temperature inversion will increase as well. The increase depends on the lapse rate above the boundary layer. This results in an expression for the change in temperature inversion over time:

$$\frac{d\Delta\theta}{dt} = -\frac{d\theta_m}{dt} + \frac{d\theta}{dz}\frac{dh_m}{dt} = -\frac{d\theta_m}{dt} + \gamma_\theta \frac{dh_m}{dt}$$

Combining these two results and rewritting the expression to obtain an expression for the change in boundary layer height due to entrainment results in:

$$\frac{dh_m}{dt} = \frac{1}{\gamma_\theta}\left[\frac{d\Delta\theta}{dt} + \frac{SHF}{\rho c_p h_m}\right] \tag{3.27}$$

Note that in these expression *SHF* is defined positive upwards.

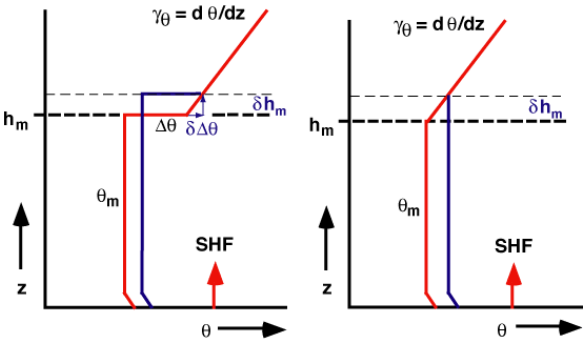

Figure 3.35: Vertical profiles of potential temperature illustrating the entrainment process (left) and the encroachment process (right).

Encroachment

Encroachment is the growth of the boundary layer arising purely from surface heating alone. It takes place in the absence of a capping inversion (Figure 3.35). As a result the increase in height of the ABL Eq. 3.27 reduces to:

$$\frac{dh_m}{dt} = \frac{SHF}{\gamma_\theta \rho c_p h_m}$$

Encroachment results in a slower increase of the depth of the ABL compared to entrainment.

3.5.4 The neutral ABL over land (Ekman or friction layer)

In the neutral ABL ($d\theta/dz = 0$) no exchange of heat takes place with the surface, only exchange of momentum, hence the term friction layer. The exchange of momentum at the surface, friction, results in a decrease in the flow speed. In addition, friction results in a turning of the wind vector, e.g. a geostrophic flow along isobars is deflected in the direction of the low pressure. This follows from the balance of forces in a stationary flow. In the case without friction the pressure gradient and coriolis force balance for a geostrophic flow. Adding friction distroys this balance (Figure 3.36a). To restore the balance the flow is deflected towards the low pressure (Figure 3.36b).

Using the momentum equations (Eq. 3.4) an expression for both wind components can be derived. Assume that friction is linearly dependent on wind speed (ku, kv), assume the flow is stationary ($d/dt = 0$) and assume a pressure gradient only in the x-direction:

$$\begin{aligned} 0 &= -\frac{1}{\rho}\frac{\partial p}{\partial x} + fv - ku \\ 0 &= -fu - kv \end{aligned}$$

The minus sign results from the fact that friction allways acts parallel and opposite to the flow. Combining these two equations result in an expression for the u and v-component of

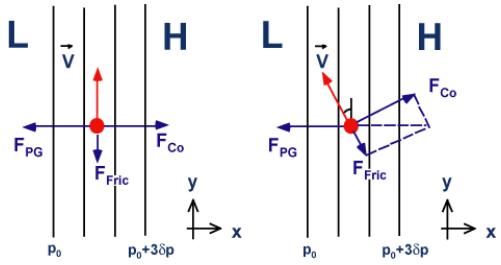

Figure 3.36: The effect of friction on a geostrophic flow.

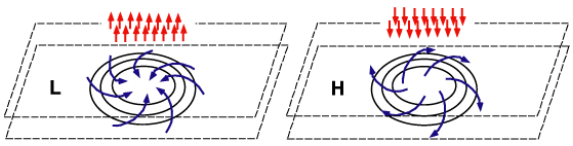

Figure 3.37: Frictional convergence and divergence.

Reynolds decomposition is a mathematical technique to separate the average and fluctuating parts of a quantity. For example describe two quantities X and Y as an average ($\overline{X}$) plus high frequency fluctuations (x'):

$$X = \overline{X} + x' \quad , \quad Y = \overline{Y} + y'$$

The overbar denotes the time average, the prime denotes the fluctuations. Some calculus rules that apply on this description are:

$\overline{x'} = 0$, the time average of the fluctuations is zero.

$\overline{\overline{X}} = \overline{X}$, the time average of the mean equals the mean.

$\overline{c\overline{X}} = c\overline{X}$, the time average of a constant times the mean equals the constant times the mean.

Furthermore:

$\overline{(\overline{XY})} = \overline{XY}$

$\overline{(\overline{X}y')} = \overline{X}\overline{y'} = 0$

And:

$$\begin{aligned}
\overline{(XY)} &= \overline{(\overline{X}+x')(\overline{Y}+y')} \\
&= \overline{\overline{X}\overline{Y} + \overline{X}y' + x'\overline{Y} + x'y'} \\
&= \overline{(\overline{X}\overline{Y})} + \overline{(\overline{X}y')} + \overline{(x'\overline{Y})} + \overline{(x'y')} \\
&= \overline{X}\overline{Y} + 0 + 0 + \overline{(x'y')} \\
&= \overline{X}\overline{Y} + \overline{(x'y')}
\end{aligned}$$

Frame 3.18: Reynolds decomposition.

the wind speed:

$$u = \frac{-\frac{k}{\rho}\frac{\partial p}{\partial x}}{k^2 + f^2} \qquad \text{and} \qquad v = \frac{-fu}{k} = \frac{+\frac{f}{\rho}\frac{\partial p}{\partial x}}{k^2 + f^2}$$

In case of Figure 3.36 $\partial p/\partial x > 0$, which results in $u < 0$ and $v > 0$. Thus, wind velocity obtains a component in the direction of the low pressure, filling up the low pressure system and draining the high pressure system (Figure 3.37). Note also that in case friction is 0, ($k = 0$), $u = 0$.

In the previous the transport of momentum / impuls is described by a linear relation between friction and flow speed. A more sophisticated way of quantifying the transport of momentum (impuls) is by looking at the contributions to the wind variation of signals with various frequencies. This can be done by describing the wind (and other variables) as a mean plus high frequency variations due to turbulence. This technique is called Reynolds decomposition and described in Frame 3.18. Reynolds decomposition in boundary layer meteorology embodies substituting the mean plus a high frequency variation term in the conservation equations (Eqs 3.4) and subsequently taking the time average of the resulting expressions. The resulting Reynolds decomposed momentum equations are:

$$\begin{aligned}
\frac{d\overline{u}}{dt} &= -\frac{1}{\rho}\frac{\partial \overline{p}}{\partial x} + f\overline{v} - \frac{\partial \overline{(u'w')}}{\partial z} \\
\frac{d\overline{v}}{dt} &= -\frac{1}{\rho}\frac{\partial \overline{p}}{\partial y} - f\overline{u} - \frac{\partial \overline{(v'w')}}{\partial z}
\end{aligned} \tag{3.28}$$

The last term on the right hand side in both equations is the friction term, or the vertical divergence of turbulent impuls. Note that the left hand side of both equations is the total derivative and therefore still includes advection of the mean flow:

$$\frac{d\overline{u}}{dt} \equiv \frac{\partial \overline{u}}{\partial t} + \overline{u}\frac{\partial \overline{u}}{\partial x} + \overline{v}\frac{\partial \overline{u}}{\partial y} + \overline{w}\frac{\partial \overline{u}}{\partial z} \; .$$

The derivation of Eq. 3.28 is given in Frame 3.19.

How to interpret this friction term in the momentum equations (Eq. 3.28). Figure 3.38 shows on the left a mean wind speed profile. A parcel with mean wind speed $\overline{u}$ is brought upwards, thus $w' > 0$. At the higher level the horizontal wind speed from this parcel is

The momentum equations without friction read:

$$\begin{aligned}\frac{\partial u}{\partial t}+u\frac{\partial u}{\partial x}+v\frac{\partial u}{\partial y}+w\frac{\partial u}{\partial z} &= -\frac{1}{\rho}\frac{\partial p}{\partial x}+fv\\ \frac{\partial v}{\partial t}+u\frac{\partial v}{\partial x}+v\frac{\partial v}{\partial y}+w\frac{\partial v}{\partial z} &= -\frac{1}{\rho}\frac{\partial p}{\partial y}-fu\end{aligned}$$

Substitute: $p=\overline{p}+p'$, $u=\overline{u}+u'$, $v=\overline{v}+v'$, $w=\overline{w}+w'$, assume ρ to be constant and average over time. Make use of the calculus rules from Frame 3.18 and the different terms become:

$$\begin{aligned}\overline{\frac{\partial u}{\partial t}} &= \frac{\overline{\partial(\overline{u}+u')}}{\partial t}=\frac{\partial\overline{u}}{\partial t}\\ \overline{u\frac{\partial u}{\partial x}} &= \overline{(\overline{u}+u')\frac{\partial(\overline{u}+u')}{\partial x}}\\ &= \overline{\overline{u}\frac{\partial\overline{u}}{\partial x}}+\overline{u'\frac{\partial\overline{u}}{\partial x}}+\overline{\overline{u}\frac{\partial u'}{\partial x}}+\overline{u'\frac{\partial u'}{\partial x}}\\ &= \overline{u}\frac{\partial\overline{u}}{\partial x}+\boxed{\overline{u'\frac{\partial u'}{\partial x}}}\\ \overline{fv} &= \overline{f(\overline{v}+v')}=\overline{f\overline{v}}+\overline{fv'}=f\overline{v}+0=f\overline{v}\end{aligned}$$

The other terms are derived similarly. The term in the box is new and appears for each advection term. The momentum equations for turbulent flow now become:

$$\begin{aligned}\frac{d\overline{u}}{dt}+\overline{u'\frac{\partial u'}{\partial x}}+\overline{v'\frac{\partial u'}{\partial y}}+\overline{w'\frac{\partial u'}{\partial z}} &= -\frac{1}{\rho}\frac{\partial\overline{p}}{\partial x}+f\overline{v}\\ \frac{d\overline{v}}{dt}+\overline{u'\frac{\partial v'}{\partial x}}+\overline{v'\frac{\partial v'}{\partial y}}+\overline{w'\frac{\partial v'}{\partial z}} &= -\frac{1}{\rho}\frac{\partial\overline{p}}{\partial y}-f\overline{u}\end{aligned}$$

The new turbulent terms can be rewritten by noting that:

$$\overline{\frac{\partial u'v'}{\partial y}}=\overline{u'\frac{\partial v'}{y}}+\overline{v'\frac{\partial u'}{y}}\,,\qquad \text{which results in :}$$

$$\begin{aligned}\overline{u'\frac{\partial u'}{\partial x}}+\overline{v'\frac{\partial u'}{\partial y}}+\overline{w'\frac{\partial u'}{\partial z}} &= \overline{\frac{\partial u'u'}{\partial x}}+\overline{\frac{\partial u'v'}{\partial y}}+\overline{\frac{\partial u'w'}{\partial z}}-\overline{u'\left[\frac{\partial u'}{\partial x}+\frac{\partial v'}{\partial y}+\frac{\partial w'}{\partial z}\right]}\\ &= \overline{\frac{\partial u'w'}{\partial z}}\end{aligned}$$

In the last step two assumptions are made. Firstly we assume incompressibility for the wind speed fluctuations, and secondly, we assume horizontal homogeneity in the ABL:

$$\frac{\partial u'}{\partial x}+\frac{\partial v'}{\partial y}+\frac{\partial w'}{\partial z}=0\,,\qquad \text{and}\qquad \overline{\frac{\partial u'u'}{\partial x}}=\overline{\frac{\partial u'v'}{\partial y}}=0\qquad \text{respectively.}$$

The end result is Eq. 3.28.

Frame 3.19: Reynolds decomposition of the momentum equations (Eq. 3.4).

smaller than the mean at that level, thus $u'<0$. Combined, $\overline{(u'w')}<0$. Similarly a parcel with mean wind speed $\overline{u}$ is brought downwards, thus $w'<0$. At the lower level the horizontal wind speed from this parcel is larger than the mean at that level, thus $u'>0$. And again combined, $\overline{(u'w')}<0$. With increasing altitude the vertical difference in wind speed becomes smaller, thus $\overline{(u'w')}$ less negative resulting in $\partial\overline{(u'w')}/\partial z>0$.

The Ekman layer

An interesting application of Eq. 3.28 is the Ekman layer. The Ekman layer describes a neutral boundary layer in which to a first approximation the Ekman solution for wind speed

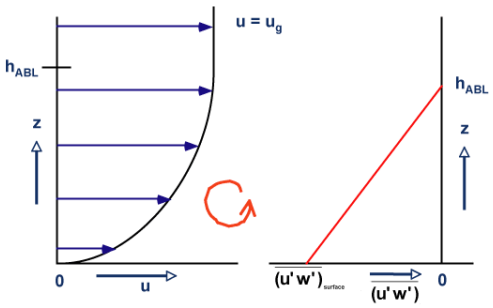

Figure 3.38: Left, mean wind profile. Right, the corresponding profile of the turbulent impuls flux.

applies. To describe the Ekman solution we assume stationary flow ($d/dt = 0$). We use the notation for geostrophic flow (Eq. 3.11) and choose the axis of our reference frame such that the geostrophic flow above the boundary layer is along the x-axis ($v_g = 0$). In Frame 3.20 is shown how the following expression for the two wind components $u(z)$ and $v(z)$ can be derived:

$$\begin{aligned} u(z) &= u_g \left[1 - \exp\left(-z\sqrt{f/2K}\right)\cos\left(z\sqrt{f/2K}\right)\right] \\ v(z) &= u_g \left[\exp\left(-z\sqrt{f/2K}\right)\sin\left(z\sqrt{f/2K}\right)\right] \end{aligned} \tag{3.29}$$

with K the eddy diffusivity, assumed constant with height. These equations show that in case $K = 0$, then $v = 0$ and $u = u_g$, i.e. pure geostrophic flow. Furthermore, $v(z) = 0$ at $z = \pi/\sqrt{f/2K} \cong 1$ km in case $K = 5\,\mathrm{m^2\,s^{-1}}$. And finally at $z = 0$ the wind vector points 45 degrees west of the geostrophic wind. Figure 3.39 illustrates this solution.

In reality the Ekman solution is very rare. This is partly because the turbulent momentum fluxes are only to a first approximation proportional to the gradient in the mean momentum (fist order closure), and partly because the eddy viscosity K is not constant with height. Especially near the surface K must vary rapidly.

The nocturnal low level jet

An interesting feature related to the rotation of the wind close to the surface due to friction effects as described in the Ekman layer, is the nocturnal low level jet (LLJ). The LLJ developes due to the development of an inertial oscillation in the remains of a convective boundary layer after sunset. After sunset dry-convective turbulent mixing almost ceases and a stable

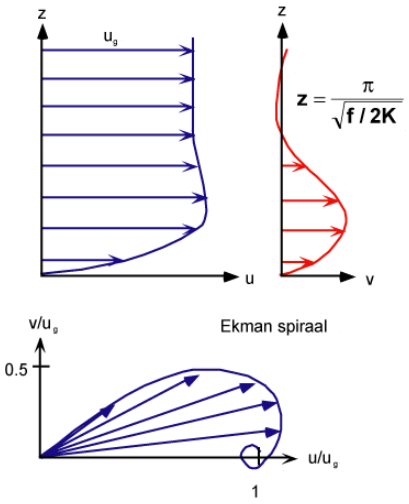

Figure 3.39: The solution for the Ekman layer on the Northern Hemisphere.

boundary layer starts to develope from the surface. As a result, in the remnants of the convective boundary layer, friction is no longer a significant force. The wind in this remnant layer starts to rotate to adjust itself to the geostrophic flow. In the absence of other forces, an inertial oscillation developes.

To describe the oscillation and the LLJ we use the momentum equations 3.4 assuming friction to be 0 and the notation for geostrophic flow (Eq. 3.11). As in the decription of the Ekman layer we choose the axis of our reference frame such that the geostrophic flow is along the x-axis ($v_g = 0$). In Frame 3.21 it is shown how the following expression for the two wind components $u(z)$ and $v(z)$ can be derived:

$$\begin{aligned} u(z) &= u_g + V_0 \sin ft + (u_0 - u_g)\cos ft \\ v(z) &= v_0 \cos ft - (u_0 - u_g)\sin ft \end{aligned} \tag{3.30}$$

Assume stationary flow ($d/dt = 0$), use the notation for geostrophic flow (Eq. 3.11) and choose the axis of the reference frame such that the geostrophic flow above the boundary layer is along the x-axis ($v_g = 0$). The momentum equations (E. 3.28) then reduce to:

$$0 = +fv - \frac{\partial \overline{(u'w')}}{\partial z} \quad , \quad 0 = -f(u - u_g) - \frac{\partial \overline{(v'w')}}{\partial z}$$

where we have left out the average bars over the independent variables. We now have a set of two equations with four unknown variables u, v, $\overline{(u'w')}$ and $\overline{(v'w')}$. To close this system of equations we must find an expression for $\overline{(u'w')}$ and $\overline{(v'w')}$ in terms of u and v. A first order closure assumption is to assume that the $\overline{(u'w')}$ and $\overline{(v'w')}$ are linearly related to the vertical gradient in u and v:

$$-\overline{(u'w')} = K\frac{\partial u}{\partial z} \quad , \quad -\overline{(v'w')} = K\frac{\partial v}{\partial z}$$

with K the eddy diffusivity, assumed constant with height. Substitute in the momentum equations:

$$\begin{aligned} 0 = \quad & +fv + \tfrac{\partial}{\partial z}K\tfrac{\partial u}{\partial z} && = +fv + K\frac{\partial^2 u}{\partial z^2} \\ 0 = \quad & -f(u - u_g) + \tfrac{\partial}{\partial z}K\tfrac{\partial v}{\partial z} && = -f(u - u_g) + K\frac{\partial^2 v}{\partial z^2} \end{aligned}$$

Combine these two equations by introducing the complex velocities $\hat{V} \equiv u + iv$ and $\hat{V}_g \equiv u_g + iv_g$ with $i = (-1)^{1/2}$, then multiply the second equation by i and add the first equation. Note that $1/i = -i$. The result is:

$$0 = \frac{\partial^2 \hat{V}}{\partial z^2} - \frac{if}{K}(\hat{V} - \hat{V}_g)$$

A general solution of this equation is: $\hat{V}(z) = A\exp\left(\sqrt{\tfrac{if}{K}}z\right) + B\exp\left(-\sqrt{\tfrac{if}{K}}z\right) + C$

The boundary conditions require that at the surface ($z = 0$) $u = 0$ and $v = 0$ thus $\hat{V}(0) = 0$, while far from the ground ($z \to \infty$) $u = u_g$, $v = v_g = 0$ and $\hat{V}(\infty) = \hat{V}_g = u_g$. Substitution of the general solution in the equation results in $C = u_g$, and the boundary conditions provide (check), $A = 0$ and $B = -u_g$. The solution now becomes:

$$\hat{V}(z) = -u_g \exp\left(-\sqrt{\frac{if}{K}}z\right) + u_g$$

The last step is to separate the Imaginary and Real part of the exponent in order to find a solution for $u(z)$ separate from $v(z)$. Make use of the fact that $\exp(-i\varphi) = \cos\varphi - i\sin\varphi$ and $\sqrt{i} = (i+1)/\sqrt{2}$. The solution now becomes (check):

$$\hat{V}(z) = u_g\left[1 - \exp\left(-\sqrt{\frac{f}{2K}}z\right)\left(\cos\sqrt{\frac{f}{2K}}z - i\sin\sqrt{\frac{f}{2K}}z\right)\right]$$

of which $u(z) = Re(\hat{V})$, the Real part and $v(z) = Im(\hat{V})$, the Imaginary part, given in Eq. 3.29.

Frame 3.20: The Ekman layer.

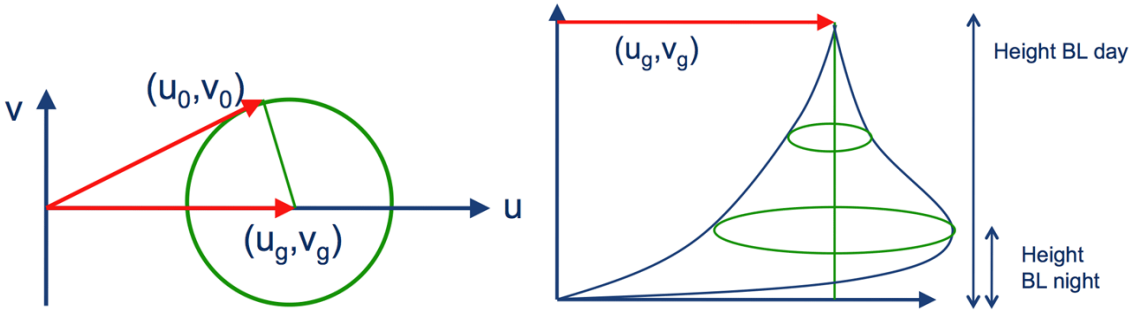

Figure 3.40: Illustration of the rotation of the wind vector resulting in a low level jet.

with (u_0, v_0) the wind vector at $t = 0$, the moment friction force becomes neglegible. The period of the oscillation P equals $2\pi/f$, which is about 15 hours for The Netherlands. Depending on the initial angle between (u_0, v_0) and the geostrophic wind (u_g, v_g), the maximum wind speed is reached about 6 to 8 hours after sunset (for The Netherlands).

Assume no friction, use the notation for geostrophic flow (Eq. 3.11) and choose the axis of the reference frame such that the geostrophic flow is along the x-axis ($v_g = 0$). The momentum equations (E. 3.28) then reduce to:

$$\frac{du}{dt} = +fv$$
$$\frac{dv}{dt} = -f(u - u_g)$$

We now have a set of two equations that describe the evolution in time of the wind components u, v. Combine these two equations by introducing the complex velocities $\hat{V} \equiv u + iv$ and $\hat{V}_g \equiv u_g + iv_g = u_g$ with $i = (-1)^{1/2}$, then multiply the second equation by i and add the first equation. Note that $1/i = -i$ and $i^2 = -1$. The result is:

$$\frac{d\hat{V}}{dt} = -if(\hat{V} - \hat{V}_g)$$

A general solution of this equation is: $\hat{V}(t) = A\exp(-ift) + B$

The boundary conditions require that at $t = 0$ $u = u_0$ and $v = v_0$, thus $\hat{V}(0) = \hat{V}_0$, and for large t $u = u_g$ and $v = v_g$ thus $\hat{V}(t) = \hat{V}_g = u_g$. Substitution of the general solution in the equation results in $B = u_g$. The boundary conditions provide (check), $A = u_0 - u_g + iv_0$ The solution now becomes:

$$\hat{V}(t) = \left(u_0 - u_g + iv_0\right)\exp(-ift) + u_g$$

The last step is to separate the Imaginary and Real part of the exponent in order to find a solution for $u(t)$ separate from $v(t)$. Make use of the fact that $\exp(-i\varphi) = \cos\varphi - i\sin\varphi$. The solution now becomes (check):

$$\hat{V}(t) = \left(u_0 - u_g + iv_0\right)(\cos ft - \sin ft) + u_g$$

of which $u(t) = Re(\hat{V})$, the Real part and $v(t) = Im(\hat{V})$, the Imaginary part, given in Eq. 3.30.

Frame 3.21: The Low Level Jet.

Chapter 4

List of constants

Below follows a list of constants as used in the reader.

Name	Value	Section
Speed of light	$c = 2.9973\times10^{8}\ \mathrm{m\,s^{-1}}$	2.1.1
Heat capacity air at constant pressure	$c_p = 1004\,\mathrm{J\,kg^{-1}\,K^{-1}}$	2.2.4
Heat capacity air at constant volume	$c_p = 717\,\mathrm{J\,kg^{-1}\,K^{-1}}$	2.2.4
Sun-Earth distance (average)	$d_{s-e} = \sim150\times10^{6}\,\mathrm{km}$	2.1.2
Gravitational constant	$G = 6.673\times10^{-11}\ \mathrm{N\,m^{2}\,kg^{-2}}$	2.5.1
Gravitational acceleration	$g = 9.81\,\mathrm{m\,s^{-2}}$	2.5.1
Planck constant	$h = 6.63\times10^{-34}\ \mathrm{J\,s}$	2.1.1
Boltzmann constant	$k = 1.38\times10^{-23}\ \mathrm{J\,K^{-1}}$	2.1.1
Latent heat of melt (ice ⟷ water)	$L_m = 3.34\times10^{5}\,\mathrm{J\,kg^{-1}}$	2.3.1
Latent heat of sublimation (ice ⟷ vapor)	$L_m = 2.84\times10^{6}\,\mathrm{J\,kg^{-1}}$	2.3.1
Latent heat of evaporation (water ⟷ vapor)	$L_m = 2.51\times10^{6}\,\mathrm{J\,kg^{-1}}$	2.3.1
Radius Earth (average)	$r_e = 6.37\times10^{6}\,\mathrm{m}$	2.1.2
Radius Sun (average)	$r_s = \sim700{,}000\,\mathrm{km}$	2.1.2
Solar constant	$S_0 = \pm1374\ \mathrm{W\,m^{-2}}$	2.1.2
Universal gas constant	$R^* = 8.314\times10^{3}\,\mathrm{J\,K^{-1}\,kmol^{-1}}$	2.2.2
Specific gas constant dry air	$R_d = 287.05\,\mathrm{J\,kg^{-1}\,K^{-1}}$	2.2.2
Specific gas constant moist air	$R_v = 462.\,\mathrm{J\,kg^{-1}\,K^{-1}}$	2.3.1
Dry adiabatic lapse rate	$\gamma_d = -\frac{g}{c_p} = \text{-}9.81\,\mathrm{K\,km^{-1}}$	2.2.4
Angular velocity Earth	$\Omega = 7.3\times10^{-5}\ \mathrm{rad\,s^{-1}}$	3.2.2
Stefan Boltzmann constant	$\sigma = 5.67\times10^{-8}\,\mathrm{W\,m^{-2}\,K^{-4}}$	2.1.1

Chapter 5

Course information

5.1 Course programme

The lectures are in room BBL 071 unless stated otherwise. Note that attendance at the guest lectures, the project presentations, the mid term exam and the final exam are required, attendance at the lectures and exercises is recommended.

Week	Date	Time	Activity	Info
17	Tues 23 Apr	9h-12h45	H01 & W01	Choose project subject
	Thur 25 Apr	13h15-17h00	H02 & W02	
18	Tues 30 Apr	9h-12h45		No class (Koninginnedag)
	Thus 2 May	13h15-17h00	H03 & W03	Discuss and hand in project plan
19	Tues 7 May	9h-12h45	H04 & W04	
	Thur 9 May	13h15-17h00		No class (Hemelvaart)
20	Tues 14 May	9h-12h45	H05 & W05	
	Thur 16 May	13h15-17h00		**Mid term exam**
21	Tues 21 May	9h-12h45	H06 & W06	**Guest lecture Hans Oerlemans**
	Thur 23 May	13h15-17h00	H07 & W07	**Guest lecture Geert Jan Roelofs**
22	Tues 28 May	9h-12h45		**Excursion to KNMI**
	Thur 30 May	13h15-17h00	H08 & W08	
23	Tues 4 June	9h-12h45	H09 & W09	
	Thur 6 June	13h15-17h00	H10 & W10	**Gast lecture Aarnout van Delden**
24	Tues 11 June	9h-12h45	H11 & W11	
	Thur 13 June	13h15-17h00	H12 & W12	
25	Tues 18 June	9h-12h45	H13 & W13	(if necessary Project presentations)
	Thur 20 June	13h15-17h00		**Project presentations**
27	4 July	14h00-17h00 h	????**Final exam**	

5.2 Contact information

If you have questions or remarks please contact:
Carleen Tijm-Reijmer (C.H.Tijm-Reijmer@uu.nl)
Room: BBL 663, Tel: 3273

5.3 Examination

The grade you receive for this course is based on your project work and presentation (25%) and the average of both written examinations (75%).
The mid term written exam includes chapter 1, the written examination at the end of the course includes all lectures (unless stated otherwise) plus chapters 2 and 3 of this reader.
The following sections are EXCLUDED:

- Section 3.4.3

5.4 Project information

The project consists of a small literature/internet study and is closed by a presentation (NO written report). You can either do it alone or team of with one other student. You choose your topic in consultation with the teacher (examples are given below). When your topic is approved you write a project plan (example is given below) research your topic and prepare an oral presentation.

Presentation and project workplan may be written in Dutch.

5.4.1 Topic examples

- Any acceptable subject
-
- Airpolution and living conditions
- Greenhouse effect
- The hole in the ozone layer
- Ozone in the troposphere
- El Nino/Southern Oscillation: impact on local weather
- Climate reconstruction from ice cores
- Ice ages
- Weather prediction and models
- Predictability of the weather and climate
- Acid rain: is there still a problem
- Extreme showers
- Extreme weather phenomena
- Observations in the atmosphere
- Wind-chill
- Large meteorological experiments: SHEBA, EPICA....
- Large ice bergs
- Sick building syndrome
- Sea ice
- IPCC
- Optical phenomena
- Volcanos and climate
- Tornados
- Huricanes
- Aerosols and clouds

5.4.2 Workplan example

Name and e-mail:
Mary Example, M.Example at students.uu.nl
Title of project:
Holocene climate changes in the Sahara

Short description and motivation

In the summer of 2006 I was in the Sahara in Morocco and there I found lots of fossils, remains of a period in which the Sahara was an ocean. I am very interested in the causes of this remarkable change from an ocean to a desert in the Holocene period. The change is due to climate changes. Therefore I am going to investigate climate changes in the Holocene and its causes and its influence in North Africa.

The main question I am going to answer in the project is:

What influences did Holocene climate changes have in the Sahara?

To answer this main question the following partial questions need to be answered:

1. What are the Holocene climate changes in the region of North Africa?
2. What are the causes of these climate changes?
3. How did the environment North Africa change?
4. What is the relation between the change of the environment and the climate changes?

The presentation will start with an introduction to the problem and a description of the Holocene period in general. Then the partial questions will be answered. The last part of the project will be the answer on the main question and eventually some statements about the future of the Sahara.

5.4.3 Presentation information

The presentation must be made in powerpoint. You will get a total of 12 minutes of which 10 are for the presentation and 2 for questions. A presentation of 10 minutes consists of about 8 sheets. When the research is carried out with 2 students, a duo-presentation is applicable. Presentations must be send by email or otherwise electronically to the teacher latest 1 day before the presentations.

In general, a presentation follows the following structure:
Title page
Contents summary
Introduction: introduce your research question
Contents
- research method
- results
Summary and conclusions

Hints for the presentation

- For short presentations possible to omit contents summary or combine Title page, Contents summary and/or Introduction.
- Do not put too much information on 1 slide.
- Take care that your figures are clear.
- Write down some key words as back up but not whole sentences.

- Do not look at the projection screen too much, look at your audience!
- Stay within your time limit, practice in front of a mirror with a stop watch!

Determination of presentation grade

- Contents of the presentation (have you put enough effort into it and do you understand the subject of your choice.
- Structure of the presentation, e.g. does your story have a clear beginning and ending.
- Slides (not too much information on 1 slide, clear figures)
- Whether you are within the time limit or not.
- Overall impression, do you address the audience enough, show enthusiasm, can answer questions etc.

5.5 Hints for the written exam

All constants you may need will be given.

5.5.1 Formulas to know by heart

Chapter 2

- Stefan Boltzmanns law
- Kirchhoffs law
- deriviation solar constant
- Definition albedo
- Radiation balance
- Ideal gas law
- Gas law for the dry atmosphere
- Gas law for water vapor
- Gas law for the moist atmosphere
- Hydrostatic balance
- Dry adiabatic lapse rate (understand the deriviation)
- Potential temperature (understand the deriviation)
- Lapse rate potential temperature
- Mixing ratio
- Perturbation analyses
- Specific moisture
- Virtual temperature
- Brunt Väisälä frequency

Chapter 3

- Centrifugal force/acceleration
- Effective gravity
- Geopotential
- Coriolis force/acceleration

- Coriolis parameter
- Pressure gradient force
- Momentum equations (in cartesion, natural and pressure coordinates)
- Total and local derivitives
- Rossby number
- Geostrofic flow (in cartesion, natural and pressure coordinates)
- Cyclostrofic flow (in natural coordinates)
- Gradient flow (in natural coordinates)
- Thermal wind
- Continuity equation
- Energy balans surface
- Sensible and latent heat fluxes

5.5.2 Formulas to recognise / able to work with / able to apply

Chapter 2

- Plancks law
- Wiens law
- Instantaneous and averaged incoming solar radiation
- Clausius Clapeyron
- Moist adiabatic lapse rate
- Equivalent potential temperature

Chapter 3

- Inertial oscillation (in cartesion and natural coordinates)
- Deriviation Centrifugal force/acceleration
- Deriviation Coriolis force/acceleration
- Deriviation momentum equation in natural coordinates
- Entrainment and encroachment
- Reynolds decomposition

Chapter 6

Exercises

6.1 Radiation balance of the Sun-Earth system

Exercise 1

Sirius has an effective temperature of 10000 K and a radius of 1.2 million km (0.008 AU). Calculate which planet in our solar system could be habitable, in terms of incoming short wave (*Shw*) radiation, if Sirius was our sun.

Planet	distance
Mars	1.5 AU
Jupiter	5.2 AU
Saturn	9.6 AU
Uranus	19.2 AU

Exercise 2

As the Sun cools, its spectrum will shift towards longer wavelengths. Estimate the change in the **Earth's black body temperature** if the peak in the *Shw* spectrum is displaced from its current position at 0.50 μm to a longer wavelength (more yellow) of 0.55 μm.

Exercise 3

The hood of a car can be modelled as a flat plate with *Lw* absorptivity of 0.9. The car is white (*Shw* reflectivity of 0.8). The atmosphere can be modeled as a gray layer with *Lw* absorptivity of 0.8, which emits radiation equally to space and the surface. The atmosphere is transparant for *Shw*. The incoming *Shw* radiation is 1100 Wm^{-2}. Assume radiation balance on the hood and in the atmosphere. Keep in mind that according to Kirchoff's law, absorptivity equals emissivity.

a. Draw a scheme including all upward and downward components of *Shw* and *Lw* radiation in the atmosphere and on the hood of the car.

b. Assume radiation balance in the atmosphere and on the hood. Estimate the hood's temperature.

c. Recalculate the hood's temperature, but now for a **red** car with reflectivity 0.4.

d. What physical process will mediate the values in **b** and **c**?

Exercise 4

How would the nature of the Earth's seasons change if the axis of the Earth's orbit was perpendicular to the plane of its orbit?

Exercise 5

What favors growth of the ice sheets: warm winters and cold summers, or cold winters and warm summers? Explain your answer.

6.2 Physical properties of the dry atmosphere

Exercise 1

Assume that the mean pressure observed in a planetary atmosphere varies with height according to:

$$p(z) = \frac{p_0}{1 + \left(\frac{z}{h}\right)^2}\ , \tag{6.1}$$

in which h is a constant. Derive an expression for the mean variation of temperature with height. *Note: in section 2.2.3, p was derived for a constant T.*

Exercise 2

Calculate the mass of the air column above you at sea level.

Exercise 3

In the mid-latitudes, air at 300 hPa level, inside the jet stream, is often observed to have temperatures as high as -40°. Calculate the corresponding potential temperature.

Exercise 4

Assume that in the troposphere a linear profile is a good approximation of temperature: $T = a + \gamma z$, with a = 288.15 K and γ = -6.5 $\mathrm{K\,km^{-1}}$. Take p_0 = 1013 hPa.

a. Calculate the pressure at z = 5 km, using the isothermal approximation (i.e. taking the average temperature of the layer).

b. Derive the expression for the tropospheric pressure distribution p(z), taking into account the lapse rate γ = dT/dz.

c. Recalculate the pressure at 5 km using the derived expression. Is the isothermal approximation in this case a good approximation?

d. Some people suffer from height sickness when they reach an altitude of 2 km. Calculate the air density at this elevation.

6.3 Atmospheric moisture

Exercise 1

One way of representing the amount of moisture in the atmosphere is by using relative humidity (RH). Assume we have two cases:

Summer	$T = 20°C$	$RH = 40\%$ $p = 1000$ hPa
Winter	$T = 5°C$	$RH = 80\%$ $p = 1000$ hPa

a. Calculate the absolute amount of moisture (specific humidity) in the air for both situations.

b. What is the importance of the relative humidity versus the specific humidity for a meteorologist?

Exercise 2

Suppose, the temperature in a kitchen is 15°C and the relative humidity is 60%. You leave the door of your refrigerator open long enough for the temperature and relative humidity in the refrigerator to take the same values as in the kitchen. Then you close the refrigerator. The temperature in the refrigerator will drop again. Calculate at which temperature the air in the refrigerator will become saturated.

Exercise 3

The föhn effect is a common phenomenon in mountainous regions. Famous föhn winds are the Mistral and Föhn winds are warm dry downslope winds that can last for days over distances of more than 100 km. In extreme cases the temperature can rise with 20°C and relative humidity can drop to values as low as 10%.

Assume a mountain with its base at 950 hPa and its top at 700 hPa. An air parcel is lifted from the base of the mountain, over the mountain. At start the parcels temperature is 283 K.

a. When the air parcel starts rising due to the presence of the mountain what is the lapse rate of the initial ascent, dry or moist adiabatic? Explain your answer. During this initial part of the ascent, what quantity is conserved? Think of temperature T, potential temperature θ and equivalent potential temperature θ_e.

b. The air parcel is lifted up from 950 hPa and saturation occurs at 900 hPa. Calculate the specific and relative humidity at 950 hPa.

c. The air parcel is lifted further. Which quantity is now conserved?

d. The air parcel is lifted to the top of the mountain. The specific humidity decreases to 2.5 g/kg at the top, due to condensation. Calculate the potential temperature of the air parcel at the top.

e. The condensed moisture is removed by rain and at the other side of the mountain the air parcel descends to 950 hPa. What is the lapse rate for the descend, dry or moist adiabatic? Calculate the new temperature and relative humidity of the parcel at 950 hPa.

6.4 Aerosols and clouds

Exercise 1

Latent heat is the heat released when water (H_2O) undergoes a change of state (water to vapor). To evaporate 1 kg of water $2.5\times10^6\,\mathrm{J\,kg^{-1}}$ (L_v, the latent heat of evaporation) energy is required.

a. Estimate the mean global precipitation rate given a global average latent heat flux (LHF) of 90 $\mathrm{W\,m^{-2}}$ from the surface to the atmosphere. *Hint:* first calculate how many kg of water evaporate per second from 1 $\mathrm{m^2}$, convert this value to mm water per second and calculate the precipitation rate per day.

b. Express the above calculation in symbols, in other words, give the equation deduced from the above (LHF in terms of precipitation rate).

Exercise 2

When potential temperature is a function of height, the atmospheric lapse rate ($\gamma = dT/dz$) will differ from the adiabatic lapse rate ($\gamma_d = -g/c_p$).

a. Show that:

$$\frac{T}{\theta}\frac{d\theta}{dz} = \gamma - \gamma_d$$

Hint: use the definition of the potential temperature $\theta = T\left(\frac{p_0}{p}\right)^{R_d/c_p}$, work from left to right ($\frac{T}{\theta}\frac{d\theta}{dz}$ towards $\gamma - \gamma_d$), remember the hydrostatic equation and the ideal gas law, and note the definitions of lapse rate given.

In case $\gamma > \gamma_d$, potential temperature θ increases with height and the atmosphere is stably stratified. In this case it can be shown that when an air parcel is moved upwards over a distance of dz, it will accelerate back to its original position according to:

$$\frac{d^2z}{dt^2} \approx \frac{g}{T}(\gamma_d - \gamma)dz \tag{6.2}$$

which is the equation of an harmonic oscillator (described by d^2x/dt^2 =frequency^2dx)

b. Describe in words the meaning of the different terms in equation 6.2.

c. Derive the expression for the Bouyancy or Brunt Väisälä frequency N in terms of the potential temperature θ. Make use of $\frac{T}{\theta}\frac{d\theta}{dz} = \gamma - \gamma_d$ and equation 6.2. Note that the Brunt Väisälä frequency is a wave frequency.

d. Altocumulus lenticularis is a cloud type resulting from a wave train around the lifting condensation level in a stable atmosphere. This type of wave can develope when an air flow is forced over a mountain. Derive an expression that describes the horizontal spacing between the clouds (wave tops) that develope behind the mountain.

e. Calculate the horizontal spacing between the clouds given a flow speed u = 10 $\mathrm{m\,s^{-1}}$, a potential temperature θ = 273 K and a lapse rate $d\theta/dz$ =5 $\mathrm{K\,km^{-1}}$.

f. The air is flowing with flow speed u, however the clouds behind the mountain seem stationary. Explain this.

6.5 Temperature and radiation in the clear atmosphere

Exercise 1: a simple model of the global atmospheric energy budget

The energy budget of a simplified Earth-atmosphere system is presented in Figure 6.1.

a. Write out the equations for energy balance in the atmosphere and at the surface. Solve the equations for the longwave emissions (Lw_{e1}= .. and Lw_{e2}= ..) and eliminate the term for short wave absorption at the surface Shw_{a2} in both expressions.

b. Give an expression for the radiation temperature at the Earth's surface.

Measurements give the following values: $S_0/4 = 343\ \mathrm{W\,m^{-2}}$; $\alpha_p = 0.3$; $Shw_{a1} = 68\ \mathrm{W\,m^{-2}}$; $t = 0.056$; $e = 0.603$; $H + LE = 106\ \mathrm{W\,m^{-2}}$.

c1. Calculate the surface temperature T_E and the atmospheric long wave emission Lw_{e2} in the case without atmosphere.

c2. Calculate the surface temperature T_E and the atmospheric long wave emission Lw_{e2} in the case with atmosphere, but without turbulence.

c3. Calculate the surface temperature T_E and the atmospheric long wave emission Lw_{e2} in the case with atmosphere and turbulence (present situation).

c4. Calculate the surface temperature T_E and the atmospheric long wave emission Lw_{e2} in the case of maximum atmospheric greenhouse effect.

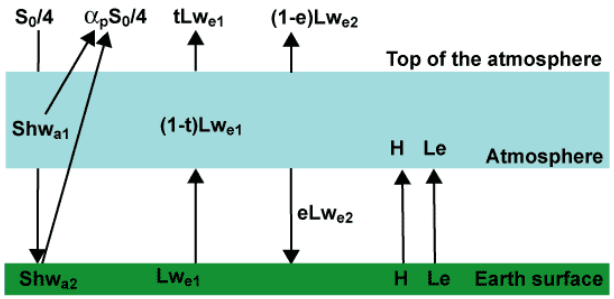

Figure 6.1: Diagram of the simplified heat budget of the Earth-atmosphere system. A is the absorption coefficient of Shw, e the emission coefficient of Lw in the atmosphere and t the transmissivity coefficient of Lw in the atmosphere.

Exercise 2

a. CO_2 is a very effective absorber of radiation. At which wavelength is the strongest absorption of CO_2 found?

b. See figure 2.3. The figures shows that in the CO_2 absorption band the emission decreases. Why does the emission not become zero?

c. Explain the thin peak in the middle of the CO_2 absorption band in Figure 2.33. *Hint:* Absorption of a gas is most effective in the middle of the absorption band. *Hint:* The rate of absorption depends on ...

Exercise 3

Figure 2.37 includes the effect of clouds in general on the energy budget of the Earth-Atmosphere system. It is expected that the amount of clouds will change in a changing climate.

a. What is the impact of an increase in high clouds (cirrus) on the short wave radiation flux? and the longwave radiation flux? Combining the effect on short and long wave radiation, does an increase in amount of high clouds result in a cooling or a warming. Motivate your answer.

b. What is the impact of an increase in thick low clouds (e.g. stratus) on the short wave radiation flux? and the longwave radiation flux? Combining the effect on short and long wave radiation, does an increase in amount of high clouds result in a cooling or a warming. Motivate your answer.

6.6 Motion in the atmosphere

Exercise 1: the centrifugal force

Like all objects, satellites endure gravity, nevertheless they never fall to the ground.

a. Derive an expression for the angular velocity (Ω) which is required to stay at a certain distance (r) from the Earth centre. Use that the gravity decrease with height (R_0 = radius of the Earth):

$$g(r) = g_0 \left(\frac{R_0}{r} \right)^2$$

b. Calculate the altitude of geostationary satellites. g_0 = 9.81 m s^{-2}, R_0 = 6378 km.

c. At what rotation speed (in m/s) should the earth be spinning for people at the equator to 'hover'?

Exercise 2: the coriolis force

a. After the great success of defeating Saddam, Mr. Bush attacks North Korea. He fires a missile (speed 1000 km/h) at Pyongyang from an American submarine in Sea of Japan (both at 39 degrees North, distance 600 km). Unluckily, he forgets that the earth rotate. Will Kim Jong-il and Pyongyang survive? Motivate your answer.

b. After his first failure, it is explained to Bush what happened. He understands he needs bigger weapons, and tries again, without compensating for the deflection he experienced earlier. This time he takes a bigger missile that travels slower than the one in (a). At what speed does the missile have to travel at least for the people in China, 100 km to the north, to be safe?

Exercise 3: the material derivative

A ship is steaming northward at a speed of 10 km/h. The surface pressure increases towards the northwest at a rate of 5 Pa/km. What is the pressure tendency recorded at a nearby island station if the pressure aboard the ship decreases at a rate of 100 Pa / 3 h?

Exercise 4

a. Calculate the geostrophic wind speed in meters per second for a pressure gradient in a low pressure area of 10 hPa per 1000 km. Let $\rho = 1.2\ \mathrm{kg\,m^{-3}}$ and $f = 10^{-4}\ \mathrm{s^{-1}}$.

Hurricanes don't form at latitudes less than 5° from the equator because there the Earth's planetary vorticity (f) is too weak to impart sufficient spinning motion. Surface winds must be at least 120 km/h to be called a hurricane.

b. What is the minimum east-west pressure gradient needed to generate hurricane-force geostrophic winds at 5° latitude?

c. What is the minimum east-west pressure gradient required at 30° latitude?

Exercise 5

a. A tornado rotates with constant angular velocity ω. Show from the cyclostrophic wind equation that the surface pressure at the centre of the tornado is given by:

$$p(0) = p(r)\exp\left(\frac{-\omega^2 r^2}{2R_d T}\right)$$

where $p(r)$ is the surface pressure at distance r from the centre, $R_d = 287\ \mathrm{J\,kg^{-1}\,K^{-1}}$ is the gas constant for dry air and T is the temperature (assumed constant).

b. If the temperature is 288 K and pressure and wind speed at 100 m from the centre are 1000 hPa and 100 m/s, respectively, what is the central pressure?

Exercise 6: Thermal wind

The mean temperature in the layer between 750 and 500 hPa decreases eastwards by 3°C per 100 km. If the 750 hPa geostrophic wind is from the south-east and 20 m/s, what is the geostrophic wind speed and direction at 500 hPa? Take $f = 10^{-4}\ \mathrm{s^{-1}}$.

Exercise 7: Horizontal divergence

The following data were received from stations 50 km to the east, north, west and south of our station, respectively:

Station	Wind direction	Wind speed
East	90°	$8\ \mathrm{m\,s^{-1}}$
North	120°	$4\ \mathrm{m\,s^{-1}}$
West	90°	$10\ \mathrm{m\,s^{-1}}$
South	60°	$4\ \mathrm{m\,s^{-1}}$

A wind direction of 0° implies a wind from the north and 90° from the east. Calculate the approximate horizontal divergence at the station.

Exercise 8: Vorticity

a. An air parcel at 30°N moves northward conserving absolute vorticity. If its initial relative vorticity is $5\times10^{-5}\ \mathrm{s^{-1}}$, what is its relative vorticity upon reaching 90°N?

b. An air column at 60°N with $\zeta_g = 0$ initially stretches from the surface to a fixed tropopause at 10 km height. The air column passes a mountain ridge of 2.5 km height at 45°N. What is its relative vorticity at the mountain ridge, assuming that the flow satisfies the barotropic potential vorticity equation?

Exercise 9: Rossby waves

Consider the relation for Rossby waves given in the lecture notes:

$$\frac{d_h(\zeta+f)}{dt} = \frac{\partial\zeta}{\partial t} + u\frac{\partial\zeta}{\partial x} + v\frac{\partial\zeta}{\partial y} + \beta v = 0$$

Assume for this exercise that the motion consists of a zonal velocity plus a small horizontal perturbation: $u = u_{av} + u'$; $v = v'$ and $\zeta = \zeta_{av} + \zeta'$. We define a perturbation stream-function ϕ' according to: $u' = -\partial\phi'/\partial y$ and $v' = \partial\phi'/\partial x$.

a. Show that:

$$\zeta' = \left(\frac{\partial^2}{\partial x^2} + \frac{\partial^2}{\partial y^2}\right)\phi' = \nabla^2\phi'.$$

The perturbation form of the relation for Rossby waves is then:

$$\left(\frac{\partial}{\partial t} + u_{av}\frac{\partial}{\partial x}\right)\nabla^2\phi^2 + \beta\frac{\partial\phi'}{\partial x} = 0 \tag{6.3}$$

in which we have neglected the terms with products of perturbations. (If you want to practise working with equations, try to derive Eq. 6.3). We seek a wave as a solution, of the form:

$$\phi' = \text{Re}\,[\Phi\exp[i(kx + ly - \omega t)]] \tag{6.4}$$

Here k and l are wave numbers in the x and y direction, respectively, Φ is a constant.

b. Find the wave velocity $c_x = \omega/k$, by substituting the Rossby wave 6.4 in equation 6.3.

c. What is the difference between this answer and the one in the example in the lecture notes?

d. Why does the wave always travel westwars relative to the mean zonal flow?

Exercise 10: Friction

We investigate the effect of friction on the airflow in a coastal area in the northern hemisphere. Assume 2 areas, both north-south oriented, one above land and one above sea (see figure 6.2). The following parameters are known for the two areas:

	Sea	Land
Pressure (2000 m)	800 hPa	800 hPa
Temperature (2000 m)	5°C	5 °C
lapse rate γ	-6.5 K/km	-10 K/km
friction (k)	$5{\cdot}10^{-5}$ s^{-1}	$10{\cdot}10^{-4}$ s^{-1}

a. Calculate pressure at sea level in above land and above sea. Show the derivation of the used equation.

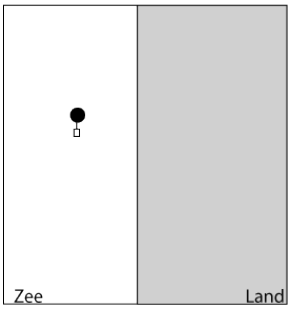

Figure 6.2: Situation sketch in exercise 10.

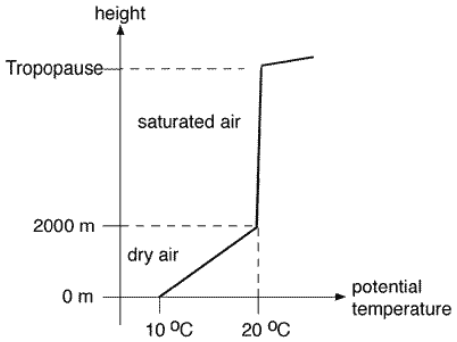

Figure 6.3: Diagram of the potential temperature profile in exercise 11.

In a stationary situation the balance of forces in the boundary layer (vertical averaged) is by approximation given by:
0 = pressure gradient force + coriolis force + friction
Assume a hot air balloon to be flying in this boundary layer above sea at 1 km from the coast (see figure 6.2).

b. Make a sketch of the forces working on the balloon (seen from above). Remember to include isobars, (geostrofic) wind direction, axis etc. Hint: assume one of the axis to coincide with the coastline. Is the balloon moving towards the coast or not. Explain.

Assume the following momentum balance in which friction is proportional to the wind speed:

$$x: \quad 0 = \quad -\frac{1}{\rho}\frac{\partial p}{\partial x} + fv - ku$$

$$y: \quad 0 = \quad -\frac{1}{\rho}\frac{\partial p}{\partial y} - fu - kv$$

c. Derive an expression for the two wind speed components (u, v) as a function of the pressure gradient and friction force.

The friction coefficient k is smaller over sea than over land. As a result frictional convergence in the coastal zone occurs. Assume the geostrophic wind to be 30 m/s (in southward direction), coriolis f = $1{\cdot}10^{-4}\,s^{-1}$, frictional coefficients K are given in the table above, the boundary layer is 2000 m thick and the adjustment from sea to land conditions takes place over a distance of 10 km.

d. Assume the wind to be blowing from the sea towards the land. When adjusting to land conditions, will the balloon change height? And if so, in what direction. Illustrate your answer with a calculation.Hint: make use of the continuity equation and calculate the vertical change at 10 km distance from the coast at the top of the boundary layer.

Exercise 11: Convection

At sunrise, the potential temperature θ profile in the atmosphere is given in figure 6.3.

a. Discuss the vertical stability of the different layers.

The convective atmospheric boundary layer starts growing when the energy balance at the surface becomes positive (at $t = 0$). The growth of this layer with depth h_m can be described with:

$$\frac{\partial h_m}{\partial t} = \frac{SHF}{\rho c_p h_m \gamma_\theta} \quad \text{in which} \quad \gamma_\theta = \frac{\partial \theta}{\partial z}$$

The turbulent sensible heat flux SHF is estimated by a sinus-function with a period of 24 hours, SHF_{max} = 500 $\mathrm{W\,m^{-2}}$ and SHF = 0 $\mathrm{W\,m^{-2}}$ at $t = 0$. Use that (ρc_p) equals 1300 $\mathrm{J\,K^{-1}\,m^{-3}}$.

b. Why is rainfall possible if h_m exceeds 2000 m?

c. Find out if showers will occur during this day. Motivate your answer with calculations.

Bibliography

Garratt, J.. 1992. *The Atmospheric Boundary Layer*. Cambridge University Press, Cambridge, UK. 316 pp.

Hartmann, D.. 1994. *Global Physical Climatology*, volume 56 of *International Geophysics series*. Academic Press. 411 pp.

Holton, J.. 1992. *An Introduction to Dynamic Meteorology*, volume 48 of *International Geophysics series*. Academic Press. 511 pp.

IPCC. 2007. Climate change 2007: The science of climate change. In: Solomon, S., D. Qin, M. Manning, M. Marquis, K. Averyt, M. Tignor, H. L. M. Jr. and Z. Chen, editors, *Contribution of Working Group I to the Fourth Assessment Report of the Intergovernmental Panel on Climate Change*. Cambridge University Press, Cambridge, UK.

Liou, K.. 1980. *An Introduction to Atmospheric Radiation*, volume 26 of *International Geophysics series*. Academic Press. 392 pp.

Wallace, J. and P. Hobbs. 2006. *Atmospheric Science: An introductory survey*. Academic Press. 483 pp.